Title

The FcuR and IgM, a Duo on Antigen Presentation and BCR Kinetics

Author

Blandino, Rebecca Alisha

Publication Date

2023

Peer reviewed|Thesis/dissertation

The FcμR and IgM, a Duo on Antigen Presentation and BCR Kinetics

By

REBECCA BLANDINO

DISSERTATION

Submitted in partial satisfaction of the requirements for the degree of

DOCTOR OF PHILOSOPHY

in

Biochemistry, Cellular & Molecular, Developmental Biology

in the

OFFICE OF GRADUATE STUDIES

of the

UNIVERSITY OF CALIFORNIA

DAVIS

Approved:

Nicole Baumgarth , Chair

Charles Bevins

David Pleasure

Committee in Charge

2023

Abstract

Efficient IgG responses are the basis for many vaccines strategies. B cells differentiate into high affinity antibody-producing plasma cells because of activation steps that involve antigen processing and presentation (via MHC class II molecules) to CD4+ "helper" T cells. Current understanding is that this process involves protein antigens becoming captured by B cells via their B cell receptor (BCR), which consists of membrane-bound IgM and associated signaling chains CD79a and CD79b (IgM-BCR). Following antigen-capture, the IgM-BCR antigen complex is internalized, protein antigens are degraded into peptides and peptides are then integrated into MHCII molecules and presented on the B cell surface to CD4 T cells. Following antigen presentation to cognate CD4 helper T cells, B and T cells will become further activated and enter differentiation programs, including the development of IgG-secreting plasma cells. Understanding the mechanisms that support maximal IgG response induction is significant, as it can be exploited for vaccine development and design as well as lead to a better understanding of immunity to infections.

The immunoglobulin isotype M (IgM) is present on cell surfaces of all developing B cells as IgM-BCR. Additionally, IgM is present in a secreted form (sIgM). IgM is the evolutionary most conserved antibody isotype and is present in all jawed vertebrates. Previous experiments have shown that mice lacking sIgM and infected with influenza virus had reduced virus-specific serum IgG, increasing their susceptibility to death and inability to clear infection. Together, this suggests that

sIgM is critical for effective IgG responses.

Although sIgM has been reported to bind various cell surface receptors, there is only one receptor that it binds with high affinity: the FcμR, a receptor highly expressed on B cells. Previously, our lab showed that mice lacking the FcμR ($FcμR^{-/-}$) have significantly reduced IgG responses after influenza infection, like sIgM-deficient mice. This dissertation was designed to test the hypothesis that the FcμR mediates the uptake and processing of sIgM-antigen complexes, augmenting presentation of antigen to helper T cells and thereby enhancing subsequent IgG responses. My dissertation work confirmed this hypothesis and in addition identified a novel function for the FcμR in supporting IgM-BCR antigen complex internalization, and antigen processing and presentation.

Chapter 1 reviews the literature on the structure and function of sIgM and the FcμR. The functions of secreted IgM have been extensively studied and are outlined in this review with focus on potential roles and connections to IgG secretion, as well as its recently discovered structure and interaction with AIM/CD5L. The FcμR, was described originally as a receptor that prevents Fas mediated apoptosis but was later rediscovered as a receptor that binds exclusively to the Fc region of IgM. The major questions raised in the review and its focus revolve around how sIgM-FcμR interactions together support maximal IgG responses.

Chapter 2 describes establishment of a system that can model the dynamics of T-dependent B cell responses *in vitro* and *in vivo*. For that, I generated a conjugate protein antigen, hen-egg lysozyme (HEL) fused to ovalbumin (OVA),

for which previously described HEL-specific BCR- and OVA-specific T cell receptor (TCR)-transgenic mice were bred and utilized. The BCR transgenic "SW_{HEL}" mice are gene "knock-in" mice that express and secrete HEL-specific IgM and can undergo class-switch recombination to secrete other Ig isotypes, such as IgG. The SW_{HEL} mice were backcrossed onto mice, which have been described previously, that lack the FcμR. The "OT-II" mouse contains a transgene encoding OVA-specific TCR presented in the context of MHC-II I-A^b, as expressed in C57BL/6 mice. In this system, B cells either expressing or not the FcμR bind to HEL, internalize, and process the HEL-OVA conjugate and present OVA peptides in MHC-II I-A^b to OT-II CD4 T cells, which are then activated to proliferate. To track antigen via confocal and STED microscopy, as well as flow cytometry, the fluorescent molecule BODIPY was conjugated to whole HEL protein. Chapter 2 outlines the generation of these reagents and assessment for their use in subsequent experiments, which are outlined in Chapter 3.

Chapter 3 demonstrates reduced serum IgG responses to subcutaneous immunization with HEL-OVA conjugate in SW_{HEL} transgenic mice lacking the FcμR compared to SW_{HEL} controls that express the FcμR, as measured by ELISA. Given that up to 20% of B cells in the SW_{HEL} mouse are HEL-binding, mixed bone marrow irradiation chimeric mice were generated that contained 2% SW_{HEL} transgenic B cells with or without the FcμR, which were similarly assessed for their IgG responses but in the context of more physiological frequencies of antigen-specific B cells. The results were consistent with those obtained with total SW_{HEL} transgenic mice. To investigate what role the FcμR plays in the B cell's ability to

internalize and present antigen to helper (CD4+) T cells, HEL-OVA construct was used containing a small peptide that when integrated into I-A^b was recognized by a commercially available monoclonal antibody. The results demonstrated significant reductions in MHC-peptide complex surface expression and reduced antigen-presentation of B cells to CD4 T cells in the absence of the FcμR. Utilization of STED and confocal microscopy assessed the protein kinetics and localization of the internalized IgM-BCR, antigen and FcμR as well as other intracellular antigen marking the pathway of endocytosis, such as RAB11, LAMP-1, and EEA1. Collectively, the results demonstrate the need for FcμR expression in IgM-BCR internalization and antigen processing. Finally, addition of HEL-specific sIgM was shown to further enhance antigen-presentation by FcμR sufficient but not deficient B cells. Thus, this chapter demonstrates that the FcμR acts as a chaperone for IgM-BCR complexed with antigen and a second, albeit less prominent role for the receptor in binding antigen-sIgM complexes further enhancing antigen presentation to CD4+ T cells.

Acknowledgments

I want to express my sincere gratitude to my mentor Dr. Nicole Baumgarth for continuous support, guidance, patience, motivation and understanding though my studies. I have learned a great deal from Nicole; not only how to write, but to conduct science and critical thinking in a productive, logical manner; I am the scientist I am today because of Dr. Baumgarth. A huge thank you to my dissertation committee members Dr. Charles Bevins and Dr. David Pleasure for always motivating and helping me with anything I needed. Their advice and insightful feedback were paramount in my dissertation.

Our collaborators:

Dr. Robert Brink

Dr. Ingrid Brust-Mascher

Dr. Jason Cyster

Dr. Mark Flajnik

Dr. Kathrin Kläsener

The current and past members of the Baumgarth laboratory: Jean Luo, Dr. Trang Nguyen, and Dr. Fauna L. Smith.

Last but certainly not least, to my mom and dad, who have always supported me in more ways I can list, my family and friends for all their encouragement and understanding throughout the years.

Table of Contents

Chapter 1

Secreted IgM: New Tricks for an Old Molecule
As published in J Leukocyte Biology
(Blandino & Baumgarth, 2019)

Abstract

Secreted IgM (sIgM) is a multifunctional evolutionary conserved antibody that is critical for the maintenance of tissue homeostasis as well as the development of fully protective humoral responses to pathogens. Constitutive secretion of self- and polyreactive natural IgM, produced mainly by B-1 cells, provides a circulating antibody that engages with autoantigens as well as invading pathogens, removing apoptotic and other cell debris and initiating strong immune responses. Pathogen-induced IgM production by B-1 and conventional B-2 cells strengthens this early, passive layer of IgM-mediated immune defense and regulates subsequent IgG production. The varied effects of secreted IgM on immune homeostasis and immune defense are facilitated through its binding to numerous different cell types via different receptors. Recent studies identified a novel function for pentameric IgM, namely as a transporter for the effector protein ″apoptosis-inhibitor of macrophages″ (AIM/CD5L). This review aims to provide a summary of the known functions and effects of sIgM on immune homeostasis and immune defense, and its interaction with its various receptors, and to highlight the many critical immune regulatory functions of this ancient and fascinating immunoglobulin.

Introduction

The humoral immune system provides an intricate and complex response to protect the host from infections and pathological alterations of cells and/or tissues. B cells, activated in response to such alterations, begin to secrete immunoglobulins that can then bind to and inactivate or eliminate the threat. The evolutionary highly conserved immunoglobulin isotype M (IgM), forms the cell surface antigen receptor (BCR) of all developing B cells of jawed vertebrates, is the first anti- body to be generated in ontogeny, and the first to be secreted during an immune response. Most secreted (s)IgM is generated as a pentameric Ig molecule, displaying 10 antigen-binding sites, which greatly enhances the avidity with which it binds cognate antigen.[1] As recently shown, IgM is an asymmetric pentamer that also forms a pocket for an effector protein, termed “apoptosis-inhibitor of macrophages” (AIM/CD5L), whose serum half-life is greatly enhanced through binding to IgM.[2] In addition to IgM’s direct effector functions and its AIM transport function, studies conducted for over 30 years have shown direct immunoregulatory functions for sIgM. Particularly intriguing are the immune-enhancing effects of sIgM for inducing maximal IgG responses and the immune-protective effects against the development of antibody-mediated autoimmune disease.[3–6] The mechanisms by which sIgM regulates these processes remain poorly understood, but recent studies have implicated the newly discovered FcμR in facilitating direct interaction of sIgM with cells of the immune system, specifically B and T cells. Mice lacking the

FcμR also show reduced IgG responses following immunization and infection and develop increased circulating autoantibody titers.[7,8] . In this article, we review the initial discovery of IgM, its structure and functions, and summarize the known interactions with various IgM-binding receptors, focusing in particular on the FcμR. Although IgM was identified more than 75 years ago, much remains to be learned about this evolutionarily highly conserved immunoglobulin, and the receptors that support its effector and regulatory functions.

The Discovery of IgM

The study of the humoral immune system was sparked In 1888 when the bacteriologist George Nuttall demonstrated antibacterial properties in the serum of animals inoculated previously with anthrax bacilli.[9–11] In a landmark paper published in 1890, Emil von Behring with Shibasaburo Kitasato reported that blood taken from rabbits vaccinated with tetanus bacteria and then injected into mice, protected the mice against lethal doses of *Clostridium tetani.*[12] Shortly thereafter, Von Behring published similar results using *Corynebacterium diphtheria* infection of guinea pigs.[13–15] In 1894, Richard Pfeiffer performed in vitro experiments with *Vibrio cholera* showing that the plasma of previously immunized guinea pigs could lyse the bacteria, terming this the “Pfeiffer’s phenomenon”.[10] and thus providing a mechanism for the earlier discovered protective capacity of serum. In 1930, Tiselius developed a technique, later adopted by Landsteiner, to separate and visualize proteins by electrophoresis.[9] Using this technique, Tiselius and Kabat In 1939 identified a major band of serum proteins (γ-globulins), which we now understand

to contain most immunoglobulins.[9,14,16] . The first inference of IgM was made in 1937 in horses immunized with pneumococcus polysaccharide. The vaccine-induced anticarbohydrate antibodies were shown to be 3–4 times larger than γ-globulins.[17] Immunoglobulin (M) (IgM) was first characterized in 1944 via immunoelectrophoresis and ultracentrifugation by Waldenström, Pederson, and Kunkel from patients with B cell lymphoma.[18,19] In these experiments, highly elevated concentrations of IgM were visualized. Originally named macroglobulin, it was not until the 1960s when the nomenclature for Ig-isotypes was developed, that macroglobulin became the "M" in IgM.[9,20,21].

Expression of IgM

All jawed vertebrates express IgM, including amphibians, reptiles, shark, fish, and mammals,[22,23] whereas jawless vertebrates, such as hagfish and lamprey, lack IgM.[24] IgM production can be detected very early, in humans as early as week 20 of gestation.[25] The fact that both antigen-free and germfree mice have serum IgM levels similar to that of SPF or conventional-housed mice (300–800 μg/ml),[22] suggesting that foreign antigen exposure does not control serum IgM concentrations.[26,27] However, whether it may affect the specificity of the circulating IgM has not been analyzed. The half-life of sIgM is very short, with reports ranging from 8 h to 2 days[28] in mice and 5–8 days in humans.[29] In contrast, the half-life of IgG is closer to 3 weeks. Obvious sexual dimorphism exists in the levels of circulating IgM, with female mice showing significantly higher serum IgM concentrations than male mice. Recent studies have linked this difference to the

regulation of IgM-secreting cells by estrogen. With that, they also linked the presence of higher levels of oligosaccharide-specific serum IgM to a selective survival advantage of females compared to males following bacterial infection.[30]. Due to its large size, ~970 kDa, pentameric IgM does not easily extravasate into tissues.[31,32] Similar to dimeric IgA, pentameric IgM can bind to the polymeric Ig receptor via its J (joining) chain, which facilitates the transport of IgM across epithelial layers into the lumen of mucosal tissues (see below[33]). The lamina propria of the human but not the mouse gastrointestinal tract contains significant frequencies of IgM plasma cells. Secreted IgM, together with secretory IgA, seems to affect the gut microbial diversity by binding to commensals and anchoring them in the mucus layer.[34] Further work is required to reveal the distinct functions of IgM and IgA binding to the microbiota and to understand the apparent species-specific differences of these processes. IgA deficiency in both humans and mice has surprisingly subtle effects on their health status, given the large daily production of IgA and its presence on mucosal surfaces. The observed compensatory increases of sIgM in IgA-deficiency may explain, at least in part, these findings.[35]

A Newly Discovered Structure for a Very Old Molecule

IgM is structurally distinct from the other immunoglobulin subtypes. This is not only because of its usually pentameric form[1,2] but also because IgM lacks a flexible hinge region.[31] Secreted and membrane forms of IgM are generated by alternative splicing,[36] with membrane- bound IgM expressing a hydrophobic transmembrane domain of ~25 amino acids at the hydroxy terminus of the Ig-heavy chain and

secreted IgM carrying a hydrophilic secretory tail at its carboxy terminus. Cysteine residues at that tail prevent premature secretion and support the assembly of the mature secreted form in the ER.[37] In the absence of the joining chain (J-chain), IgM usually aggregates into hexamers, which seems to bind complement more efficiently.[28,38] Increased hexameric IgM in humans is present in disorders such as macroglobulinemia, whereas, for example, in Xenopus hexameric IgM is the predominant form of IgM.[39] Very little information exists about the hexameric form and its potential physiologic functions. Pentameric and monomeric IgMs have been notoriously difficult to crystallize. The first inference of the structure of IgM stems from negative stain electron microscopy.[2,40,41] Without antigen, IgM exhibited a planar, star-shaped complex. However, when bound to its cognate antigen (flagella from *Salmonella* sp.), a conformational change was visualized, with IgM adopting a table-like conformation.[40] More recently, through cryoatomic force microscopy, modeling of the antigen-free IgM pentamer was revised showing that IgM adopts a nonplanar, mushroom-shaped structure. Furthermore, the table-like conformation following antigen binding was shown to expose the C1q-binding site on the heavy chain constant region.[40] Most recently, using single-particle electron microscopy it was revealed that the IgM pentamer does not form a symmetric pentameric star, as always assumed, but rather takes the form of an asymmetric pentagon with one large gap at a 50° angle between two of the five IgM monomers.[2] Surprisingly, this gap contained a serum protein, the “apoptosis inhibitor expressed by macrophages” (AIM/CD5L). Thus, the data identified secreted IgM not only as an effector protein but also as a transporter for another effector protein (Fig. 1).

AIM/CD5L/SP-α is a member of the scavenger–receptor cysteine- like domain superfamily and is produced by macrophages.[42] AIM is present in the serum, where its half-life is greatly enhanced by binding to IgM.[42–45] *In vitro* and *in vivo* studies with gene-targeted mice suggested that AIM is involved in the regulation of apoptosis of developing CD4/CD8 double-positive thymocytes. However, its high expression by tissue macrophages, including macrophages in the liver, peritoneal cavity, and splenic red pulp, and its binding to low- density lipoproteins, among other cholesterol-containing antigens, suggests that this molecule has additional functions that require further study.[46] Specifically, it will be important to reexamine whether any of the many defects observed in mice lacking sIgM may be explained in fact by the lack of-or an altered availability of AIM. Each human IgM heavy chain carries five N-linked glycosylation sites and an additional site on the J-chain[47] (Fig. 1), accounting for 12–14% of its molecular weight and making it the most heavily N-glycosylated antibody of humans.[48] IgM's function is significantly affected by glycosylation. For example, sialylation was reported to support the internalization of IgM by T cells, leading to inhibition of T cell responses, an effect diminished by the absence of sialic acid.[47] Glycosylation of IgM at position 46 (N46) was shown to be required for pre-BCR function,[49] and mutation of Asn-402 disables complement protein C1-binding.[50] In contrast to IgG, whose interactions with the various FcμR were shown to be critically affected by its glycosylation,[48,51] interaction of IgM with the hFCMR appears to be glycan independent.[51]

Natural IgM production: Two sides to a coin

Principally two types of secreted IgM have been distinguished in the literature based on their cellular origins, regulation of their production, and overall function: natural IgM and immune/induced IgM. Whereas the former is thought to be produced constitutively without stimulation by a foreign antigen, induced IgM production is the direct outcome of a tissue insult and/or infection. The two types of IgM have distinct modes of induction and distinct repertoires, fulfilling a myriad of effector functions that we will outline below (Fig. 2). In mice, natural IgM production has been linked to a small subset of B cells, termed B-1 cells. These cells are of fetal/neonatal origin and are the initial source of IgM after birth. Early adoptive transfer studies showed that much of the circulating IgM was produced by these cells[52] and subsequent studies using transfer of B-1 cells into neonatal B cell-depleted mice showed that amount to be more than 90%.[53,54] Others reported that marginal zone (MZ) B cells also contribute to natural antibody production in both humans and mice.[55,56]

Serum concentrations of natural IgM are similar between mice held under standard housing conditions and those kept free of microbiota or even solid food antigens.[57] The CD5+ B-1 cells in spleen and body cavities of germfree, as well as SPF-housed, mice also showed very similar Ig-VH gene repertoires, supporting the long-held concept of “natural” IgM production, that is, production of IgM that is independent of foreign antigen.[58] This was further supported by findings that depletion or genetic ablation of T cells had little effect on serum IgM levels, whereas most IgG subtypes were strongly reduced, suggesting that B-1 cells do not require T

cell-mediated activation in order to secrete IgM.[59,60].

Natural or “spontaneous” IgM production occurs mainly in the spleen and the bone marrow.[57,61–63] Two cell populations producing these antibodies have recently been identified: “classical” non-terminally differentiated CD19+ Blimp-1^{neg} CD43+ B-1 cells and B-1-derived CD19$^{lo/-}$ CD43+ Blimp-1^{pos} plasma cells.[61,63,64]Our studies showed that the Blimp-1^{neg} IgM-secreting cells did not upregulate Blimp-1 expression and continued to secrete IgM in the absence of Blimp-1 in conditional, B cell-specific Blimp-1 deficient mice.[63] This is significant, as it suggests that only some B-1 cells are activated to terminally differentiate to plasma cells to secrete IgM. It raises the question of what are the stimuli inducing the differentiation of B-1 cells forming B-1 PC versus those inducing IgM secretion without terminal differentiation. It may also indicate that the antigen specificity of the IgM secreted by those distinct activation events differ. There have been no reports of B-1 cells participating in germinal center responses, thus it is unlikely that the plasma cells have emerged from such response. Their recent extensive RNA sequencing experiments also provided no evidence that B-1 cells undergo extensive somatic hypermutation, with significant components being germline encoded. Although an analysis of only IgM-secreting B-1 cells was not conducted.[58,65] With regard to the specificity of IgM, current evidence suggests that the pool of natural IgM-secreting B-1 cells is positively selected upon the recognition of self-antigens during development.[66] This explains the highly skewed, self-reactive repertoire of natural IgM and the fact that the antigen-specificity of B-1 cells is tightly linked to their unique functions.[67] Given the similarity in the B-1a cell repertoire of gnotobiotic and

conventional-housed mice, it then appears that self- antigen recognition shapes the B-1 cell repertoire through activation and clonal expansion, which explains the strong changes in VH-usage over the first few months of life.[58,65] How B-1 cells can be selected and then differentially activated by self-antigens to secrete self-reactive IgM, without this process resulting in autoimmune disease development is a further important but unresolved question.

One possible explanation might be the unique structure and the size of natural IgM, which ensures that IgM remains circulating in the blood without extravasation unless tissue destruction or extensive inflammation leads to endothelial cell damage/leakage. In the circulation, IgM has been associated with protection from systemic infections, that is, bacteremia and viremia, such as after infection with *Borrelia hermsii* [68] enteropathogenic *Escherichia coli* [30] or during more general sepsis.[4] It has also been shown to be protective in atherosclerosis, plaque formation in the blood vessel wall, where natural IgM is believed to help remove modified LDL and apoptotic and necrotic cell debris, thereby reducing triggers of inflammation.[69,70] .A potential clinical application for natural IgM was indicated by recent reports that enhancing the number of IgM-secreting B-1 cells via treatment of mice with anti-TIM-1 attenuated atherosclerosis development, providing a promising potential therapeutic approach that requires exploration in humans.[71,72] .In contrast, when IgM extravasates into tissues, such as during endothelial damage and leakage created by a lack of blood per- fusion and subsequent reperfusion of an organ, as occurs for example following surgery, the presence of IgM in these tissues causes excessive activation of complement and resultant tissue and organ damage.[73,74] The

ability of IgM to contribute to immune homeostasis by binding to and helping to remove a large number of “altered” self-antigens, coupled with the ability to also bind to shared molecules on pathogens is a hallmark of natural IgM. The classic example is the simultaneous recognition of both *Streptococcus pneumoniae* and oxidized LDLs by a particular IgM natural antibody.[75] These unique polyreactive proper- ties of IgM may provide a powerful evolutionary advantage, explaining why IgM, but not other immunoglobulins are shared among all jawed vertebrates.[76–78] The polyreactive nature of natural IgM has long been recognized {reviewed in Ref. 79}. A possible mechanistic explanation for its polyreactivity is that natural IgM is encoded by V regions containing higher frequencies of tyrosine and serine residues, which contain hydroxylated side chains that enable IgM greater binding flexibility (reviewed in Ref. 22). With regard to the specificity of IgM, in addition to the antigens mentioned above, natural IgM also binds to various epitopes on phosphorylcholine and other phospholipids, carbohydrates such as phosphatidylcholine, ssDNA and dsDNA, oxidized LDL, and certain PAMPS.[80–83] Although their polyreactivity is overall characterized by low-affinity antigen interactions, the ten binding sites of IgM still enable overall higher avidity binding.[84] Taken together, natural IgM is a self-reactive, serum protein with unique structural characteristics that enable its effectiveness in binding to self-antigens and thereby contributing to immune homeostasis by reducing the threat of inflammation and tissue damage (Fig. 2). In situations of chronic or extreme inflammation, however, this otherwise highly protective immune effector molecule can gain access to tissues otherwise inaccessible, where it can promote inflammation and there- fore often also tissue damage and disease.

Immune/Induced IgM

Remarkably little attention has been paid to the initial and transient induction of IgM secretion, which is one of the first contributions of the adaptive immune system to immune defense. Induced IgM is generated by either the activation of B-1 cells and/or by activation of conventional B (B-2) cells. It is generally assumed that early IgM production occurs because all B cells first express IgM and that the generation of other Ig-isotypes requires time for class-switch recombination to occur, while IgM secretion occurs rapidly through alternative RNA splicing, excluding the membrane domain usually tethering the IgM (B cell receptor) onto the surface of developing B cells. However, we now understand that a sizable population of memory B cells remains nonclass switched, while having undergone activation events that drove them toward memory development, even hyper affinity maturation in germinal centers,[85,86] suggesting that the production of IgM is about more than simply "being there early." Effector functions of IgM, such as effective activation of complement might be critical for early immune defense,[87] or the ability to bind to various IgM-binding receptors (see below). The presence of early IgM was also shown to be important for maximal IgG response induction (Table 1). Finally, the lack of easy diffusion may ensure that locally produced IgM remains mainly at the site of production, that is, the secondary lymphoid tissues, where it could support the filter function of lymph nodes. In support, we showed previously that B-1 cell-derived IgM production in the respiratory tract regional lymph nodes following influenza infection, measured by ELISPOT, was not reflected in the

serum, where B-1 derived IgM titers were unchanged, whereas conventional B cell-derived serum IgM did increase transiently in response to the infection. The tissue location of the IgM-secreting conventional B cells giving rise to this systemically-produced IgM was more difficult to discern, however, as conventional, but not B-1 cell-derived increased IgM production also occurs in the spleen after influenza infection and is not restricted to the draining lymph nodes of infected mice.[3,88,89] Splenic IgM-producing cells have been found mainly in the marginal zone and the red pulp, both areas with immediate access to the circulating blood. Both, B-1 and conventional B-2 cells generate secreted IgM in the draining lymph nodes early after influenza infection, and both contributed to immune defense.[88,938.8,93] Whether B-1 cells are activated via antigen-specific or innate signals remains an open question. They are exquisitely responsive to TLR-mediated stimulation but unable to respond to BCR-mediated signaling with clonal expansion. Yet, observations of antigen-specific B-1 cells responses have been made in response to numerous pathogens, including *B. hermsii, Francisella tularensis, Salmonella typhimurium, and S. pneumoniae,*[68,84,94–96] suggesting that B-1 cells in vivo can respond to BCR-mediated signals and thus act as part of the adaptive rather than the innate response. We refer to our recent in-depth discussion on this topic elsewhere.[97]

The antigen-specific, T-dependent, and T-independent activation of conventional B cells results in a transient induction of sIgM that lasts for 1–2 weeks after the insult. This temporary induction, measurable also in the blood, has been exploited clinically for distinguishing early from longer-term infections by determining the ratio of antigen-specific IgM and IgG levels in repeated blood draws. The

transient production of IgM coupled with its very short half-life explains its only brief presence in most acute infections. Given the early effectiveness of IgM in suppressing infections,[3,4,98] it is unclear what benefit the rapid curtailment of IgM production may have, an intriguing yet unexplored question. However, some chronic infections do induce continued IgM production, for example, following infection with *Ehrlichia muris*, where a protective, T-independent and BAFF-dependent IgM response was shown to be induced long-term by plasmablasts in spleen and bone marrow.[99–101] We have made similar observations during chronic infection of mice with *Borrelia burgdorferi* (Hastey CJ, Elsner, RA, Olsen, K., and Baumgarth, N. in preparation). Interestingly, in humans infected with *Borrelia burgdorferi,* patients may remain seropositive for IgM or IgG for up to 20 years.[102–104] In addition, humans infected with West Nile virus have shown persistent IgM levels from one up to 8 years postinfection.[105] Continued and in fact enhanced IgM production was also reported after recovery from *Plasmodium vivax* infection. However, the time point of analysis was only 30 days after completion of treatment.[106]

Effects of IgM deficiency

Mice that lack secreted but not membrane-bound IgM developed antibody-mediated autoimmune disease, suggesting that sIgM plays a regulatory role in the development of self- and foreign-antigen induced humoral immunity (Table 1). Similar findings have been made in humans with a primary IgM-deficiency.[107] At least three distinct, nonmutually exclusive mechanisms for autoimmune antibody-development have been suggested: First, natural IgM usually rapidly removes self- antigens, such

as cellular debris, from the body.[108] In IgM-deficiency such cellular content could act as damage-associated molecular pat- terns (DAMPS) and stimulate inflammatory responses, enhancing the risk of autoimmune-disease development.[109,110] Furthermore, natural IgM recognition of such antigens also appeared to drive IL-10 production by B and T cells, further reducing the risk of inflammation- induced tissue damage.[4,92,111] Second, Tsiantoulas et al. reported that sIgM-/- mice showed increased BCR signaling, a process that was reversed with treatment with a Btk inhibitor at low doses. The authors suggested that sIgM may act as a "decoy receptor" competing for binding between sIgM and membrane-IgM, reducing the likelihood by which B cells respond to self-antigens.[91] Third, we observed that bone marrow B cell development and peripheral B cell repertoires were significantly altered in sIgM-/- mice, concomitant with the appearance of anergic CD5+ B cells in the periphery. The data suggested that the lack of central tolerance induction during B cell development in the absence of sIgM may explain the increased production of autoreactive IgG.[90]

Deletion of sIgM also significantly reduced immune protection against numerous infectious agents, as outlined above. This strong effect of sIgM on protection might be due, at least in part, to the enhancing effects of sIgM in the development of maximal IgG responses (Table 1). Although the phenomenon of IgM-enhanced IgG production has been reported for many years and appears to be strongest during immune induction to limiting amounts of antigen and following infections,[3–5,112] we still do not fully understand the mechanism underlying these effects. We will return to this topic below in the context of sIgM interaction with its

receptors. In summary, sIgM has many functions both in maintaining homeostasis and system health, as well as in the immediate protection from infectious and other noxious insults. Its production is tightly con- trolled in time, and its functions are closely associated with its unique structure. The apparent immune regulatory functions of sIgM require further investigation, to obtain a better molecular understanding of how sIgM might be exploited therapeutically for enhancing immunity and reducing metabolic and autoimmune diseases.

Receptors that Bind IgM

Multiple receptors expressed by a variety of cell types can bind IgM. These include the complement receptors (CR1/CR2), Fc$\alpha\mu$R polymeric Ig receptor, and the FcμR (Fig. 3). The latter is the only bona fide Fc-receptor for IgM and the most recently identified receptor.[113] Below is a brief review of these receptors and how they may support the various functions of sIgM.

Complement Receptors

Complement receptors 1 and 2 (CD35/CD21) are primarily expressed on B cells and on follicular dendritic cells (FDCs).[114,115] Complement receptor engagement has been shown to be critically involved in the induction of maximal antibody responses following immunization (reviewed in Ref. 116). Secreted IgM is an effective activator of complement and complement itself was shown to support maximal IgG response induction. However, a mouse in which the complement binding site on the CH3 domain of the IgM heavy chain was inactivated, showed no

effect on IgG responses during primary or secondary responses following immunization with sheep red blood cells, KLH, and NP-KLH.[117] The conclusion that IgM-mediated enhancement of IgG responses can occur without complement activation is supported by studies on influenza infection in mice, where removal of complement via injection of cobra venom factor did not significantly affect the over- all IgG response, while the lack of sIgM and the lack of FcμR expression on B cells showed significant and continuing IgG reductions.[8] In apparent contrast to those studies, when antigen-specific IgM was co-administered with antigen, the ensuing IgG response was greatly enhanced, while the same experiment conducted with sIgM unable to bind C1q did not provide such enhancement. The complement-binding dependent IgM-enhancing effects on IgG responses required the presence of CR1/2 on both B cells and FDC.[118,119]

The data suggest a fundamental difference in the kinetics and functions of IgM and complement under those two very distinct situations. In one case, sIgM was coadministered and thus already bound to anti- gen, thus forming a large antigen–antibody complex, while in the other case sIgM must have first been produced and then engage with anti- gen. It has been concluded from those data that pre-existing natural IgM may not act via complement-mediated immune response enhancement, or that natural sIgM may not have been present at the site of antigen deposition, as immediate IgG enhancement was not seen when antigen was injected without first being mixed with sIgM.[116] This hypothesis appears less likely to us, however, as at least during an infection both, pre-existing natural and antigen-induced IgM, were shown to be necessary for maximal IgG responses[3] and both types of IgM were present in the

regional lymph nodes of influenza-infected mice, the main tissue source of anti-influenza IgG.[88,93] An intriguing alternative possibility is that the observed differences in the effects of sIgM on the IgG response, and the role of the complement receptors, are due to the distinct pathways soluble and sIgM-complexed antigen would take traveling to and through the secondary lymphoid tissues, due to their large differences in size. At the molecular level, IgM-CR1/2 interactions may enhance IgG responses via enhanced BCR-signaling through colligation of antigen with CR1/2 and the BCR. It has also been shown that sIgM-CR1/2- mediated binding to splenic MZ B cells supported the shuffling of anti- gen from the splenic MZ to the follicle via migration of the MZ B cells in and out of the follicle.[120] IgM-complement receptor-mediated enhanced presentation of antigen to B cells can also occur via tethering of sIgM–antigen complexes onto the FDC in germinal centers. Indeed, expression of CR1/2 is particularly high on those cells. A recent review article by Heyman and colleagues provides a more in-depth discussion on that topic.[116]

Fc$\alpha\mu$R

The Fc$\alpha\mu$R is a transmembrane protein that binds both IgA and IgM. Interestingly, binding of sIgM to the Fc$\alpha\mu$R was greatly reduced when pentameric sIgM was complexed with AIM.[121] The Fc$\alpha\mu$R appears to be expressed predominantly on antigen-presenting cells, including macrophages, and to be particularly abundant on FDC, while it is not expressed on granulocytes, T cells or NK cells.[122–125]

The presence of the Fc$\alpha\mu$R appeared to be largely dispensable for mediating

the immune protective role of sIgM following *B. hermsii* infection, and therefore opsonization of antigen for macrophage uptake.[126] Instead, the receptor has been shown to mediate the endo- cytosis of IgM-coated bacteria by B cells[123,124] and the binding and internalization of sIgM-antigen complexes by FDC. Thus, the receptor can promote antigen processing and presentation to CD4 helper T cells via binding to sIgM and IgA-antigen complexes,[124] while reducing the availability of antigen tethering on the surface of FDC, and thus anti- gen presentation to B cells.[121] The data suggest that sIgM binds to at least two distinct types of receptors on the FDC: the complement receptors and the Fc$\alpha\mu$R. Given that AIM complexing affected binding of sIgM to the Fc$\alpha\mu$R but not to complement receptors, the antigen-presenting function of FDC is greatly affected by the nature of the sIgM–antigen complexes. Secreted IgM–antigen complexes containing AIM mainly were tethered onto the FDC surface via binding to the complement receptors, while those lacking AIM bound to the Fc$\alpha\mu$R and were internalized for processing and presentation on MHCII.

Despite these notable effects of the Fc$\alpha\mu$R concentrations of virus-specific serum IgG in *Fcamr-/-* mice infected with influenza virus were similar to those of wild-type mice, indicating that regulation B cell responses by sIgM were independent of the Fc$\alpha\mu$R.[8] This finding was supported by studies in AIM-/- mice that showed no difference in germinal center formation following immunization. Instead, studies in these mice suggested that by removing natural IgM-autoantigen complexes, the Fc$\alpha\mu$R facilitates the previously observed sIgM-mediated suppressive effects on IgG autoantibody generation and autoimmune disease, a process that is enhanced in the

absence of AIM.[121] Taken together, current evidence suggests an important role for sIgM– Fc$\alpha\mu$R interaction in the regulation of immune homeostasis by the FDC.

Polymeric Immunoglobulin Receptor

The polymeric immunoglobulin receptor (pIgR) is a highly conserved glycosylated receptor of about 81 kDa that is expressed principally by mucosal epithelial cells. The receptor binds both, dimeric IgA as well as pentameric sIgM via recognition of the J-chain.[115,127–130] The main function of the pIgR appears to be linked to the transepithelial trans- port of dimeric IgA, generated by plasma cells in the mucosal lamina propria, across the epithelial cell layer. This is followed by exocytosis into the lumen of mucosal tissues following cleavage of the pIgR, causing the retention of a small piece of the pIgR as “secretory component” on the sIgA. Although sIgM can bind to and be transported by the pIgR, mucosal tissues of mice usually contain much higher frequencies of IgA-compared to IgM-secreting plasma cells and thus effects of pIgR deficiencies measured in mice are mostly on homeostasis of IgA rather than sIgM.[129,131] However, as outlined above, sIgM-secreting plasma cells appear to be more numerous in humans compared to mice and thus it is possible that the pIgR plays a larger role in the transport of sIgM onto the mucosal surfaces than indicated by studies on mice.

FcμR (Faim3/TOSO)

The FcμR, a 60-kDa transmembrane protein, was originally identified as "Fas apoptosis inhibitory molecule 3" (FAIM3 or TOSO), as its expression in Jurkat T cells prevented Fas (CD95)-mediated apoptosis induced by an anti-Fas antibody.[132,133] Later studies identified the same surface protein as a sIgM-binding receptor on the surface of human and mouse B cells. While the receptor's ability to bind sIgM has been repeatedly demonstrated, the originally reported antiapoptotic function of this molecule appeared to have been due to the use of an anti-Fas antibody of the IgM isotype, as the antiapoptotic activity was not seen with an IgG anti-Fas antibody.[113,134] Although further studies are required to resolve some of the apparent discordant data, these findings have since led to the proposal to rename this gene "FCMR".[113,135]

In humans, the FCMR is located on chromosome 1q32.2, adjacent to the *PIGR* and the *FCAMR.*[113,125] The FCMR shares sequence homology with those receptors, further supporting its function as an Ig-binding protein, although it is more distantly related than the PIGR and FCAMR are related to each other.[113] A splice variant of the FcμR lacking the transmembrane exon seems to encode a soluble form of the receptor. It has been proposed that the soluble receptor serves as a "decoy" for sIgM-interaction with cell[113,136]; however, more follow-up studies are required to confirm these findings and their biological significance. The FcμR is a high-affinity sIgM receptor, binding to IgM mainly via the Cμ4 domain and independent of the J-chain. This explains why the FcμR can bind both, monomeric IgM and pentameric sIgM,

although binding to pentameric IgM occurs with higher affinity.[51,113,122,137,138] In both, humans and mice, expression of the FcμR is strongest on B cells, where it can be readily visualized by flow cytometry. In addition, low expression has also been observed on granulocytes, macrophages, and dendritic cells in mice. In humans, the receptor was shown to be expressed on T and NK cells, but not on myeloid cells.[7,8,22,125,134,137–141] Expression on human T cells was higher on $\alpha\beta$T cells than $\gamma\delta$ T cells, and higher on CD4+ than on CD8+ T cells.[125] It will be important to understand the functional significance of these expression differences between mice and humans.

On murine B cells, *Fcmr* expression is induced first after the pre-B cell stage in the bone marrow.[7,8,134,140] The FcμR is rapidly upregulated in immature B cells, thus at the time the fully rear- ranged IgM is first being generated and cells are undergoing negative selection. Here the receptor is found at high levels colocalized with IgM in the Golgi transport network and to a lesser extent on the cell surface.[7,8] The FcμR was shown to inhibit the transport and expression of the IgM–BCR onto the cell surface, such that B cells lacking the FcμR express about 30% higher levels of surface IgM–BCR, while IgD–BCR levels were unchanged.[8] This explains why in chronic lymphocytic leukemia (CLL), where the FcμR is highly expressed, surface expression of IgM–BCR is low.[125,141,142] While the process that inhibits BCR–IgM transport to the cell surface remains to be fully revealed, the outcome of this enhanced IgM–BCR expression was linked to changes in B cell selection.[8] The data provide a potential mechanistic explanation for the increases in autoantibody production seen by multiple investigators in FcμR knock out

mice.[7,140,143] Furthermore, they explain the increased activation and terminal differentiation of B-1 cells, resulting in significantly increased frequencies of B-1 derived IgM-plasma cells in spleen and bone marrow with concomitant increases in serum sIgM levels in these mice.[8]

On resting peripheral B cells, the FcμR is expressed mainly on the cell surface, at least some colocalized with IgM–BCR.[8,134,140] Some modest gene expression differences were observed between B-1, MZ B and follicular B cells,[7,8] but the functional significance of these differences is unclear. As stated above, in CLL the FcμR is strongly expressed, possibly linked to the chronic activation of these cells through BCR- mediated signaling, which was shown to increase FcμR expression.[142] Stimulation through TLR, CD40L, and IL-4 strongly inhibited FcμR expression in normal human B cells, as well as in CLL,[113,141,142,144] consistent with the loss of FcμR expression among germinal center B cells.[7] The FcμR appears to be re-expressed on more differentiated cells, however, as it was found on IgG^+ and IgA^+ memory B cells and $CD138^+$ plasma cells in spleen and lymph nodes, as well as on a subset of CD138+ bone marrow plasma cells.[125,134] This dynamic up and downregulation of FcμR surface expression suggests differentiation-stage specific functional consequences following FcμR engagement. Using Ig-allotype-disparate B cells, we were able to differentiate sIgM binding from IgM–BCR surface expression and showed constitutive binding of sIgM onto the cell surface of B cells in vivo, which was reduced in the absence of the FcμR.[8] Studies in transfected HeLa cells, as well as primary mouse B cells, showed that sIgM binding to surface-expressed FcμR caused the rapid internalization and degradation of the complex through the

endocytic pathway,[115,139,141] a process that in CLL was shown to depend on the state of FcμR glycosylation.[141] Interestingly, some sIgM uptake was shown to occur also in the absence of the FcμR, suggesting that not all sIgM internalization is mediated by the FcμR.[115,139] Recent studies showed rapid FcμR -mediated sIgM internalization by human CD4 T cells.[145] The internalization triggered a positive feed-forward mechanism resulting in increased FcμR expression as well as upregulation of the TCR and costimulatory molecules. This, in turn, triggered increased T cell responses after low-, but not high-dose stimulation.[145] The data provide an intriguing mechanism by which early production of antigen-specific sIgM in secondary lymphoid tissues could facilitate uptake by T cells, enhancing their responses. Presumably, such enhancement could not replace T cell priming, but rather enhance already primed and activated T cells, independent of their specificity. It is unclear how the uptake of IgM and/or antigen may affect T cell responses, other than through signaling through the FcμR. In the steady state, however, most if not all sIgM is natural, self-reactive. Its continued uptake presumably contributes to immune quiescence and enforcement of T cell tolerance rather than immune activation. Studies showing that the lack of the FcμR causes increased autoantibody formation over time, like the changes seen in mice lacking sIgM[4,90,92] may suggest additional mechanisms by which FcμR/sIgM interactions contribute to immune homeostasis.

Thus, the FcμR seems to serve multiple functions in the steady state: maintaining appropriate IgM–BCR expression levels in development, preventing the overshooting activation of self-reactive B cells, specifically B-1, and preventing the development of autoimmune antibody-mediated diseases. Following foreign antigen expo- sure,

depending on the antigen dose, the FcμR may modify the strength of the B cell response directly by binding to B cells and, at least in humans, also indirectly by enhancing T cell responses. The fact that both, enhancing and suppressive effects of FcμR expression have been reported on the humoral response to T-independent and T-dependent antigens,[7,8,122,140] suggests the potential of additional mechanisms of regulation that are antigen-type, dose, and cell subset specific. The dys-regulation of surface IgM–BCR expression in FcμR -/- mice remains to be fully considered for its potential effects, however, as it may con- tribute to the observed effects on immune response development in the absence of the FcμR.

Concluding Remarks

The identification of the FcμR as a bona fide receptor for sIgM and the identification of sIgM as a transport molecule for AIM have increased our ability to further resolve the complex functions of sIgM, a structurally and functionally unique, yet highly evolutionary conserved immunoglobulin that support immune homeostasis and immune defense. The functions of sIgM are intimately linked to the functions of natural IgM-secreting B-1 cells and perhaps distinguishable from the early burst of sIgM produced in response to an insult or infection by B-1 and B-2 cells. Further clarity may come from beginning to distinguish the source of the sIgM as much as the cell types with which the molecule interacts in each situation. The limited tissue penetrability of sIgM and its ability to act as a Trojan horse carrying and increasing the half-life and thus availability of an effector protein in the blood offer some potential exciting future therapeutic intervention strategies.

References

Alugupalli, K. R., Leong, J. M., Woodland, R. T., Muramatsu, M., Honjo, T., & Gerstein, R. M. (2004). B1b lymphocytes confer T cell-independent long-lasting immunity. *Immunity, 21*(3), 379-390. doi:10.1016/j.immuni.2004.06.019

Anelli, T., & van Anken, E. (2013). Missing links in antibody assembly control. *Int J Cell Biol, 2013*, 606703. doi:10.1155/2013/606703

Appelgren, D., Eriksson, P., Ernerudh, J., & Segelmark, M. (2018). Marginal-Zone B-Cells Are Main Producers of IgM in Humans, and Are Reduced in Patients With Autoimmune Vasculitis. *Front Immunol, 9*, 2242. doi:10.3389/fimmu.2018.02242

Arai, S., Maehara, N., Iwamura, Y., Honda, S., Nakashima, K., Kai, T., . . . Miyazaki, T. (2013). Obesity-associated autoantibody production requires AIM to retain the immunoglobulin M immune complex on follicular dendritic cells. *Cell Rep, 3*(4), 1187-1198. doi:10.1016/j.celrep.2013.03.006

Arai, S., Shelton, J. M., Chen, M., Bradley, M. N., Castrillo, A., Bookout, A. L., . . . Miyazaki, T. (2005). A role for the apoptosis inhibitory factor AIM/Spalpha/Api6 in atherosclerosis development. *Cell Metab, 1*(3), 201-213. doi:10.1016/j.cmet.2005.02.002

Arnold, J. N., Wormald, M. R., Sim, R. B., Rudd, P. M., & Dwek, R. A. (2007). The impact of glycosylation on the biological function and structure of human

immunoglobulins. *Annu Rev Immunol, 25*, 21-50. doi:10.1146/annurev.immunol.25.022106.141702

Asano, M., & Komiyama, K. (2011). Polymeric immunoglobulin receptor. *J Oral Sci, 53*(2), 147-156.

Baumgarth, N. (2011). The double life of a B-1 cell: self-reactivity selects for protective effector functions. *Nat Rev Immunol, 11*(1), 34-46. doi:10.1038/nri2901

Baumgarth, N. (2016). B-1 Cell Heterogeneity and the Regulation of Natural and Antigen-Induced IgM Production. *Front Immunol, 7*, 324. doi:10.3389/fimmu.2016.00324

Baumgarth, N., Herman, O. C., Jager, G. C., Brown, L. E., Herzenberg, L. A., & Chen, J. (2000). B-1 and B-2 cell-derived immunoglobulin M antibodies are nonredundant components of the protective response to influenza virus infection. *J Exp Med, 192*(2), 271-280.

Baumgarth, N., Jager, G. C., Herman, O. C., Herzenberg, L. A., & Herzenberg, L. A. (2000). CD4⁺ T cells derived from B cell-deficient mice inhibit the establishment of peripheral B cell pools. *Proceedings of the National Academy of Sciences, 97*(9), 4766-4771. doi:10.1073/pnas.97.9.4766

Baumgarth, N., Tung, J. W., & Herzenberg, L. A. (2005). Inherent specificities in natural antibodies: a key to immune defense against pathogen invasion. *Springer Semin Immunopathol, 26*(4), 347-362. doi:10.1007/s00281-004-0182-2

Behring, E. v. (1890a). Über das zustandekommen der diphtherie-immunität und der tetanus-immunität bei thieren.

Behring, E. v. (1890b). Untersuchungen über das Zustandekommen der Diphtherie-Immunität bei Thieren.

Binder, C. J., Horkko, S., Dewan, A., Chang, M. K., Kieu, E. P., Goodyear, C. S., . . . Silverman, G. J. (2003). Pneumococcal vaccination decreases atherosclerotic lesion formation: molecular mimicry between Streptococcus pneumoniae and oxidized LDL. *Nat Med, 9*(6), 736-743. doi:10.1038/nm876

Binder, C. J., & Silverman, G. J. (2005). Natural antibodies and the autoimmunity of atherosclerosis. *Springer Seminars in Immunopathology, 26*(4), 385-404. doi:10.1007/s00281-004-0185-z

Black, C. A. (1997). A brief history of the discovery of the immunoglobulins and the origin of the modern immunoglobulin nomenclature. *Immunol Cell Biol, 75*(1), 65-68. doi:10.1038/icb.1997.10

Boes, M., Esau, C., Fischer, M. B., Schmidt, T., Carroll, M., & Chen, J. (1998). Enhanced B-1 cell development, but impaired IgG antibody responses in mice deficient in secreted IgM. *J Immunol, 160*(10), 4776-4787.

Boyden, S. V. (1966). Natural antibodies and the immune response. *Adv Immunol, 5*, 1-28.

Brekke, O. H., & Sandlie, I. (2003). Therapeutic antibodies for human diseases at the dawn of the twenty-first century. *Nature Reviews Drug Discovery, 2*, 52. doi:10.1038/nrd984

Casali, P. (1998). IgM. In P. J. Delves (Ed.), *Encyclopedia of Immunology (Second Edition)* (pp. 1212-1217). Oxford: Elsevier.

Choi, J. G., Lee, Y. J., Kim, Y. J., Lee, E. K., Jeong, O. M., Sung, H. W., . . . Kwon, J. H. (2008). An inactivated vaccine to control the current H9N2 low pathogenic avian influenza in Korea. *J Vet Sci, 9*(1), 67-74.

Choi, S. C., Wang, H., Tian, L., Murakami, Y., Shin, D. M., Borrego, F., . . . Coligan, J. E. (2013). Mouse IgM Fc receptor, FCMR, promotes B cell development and modulates antigen-driven immune responses. *J Immunol, 190*(3), 987-996. doi:10.4049/jimmunol.1202227

Choi, Y. S., Dieter, J. A., Rothaeusler, K., Luo, Z., & Baumgarth, N. (2012). B-1 cells in the bone marrow are a significant source of natural IgM. *Eur J Immunol, 42*(1), 120-129. doi:10.1002/eji.201141890

Cinamon, G., Zachariah, M. A., Lam, O. M., Foss, F. W., Jr., & Cyster, J. G. (2008). Follicular shuttling of marginal zone B cells facilitates antigen transport. *Nat Immunol, 9*(1), 54-62. doi:10.1038/ni1542

Cohen, S. (1965). Nomenclature of Human Immunoglobulins. *Immunology, 8*, 1-5.

Colombo, M. J., Abraham, D., Shibuya, A., & Alugupalli, K. R. (2011). B1b lymphocyte-derived antibodies control Borrelia hermsii independent of Fcalpha/mu receptor and in the absence of host cell contact. *Immunol Res, 51*(2-3), 249-256. doi:10.1007/s12026-011-8260-8

Colucci, M., Stockmann, H., Butera, A., Masotti, A., Baldassarre, A., Giorda, E., . . . Vivarelli, M. (2015). Sialylation of N-linked glycans influences the

immunomodulatory effects of IgM on T cells. *J Immunol, 194*(1), 151-157. doi:10.4049/jimmunol.1402025

Crist, E., & Tauber, A. I. (1997). Debating humoral immunity and epistemology: the rivalry of the immunochemists Jules Bordet and Paul Ehrlich. *J Hist Biol, 30*(3), 321-356.

Czajkowsky, D. M., & Shao, Z. (2009). The human IgM pentamer is a mushroom-shaped molecule with a flexural bias. *Proc Natl Acad Sci U S A, 106*(35), 14960-14965. doi:10.1073/pnas.0903805106

Donius, L. R., Handy, J. M., Weis, J. J., & Weis, J. H. (2013). Optimal germinal center B cell activation and T-dependent antibody responses require expression of the mouse complement receptor Cr1. *J Immunol, 191*(1), 434-447. doi:10.4049/jimmunol.1203176

Ehrenstein, M. R., Cook, H. T., & Neuberger, M. S. (2000). Deficiency in serum immunoglobulin (Ig)M predisposes to development of IgG autoantibodies. *J Exp Med, 191*(7), 1253-1258.

Ehrenstein, M. R., & Notley, C. A. (2010). The importance of natural IgM: scavenger, protector and regulator. *Nat Rev Immunol, 10*(11), 778-786. doi:10.1038/nri2849

Fehr, T., Naim, H. Y., Bachmann, M. F., Ochsenbein, A. F., Spielhofer, P., Bucher, E., . . . Zinkernagel, R. M. (1998). T-cell independent IgM and enduring protective IgG antibodies induced by chimeric measles viruses. *Nat Med, 4*(8), 945-948.

Feinstein, A., & Munn, E. A. (1969). Conformation of the free and antigen-bound IgM antibody molecules. *Nature, 224*(5226), 1307-1309.

Flajnik, M. F. (2002). Comparative analyses of immunoglobulin genes: surprises and portents. *Nat Rev Immunol, 2*(9), 688-698. doi:10.1038/nri889

Forster, I., & Rajewsky, K. (1987). Expansion and functional activity of Ly-1+ B cells upon transfer of peritoneal cells into allotype-congenic, newborn mice. *Eur J Immunol, 17*(4), 521-528. doi:10.1002/eji.1830170414

Frenzel, A., Labi, V., Chmelewskij, W., Ploner, C., Geley, S., Fiegl, H., . . . Villunger, A. (2010). Suppression of B-cell lymphomagenesis by the BH3-only proteins Bmf and Bad. *Blood, 115*(5), 995-1005. doi:10.1182/blood-2009-03-212670

Furth, R. (1965). *THE IMMUNOLOGICAL DEVELOPMENT OF THE HUMAN FETUS* (Vol. 122).

Gil-Cruz, C., Bobat, S., Marshall, J. L., Kingsley, R. A., Ross, E. A., Henderson, I. R., . . . Cunningham, A. F. (2009). The porin OmpD from nontyphoidal Salmonella is a key target for a protective B1b cell antibody response. *Proceedings of the National Academy of Sciences, 106*(24), 9803-9808. doi:10.1073/pnas.0812431106

Graf, R., Seagal, J., Otipoby, K. L., Lam, K. P., Ayoub, S., Zhang, B., . . . Rajewsky, K. (2019). BCR-dependent lineage plasticity in mature B cells. *Science, 363*(6428), 748-753. doi:10.1126/science.aau8475

Gronwall, C., & Silverman, G. J. (2014). Natural IgM: beneficial autoantibodies for the control of inflammatory and autoimmune disease. *J Clin Immunol, 34 Suppl 1*, S12-21. doi:10.1007/s10875-014-0025-4

Gronwall, C., Vas, J., & Silverman, G. J. (2012). Protective Roles of Natural IgM Antibodies. *Front Immunol, 3*, 66. doi:10.3389/fimmu.2012.00066

Gunti, S., & Notkins, A. L. (2015). Polyreactive Antibodies: Function and Quantification. *J Infect Dis, 212 Suppl 1*, S42-46. doi:10.1093/infdis/jiu512

Gupta, S., & Gupta, A. (2017). Selective IgM Deficiency-An Underestimated Primary Immunodeficiency. *Front Immunol, 8*, 1056. doi:10.3389/fimmu.2017.01056

Haaijman, J. J., Slingerland-Teunissen, J., Benner, R., & Van Oudenaren, A. (1979). The distribution of cytoplasmic immunoglobulin containing cells over various lymphoid organs of congenitally athymic (nude) mice as a function of age. *Immunology, 36*(2), 271-278.

Haas, K. M., Poe, J. C., Steeber, D. A., & Tedder, T. F. (2005). B-1a and B-1b cells exhibit distinct developmental requirements and have unique functional roles in innate and adaptive immunity to S. pneumoniae. *Immunity, 23*(1), 7-18. doi:10.1016/j.immuni.2005.04.011

Halperin, J. J., Baker, P., & Wormser, G. P. (2013). Common misconceptions about Lyme disease. *Am J Med, 126*(3), 264 e261-267. doi:10.1016/j.amjmed.2012.10.008

Hammers-Berggren, S., Hansen, K., Lebech, A. M., & Karlsson, M. (1993). Borrelia burgdorferi-specific intrathecal antibody production in neuroborreliosis: a follow-up study. *Neurology, 43*(1), 169-175. doi:10.1212/wnl.43.1_part_1.169

Haury, M., Sundblad, A., Grandien, A., Barreau, C., Coutinho, A., & Nobrega, A. (1997). The repertoire of serum IgM in normal mice is largely independent of

external antigenic contact. *Eur J Immunol, 27*(6), 1557-1563. doi:10.1002/eji.1830270635

Hayakawa, K., Asano, M., Shinton, S. A., Gui, M., Allman, D., Stewart, C. L., . . . Hardy, R. R. (1999). Positive selection of natural autoreactive B cells. *Science, 285*(5424), 113-116.

Heidelberger, M., & Pedersen, K. O. (1937). The Molecular Weight of Antibodies. *J Exp Med, 65*(3), 393-414.

Henry, C., & Jerne, N. K. (1968). Competition of 19S and 7S antigen receptors in the regulation of the primary immune response. *J Exp Med, 128*(1), 133-152. doi:10.1084/jem.128.1.133

Heyman, B., Pilstrom, L., & Shulman, M. J. (1988). Complement activation is required for IgM-mediated enhancement of the antibody response. *J Exp Med, 167*(6), 1999-2004.

Hiramoto, E., Tsutsumi, A., Suzuki, R., Matsuoka, S., Arai, S., Kikkawa, M., & Miyazaki, T. (2018). The IgM pentamer is an asymmetric pentagon with an open groove that binds the AIM protein. *Sci Adv, 4*(10), eaau1199. doi:10.1126/sciadv.aau1199

Hitoshi, Y., Lorens, J., Kitada, S. I., Fisher, J., LaBarge, M., Ring, H. Z., . . . Nolan, G. P. (1998). Toso, a cell surface, specific regulator of Fas-induced apoptosis in T cells. *Immunity, 8*(4), 461-471.

Honda, S., Kurita, N., Miyamoto, A., Cho, Y., Usui, K., Takeshita, K., . . . Shibuya, A. (2009). Enhanced humoral immune responses against T-independent

antigens in Fc alpha/muR-deficient mice. *Proc Natl Acad Sci U S A, 106*(27), 11230-11235. doi:10.1073/pnas.0809917106

Honjo, K., Kubagawa, Y., Jones, D. M., Dizon, B., Zhu, Z., Ohno, H., . . . Kubagawa, H. (2012). Altered Ig levels and antibody responses in mice deficient for the Fc receptor for IgM (FcmuR). *Proc Natl Acad Sci U S A, 109*(39), 15882-15887. doi:10.1073/pnas.1206567109

Honjo, K., Kubagawa, Y., Suzuki, Y., Takagi, M., Ohno, H., Bucy, R. P., . . . Kubagawa, H. (2014). Enhanced auto-antibody production and Mott cell formation in FcmuR-deficient autoimmune mice. *Int Immunol, 26*(12), 659-672. doi:10.1093/intimm/dxu070

Hooijkaas, H., Benner, R., Pleasants, J. R., & Wostmann, B. S. (1984). Isotypes and specificities of immunoglobulins produced by germ-free mice fed chemically defined ultrafiltered "antigen-free" diet. *Eur J Immunol, 14*(12), 1127-1130. doi:10.1002/eji.1830141212

Hooper, J. A. (2015). The history and evolution of immunoglobulin products and their clinical indications. *LymphoSign Journal, 2*(4), 181-194. doi:10.14785/lpsn-2014-0025

Hosseini, H., Li, Y., Kanellakis, P., Tay, C., Cao, A., Tipping, P., . . . Kyaw, T. (2015). Phosphatidylserine liposomes mimic apoptotic cells to attenuate atherosclerosis by expanding polyreactive IgM producing B1a lymphocytes. *Cardiovascular Research, 106*(3), 443-452. doi:10.1093/cvr/cvv037

Hosseini, H., Yi, L., Kanellakis, P., Cao, A., Tay, C., Peter, K., . . . Kyaw, T. (2018). Anti-TIM-1 Monoclonal Antibody (RMT1-10) Attenuates Atherosclerosis By

Expanding IgM-producing B1a Cells. *J Am Heart Assoc, 7*(13). doi:10.1161/JAHA.117.008447

Hughey, C. T., Brewer, J. W., Colosia, A. D., Rosse, W. F., & Corley, R. B. (1998). Production of IgM hexamers by normal and autoimmune B cells: implications for the physiologic role of hexameric IgM. *J Immunol, 161*(8), 4091-4097.

Ichikawa, D., Asano, M., Shinton, S. A., Brill-Dashoff, J., Formica, A. M., Velcich, A., . . . Hayakawa, K. (2015). Natural anti-intestinal goblet cell autoantibody production from marginal zone B cells. *J Immunol, 194*(2), 606-614. doi:10.4049/jimmunol.1402383

Jayasekera, J. P., Moseman, E. A., & Carroll, M. C. (2007). Natural antibody and complement mediate neutralization of influenza virus in the absence of prior immunity. *J Virol, 81*(7), 3487-3494. doi:10.1128/JVI.02128-06

Jones, D. D., DeIulio, G. A., & Winslow, G. M. (2012). Antigen-driven induction of polyreactive IgM during intracellular bacterial infection. *J Immunol, 189*(3), 1440-1447. doi:10.4049/jimmunol.1200878

Jones, D. D., Jones, M., DeIulio, G. A., Racine, R., MacNamara, K. C., & Winslow, G. M. (2013). B cell activating factor inhibition impairs bacterial immunity by reducing T cell-independent IgM secretion. *Infect Immun, 81*(12), 4490-4497. doi:10.1128/IAI.00998-13

Jones, P. D., & Ada, G. L. (1986). Influenza virus-specific antibody-secreting cells in the murine lung during primary influenza virus infection. *J Virol, 60*(2), 614-619.

Kalish, R. A., McHugh, G., Granquist, J., Shea, B., Ruthazer, R., & Steere, A. C. (2001). Persistence of immunoglobulin M or immunoglobulin G antibody responses to Borrelia burgdorferi 10-20 years after active Lyme disease. *Clin Infect Dis, 33*(6), 780-785. doi:10.1086/322669

Kantha, S. S. (1991). A centennial review; the 1890 tetanus antitoxin paper of von Behring and Kitasato and the related developments. *Keio J Med, 40*(1), 35-39.

Kawano, M., & Nagata, S. (2018). Efferocytosis and autoimmune disease. *Int Immunol, 30*(12), 551-558. doi:10.1093/intimm/dxy055

Klimovich, V. B. (2011). IgM and its receptors: structural and functional aspects. *Biochemistry (Mosc), 76*(5), 534-549. doi:10.1134/S0006297911050038

Koyama, N., Yamazaki, T., Kanetsuki, Y., Hirota, J., Asai, T., Mitsumoto, Y., . . . Okanoue, T. (2018). Activation of apoptosis inhibitor of macrophage is a sensitive diagnostic marker for NASH-associated hepatocellular carcinoma. *J Gastroenterol, 53*(6), 770-779. doi:10.1007/s00535-017-1398-y

Kranich, J., & Krautler, N. J. (2016). How Follicular Dendritic Cells Shape the B-Cell Antigenome. *Frontiers in Immunology, 7*(225). doi:10.3389/fimmu.2016.00225

Kubagawa, H., Carroll, M. C., Jacob, C. O., Lang, K. S., Lee, K. H., Mak, T., . . . Coligan, J. E. (2015). Nomenclature of Toso, Fas apoptosis inhibitory molecule 3, and IgM FcR. *J Immunol, 194*(9), 4055-4057. doi:10.4049/jimmunol.1500222

Kubagawa, H., Kubagawa, Y., Jones, D., Nasti, T. H., Walter, M. R., & Honjo, K. (2014). The old but new IgM Fc receptor (FcmuR). *Curr Top Microbiol Immunol, 382*, 3-28. doi:10.1007/978-3-319-07911-0_1

Kubagawa, H., Oka, S., Kubagawa, Y., Torii, I., Takayama, E., Kang, D. W., . . . Wang, J. Y. (2009). Identity of the elusive IgM Fc receptor (FcmuR) in humans. *J Exp Med, 206*(12), 2779-2793. doi:10.1084/jem.20091107

Kubagawa, H., Oka, S., Kubagawa, Y., Torii, I., Takayama, E., Kang, D. W., . . . Honjo, K. (2014). The long elusive IgM Fc receptor, FcmuR. *J Clin Immunol, 34 Suppl 1*, S35-45. doi:10.1007/s10875-014-0022-7

Kubagawa, H., Skopnik, C. M., Zimmermann, J., Durek, P., Chang, H. D., Yoo, E., . . . Radbruch, A. (2017). Authentic IgM Fc Receptor (FcmuR). *Curr Top Microbiol Immunol, 408*, 25-45. doi:10.1007/82_2017_23

Kushnir, N., Bos, N. A., Zuercher, A. W., Coffin, S. E., Moser, C. A., Offit, P. A., & Cebra, J. J. (2001). B2 but Not B1 Cells Can Contribute to CD4⁺ T-Cell-Mediated Clearance of Rotavirus in SCID Mice. *Journal of Virology, 75*(12), 5482-5490. doi:10.1128/jvi.75.12.5482-5490.2001

Kyaw, T., Tipping, P., Bobik, A., & Toh, B.-H. (2012). Protective role of natural IgM-producing B1a cells in atherosclerosis. *Trends in cardiovascular medicine, 22*(2), 48-53.

Lalor, P. A., Herzenberg, L. A., Adams, S., & Stall, A. M. (1989). Feedback regulation of murine Ly-1 B cell development. *European Journal of Immunology, 19*(3), 507-513. doi:10.1002/eji.1830190315

Lleo, A., Selmi, C., Invernizzi, P., Podda, M., & Gershwin, M. E. (2008). The consequences of apoptosis in autoimmunity. *J Autoimmun, 31*(3), 257-262. doi:10.1016/j.jaut.2008.04.009

Lloyd, K. A., Wang, J., Urban, B. C., Czajkowsky, D. M., & Pleass, R. J. (2017). Glycan-independent binding and internalization of human IgM to FCMR, its cognate cellular receptor. *Sci Rep, 7*, 42989. doi:10.1038/srep42989

Lobo, P. I. (2016). Role of Natural Autoantibodies and Natural IgM Anti-Leucocyte Autoantibodies in Health and Disease. *Front Immunol, 7*, 198. doi:10.3389/fimmu.2016.00198

Magri, G., Comerma, L., Pybus, M., Sintes, J., Lligé, D., Segura-Garzón, D., . . . Cerutti, A. (2017). Human Secretory IgM Emerges from Plasma Cells Clonally Related to Gut Memory B Cells and Targets Highly Diverse Commensals. *Immunity, 47*(1), 118-134.e118. doi:10.1016/j.immuni.2017.06.013

Meryk, A., Pangrazzi, L., Hagen, M., Hatzmann, F., Jenewein, B., Jakic, B., . . . Grubeck-Loebenstein, B. (2019). Fcmu receptor as a Costimulatory Molecule for T Cells. *Cell Rep, 26*(10), 2681-2691 e2685. doi:10.1016/j.celrep.2019.02.024

Miyazaki, T., Hirokami, Y., Matsuhashi, N., Takatsuka, H., & Naito, M. (1999). Increased Susceptibility of Thymocytes to Apoptosis in Mice Lacking AIM, a Novel Murine Macrophage-derived Soluble Factor Belonging to the Scavenger Receptor Cysteine-rich Domain Superfamily. *The Journal of Experimental Medicine, 189*(2), 413-422. doi:10.1084/jem.189.2.413

Miyazaki, T., Yamazaki, T., Sugisawa, R., Gershwin, M. E., & Arai, S. (2018). AIM associated with the IgM pentamer: attackers on stand-by at aircraft carrier. *Cell Mol Immunol, 15*(6), 563-574. doi:10.1038/cmi.2017.141

Moh, E. S., Lin, C. H., Thaysen-Andersen, M., & Packer, N. H. (2016). Site-Specific N-Glycosylation of Recombinant Pentameric and Hexameric Human IgM. *J Am Soc Mass Spectrom, 27*(7), 1143-1155. doi:10.1007/s13361-016-1378-0

Murakami, Y., Narayanan, S., Su, S., Childs, R., Krzewski, K., Borrego, F., . . . Coligan, J. E. (2012). Toso, a functional IgM receptor, is regulated by IL-2 in T and NK cells. *J Immunol, 189*(2), 587-597. doi:10.4049/jimmunol.1200840

Murray, K. O., Garcia, M. N., Yan, C., & Gorchakov, R. (2013). Persistence of detectable immunoglobulin M antibodies up to 8 years after infection with West Nile virus. *Am J Trop Med Hyg, 89*(5), 996-1000. doi:10.4269/ajtmh.13-0232

Nguyen, T. T., & Baumgarth, N. (2016). Natural IgM and the Development of B Cell-Mediated Autoimmune Diseases. *Crit Rev Immunol, 36*(2), 163-177. doi:10.1615/CritRevImmunol.2016018175

Nguyen, T. T., Elsner, R. A., & Baumgarth, N. (2015). Natural IgM prevents autoimmunity by enforcing B cell central tolerance induction. *J Immunol, 194*(4), 1489-1502. doi:10.4049/jimmunol.1401880

Nguyen, T. T., Klasener, K., Zurn, C., Castillo, P. A., Brust-Mascher, I., Imai, D. M., . . . Baumgarth, N. (2017). The IgM receptor FcmuR limits tonic BCR signaling by regulating expression of the IgM BCR. *Nat Immunol, 18*(3), 321-333. doi:10.1038/ni.3677

Nguyen, T. T. T., Graf, B. A., Randall, T. D., & Baumgarth, N. (2017). sIgM-FcmuR Interactions Regulate Early B Cell Activation and Plasma Cell Development

after Influenza Virus Infection. *J Immunol, 199*(5), 1635-1646. doi:10.4049/jimmunol.1700560

Notley, C. A., Brown, M. A., Wright, G. P., & Ehrenstein, M. R. (2011). Natural IgM is required for suppression of inflammatory arthritis by apoptotic cells. *J Immunol, 186*(8), 4967-4972. doi:10.4049/jimmunol.1003021

Ochsenbein, A. F., Fehr, T., Lutz, C., Suter, M., Brombacher, F., Hengartner, H., & Zinkernagel, R. M. (1999). Control of early viral and bacterial distribution and disease by natural antibodies. *Science, 286*(5447), 2156-2159.

Ogden, C. A., Kowalewski, R., Peng, Y., Montenegro, V., & Elkon, K. B. (2005). IGM is required for efficient complement mediated phagocytosis of apoptotic cells in vivo. *Autoimmunity, 38*(4), 259-264.

Ouchida, R., Mori, H., Hase, K., Takatsu, H., Kurosaki, T., Tokuhisa, T., . . . Wang, J. Y. (2012). Critical role of the IgM Fc receptor in IgM homeostasis, B-cell survival, and humoral immune responses. *Proc Natl Acad Sci U S A, 109*(40), E2699-2706. doi:10.1073/pnas.1210706109

Pallasch, C. P., Schulz, A., Kutsch, N., Schwamb, J., Hagist, S., Kashkar, H., . . . Wendtner, C. M. (2008). Overexpression of TOSO in CLL is triggered by B-cell receptor signaling and associated with progressive disease. *Blood, 112*(10), 4213-4219. doi:10.1182/blood-2008-05-157255

Pape, K. A., Maul, R. W., Dileepan, T., Paustian, A. S., Gearhart, P. J., & Jenkins, M. K. (2018). Naive B Cells with High-Avidity Germline-Encoded Antigen Receptors Produce Persistent IgM(+) and Transient IgG(+) Memory B Cells. *Immunity, 48*(6), 1135-1143 e1134. doi:10.1016/j.immuni.2018.04.019

Pape, K. A., Taylor, J. J., Maul, R. W., Gearhart, P. J., & Jenkins, M. K. (2011). Different B cell populations mediate early and late memory during an endogenous immune response. *Science, 331*(6021), 1203-1207. doi:10.1126/science.1201730

Parkhouse, R. M., Askonas, B. A., & Dourmashkin, R. R. (1970). Electron microscopic studies of mouse immunoglobulin M; structure and reconstitution following reduction. *Immunology, 18*(4), 575-584.

Petrusic, V., Zivkovic, I., Stojanovic, M., Stojicevic, I., Marinkovic, E., & Dimitrijevic, L. (2011). Hexameric immunoglobulin M in humans: desired or unwanted? *Med Hypotheses, 77*(6), 959-961. doi:10.1016/j.mehy.2011.08.018

Plomp, R., Bondt, A., de Haan, N., Rombouts, Y., & Wuhrer, M. (2016). Recent Advances in Clinical Glycoproteomics of Immunoglobulins (Igs). *Mol Cell Proteomics, 15*(7), 2217-2228. doi:10.1074/mcp.O116.058503

Prohaska, T. A., Que, X., Diehl, C. J., Hendrikx, S., Chang, M. W., Jepsen, K., . . . Witztum, J. L. (2018). Massively Parallel Sequencing of Peritoneal and Splenic B Cell Repertoires Highlights Unique Properties of B-1 Cell Antibodies. *The Journal of Immunology, 200*(5), 1702-1717. doi:10.4049/jimmunol.1700568

R Ceppellini, S. D., G Edelman, J Fahey, F Franěk, E Franklin, H.C Goodman, P Grabar, A.E Gurvich, J.F Heremans, H Isliker, F Karush, E Press, Z Trnka. (1964). Nomenclature for human immunoglobulins. *Immunochemistry, 1*(3), 145-149.

Racine, R., Chatterjee, M., & Winslow, G. M. (2008). CD11c Expression Identifies a Population of Extrafollicular Antigen-Specific Splenic Plasmablasts Responsible for CD4 T-Independent Antibody Responses during Intracellular Bacterial Infection. *The Journal of Immunology, 181*(2), 1375-1385. doi:10.4049/jimmunol.181.2.1375

Racine, R., McLaughlin, M., Jones, D. D., Wittmer, S. T., MacNamara, K. C., Woodland, D. L., & Winslow, G. M. (2011). IgM Production by Bone Marrow Plasmablasts Contributes to Long-Term Protection against Intracellular Bacterial Infection. *The Journal of Immunology, 186*(2), 1011-1021. doi:10.4049/jimmunol.1002836

Reynolds, A. E., Kuraoka, M., & Kelsoe, G. (2015). Natural IgM is produced by CD5- plasma cells that occupy a distinct survival niche in bone marrow. *J Immunol, 194*(1), 231-242. doi:10.4049/jimmunol.1401203

Rothstein, T. L., Griffin, D. O., Holodick, N. E., Quach, T. D., & Kaku, H. (2013). Human B-1 cells take the stage. *Ann N Y Acad Sci, 1285*, 97-114. doi:10.1111/nyas.12137

Rowley, D., & Wardlaw, A. C. (1958). Lysis of gram-negative bacteria by serum. *J Gen Microbiol, 18*(2), 529-533. doi:10.1099/00221287-18-2-529

Rutemark, C., Alicot, E., Bergman, A., Ma, M., Getahun, A., Ellmerich, S., . . . Heyman, B. (2011). Requirement for complement in antibody responses is not explained by the classic pathway activator IgM. *Proceedings of the National Academy of Sciences, 108*(43), 17589-17590.

Rutemark, C., Bergman, A., Getahun, A., Hallgren, J., Henningsson, F., & Heyman, B. (2012). Complement receptors 1 and 2 in murine antibody responses to IgM-complexed and uncomplexed sheep erythrocytes. *PLoS One, 7*(7), e41968. doi:10.1371/journal.pone.0041968

Sakamoto, N., Shibuya, K., Shimizu, Y., Yotsumoto, K., Miyabayashi, T., Sakano, S., . . . Shibuya, A. (2001). A novel Fc receptor for IgA and IgM is expressed on both hematopoietic and non-hematopoietic tissues. *Eur J Immunol, 31*(5), 1310-1316. doi:10.1002/1521-4141(200105)31:5<1310::AID-IMMU1310>3.0.CO;2-N

Savage, H. P., Yenson, V. M., Sawhney, S. S., Mousseau, B. J., Lund, F. E., & Baumgarth, N. (2017). Blimp-1-dependent and -independent natural antibody production by B-1 and B-1-derived plasma cells. *J Exp Med, 214*(9), 2777-2794. doi:10.1084/jem.20161122

Schroeder, H. W., Jr., & Cavacini, L. (2010). Structure and function of immunoglobulins. *J Allergy Clin Immunol, 125*(2 Suppl 2), S41-52. doi:10.1016/j.jaci.2009.09.046

Shaw, P. X., Horkko, S., Chang, M. K., Curtiss, L. K., Palinski, W., Silverman, G. J., & Witztum, J. L. (2000). Natural antibodies with the T15 idiotype may act in atherosclerosis, apoptotic clearance, and protective immunity. *J Clin Invest, 105*(12), 1731-1740. doi:10.1172/JCI8472

Shibuya, A., Sakamoto, N., Shimizu, Y., Shibuya, K., Osawa, M., Hiroyama, T., . . . Nakauchi, H. (2000). Fc alpha/mu receptor mediates endocytosis of IgM-coated microbes. *Nat Immunol, 1*(5), 441-446. doi:10.1038/80886

Shima, H., Takatsu, H., Fukuda, S., Ohmae, M., Hase, K., Kubagawa, H., . . . Ohno, H. (2010). Identification of TOSO/FAIM3 as an Fc receptor for IgM. *Int Immunol, 22*(3), 149-156. doi:10.1093/intimm/dxp121

Shimada, S., Kawaguchi-Miyashita, M., Kushiro, A., Sato, T., Nanno, M., Sako, T., . . . Ohwaki, M. (1999). Generation of polymeric immunoglobulin receptor-deficient mouse with marked reduction of secretory IgA. *J Immunol, 163*(10), 5367-5373.

Sitia, R., Neuberger, M., Alberini, C., Bet, P., Fra, A., Valetti, C., . . . Milstein, C. (1990). Developmental regulation of IgM secretion: the role of the carboxy-terminal cysteine. *Cell, 60*(5), 781-790.

Song, Y., & Jacob, C. O. (2005). The mouse cell surface protein TOSO regulates Fas/Fas ligand-induced apoptosis through its binding to Fas-associated death domain. *J Biol Chem, 280*(10), 9618-9626. doi:10.1074/jbc.M413609200

Sorman, A., Zhang, L., Ding, Z., & Heyman, B. (2014). How antibodies use complement to regulate antibody responses. *Mol Immunol, 61*(2), 79-88. doi:10.1016/j.molimm.2014.06.010

Tiselius, A., & Kabat, E. A. (1939). An Electrophoretic Study of Immune Sera and Purified Antibody Preparations. *J Exp Med, 69*(1), 119-131.

Tissot, J. D., Sanchez, J. C., Vuadens, F., Scherl, A., Schifferli, J. A., Hochstrasser, D. F., . . . Duchosal, M. A. (2002). IgM are associated to Sp alpha (CD5 antigen-like). *Electrophoresis, 23*(7-8), 1203-1206. doi:10.1002/1522-2683(200204)23:7/8<1203::AID-ELPS1203>3.0.CO;2-1

Tjarnlund, A., Rodriguez, A., Cardona, P. J., Guirado, E., Ivanyi, J., Singh, M., . . . Fernandez, C. (2006). Polymeric IgR knockout mice are more susceptible to mycobacterial infections in the respiratory tract than wild-type mice. *Int Immunol, 18*(5), 807-816. doi:10.1093/intimm/dxl017

Tsiantoulas, D., Kiss, M., Bartolini-Gritti, B., Bergthaler, A., Mallat, Z., Jumaa, H., & Binder, C. J. (2017). Secreted IgM deficiency leads to increased BCR signaling that results in abnormal splenic B cell development. *Sci Rep, 7*(1), 3540. doi:10.1038/s41598-017-03688-8

Turula, H., & Wobus, C. E. (2018). The Role of the Polymeric Immunoglobulin Receptor and Secretory Immunoglobulins during Mucosal Infection and Immunity. *Viruses, 10*(5). doi:10.3390/v10050237

Ubelhart, R., Bach, M. P., Eschbach, C., Wossning, T., Reth, M., & Jumaa, H. (2010). N-linked glycosylation selectively regulates autonomous precursor BCR function. *Nat Immunol, 11*(8), 759-765. doi:10.1038/ni.1903

Vire, B., David, A., & Wiestner, A. (2011). TOSO, the Fcmicro receptor, is highly expressed on chronic lymphocytic leukemia B cells, internalizes upon IgM binding, shuttles to the lysosome, and is downregulated in response to TLR activation. *J Immunol, 187*(8), 4040-4050. doi:10.4049/jimmunol.1100532

Waffarn, E. E., Hastey, C. J., Dixit, N., Soo Choi, Y., Cherry, S., Kalinke, U., . . . Baumgarth, N. (2015). Infection-induced type I interferons activate CD11b on B-1 cells for subsequent lymph node accumulation. *Nat Commun, 6*, 8991. doi:10.1038/ncomms9991

WALDENSTRÖM, J. (1944). Incipient myelomatosis or «essential« hyperglobulinemia with fibrinogenopenia — a new syndrome? *Acta Medica Scandinavica, 117*(3-4), 216-247. doi:10.1111/j.0954-6820.1944.tb03955.x

Wallenius, G., Trautman, R., Kunkel, H. G., & Franklin, E. C. (1957). Ultracentrifugal studies of major non-lipide electrophoretic components of normal human serum. *J Biol Chem, 225*(1), 253-267.

Wang, H., Coligan, J. E., & Morse, H. C., 3rd. (2016). Emerging Functions of Natural IgM and Its Fc Receptor FCMR in Immune Homeostasis. *Front Immunol, 7*, 99. doi:10.3389/fimmu.2016.00099

Wright, J. F., Shulman, M. J., Isenman, D. E., & Painter, R. H. (1990). C1 binding by mouse IgM. The effect of abnormal glycosylation at position 402 resulting from a serine to asparagine exchange at residue 406 of the mu-chain. *J Biol Chem, 265*(18), 10506-10513.

Yang, Y., Ghosn, E. E. B., Cole, L. E., Obukhanych, T. V., Sadate-Ngatchou, P., Vogel, S. N., . . . Herzenberg, L. A. (2012). Antigen-specific memory in B-1a and its relationship to natural immunity. *Proceedings of the National Academy of Sciences, 109*(14), 5388-5393. doi:10.1073/pnas.1121627109

Yang, Y., Wang, C., Yang, Q., Kantor, A. B., Chu, H., Ghosn, E. E., . . . Herzenberg, L. A. (2015). Distinct mechanisms define murine B cell lineage immunoglobulin heavy chain (IgH) repertoires. *Elife, 4*, e09083. doi:10.7554/eLife.09083

Yel, L. (2010). Selective IgA deficiency. *J Clin Immunol, 30*(1), 10-16. doi:10.1007/s10875-009-9357-x

Zeng, Z., Surewaard, B. G. J., Wong, C. H. Y., Guettler, C., Petri, B., Burkhard, R., . . . Kubes, P. (2018). Sex-hormone-driven innate antibodies protect females and infants against EPEC infection. *Nat Immunol, 19*(10), 1100-1111. doi:10.1038/s41590-018-0211-2

Zhang, M., Austen, W. G., Chiu, I., Alicot, E. M., Hung, R., Ma, M., . . . Carroll, M. C. (2004). Identification of a specific self-reactive IgM antibody that initiates intestinal ischemia/reperfusion injury. *Proceedings of the National Academy of Sciences of the United States of America, 101*(11), 3886-3891. doi:10.1073/pnas.0400347101

Zhang, M., Takahashi, K., Alicot, E. M., Vorup-Jensen, T., Kessler, B., Thiel, S., . . . Carroll, M. C. (2006). Activation of the Lectin Pathway by Natural IgM in a Model of Ischemia/Reperfusion Injury. *The Journal of Immunology, 177*(7), 4727-4734. doi:10.4049/jimmunol.177.7.4727

Zhou, Z. H., Tzioufas, A. G., & Notkins, A. L. (2007). Properties and function of polyreactive antibodies and polyreactive antigen-binding B cells. *J Autoimmun, 29*(4), 219-228. doi:10.1016/j.jaut.2007.07.015

Table 1: Effects of IgM-deficiency on humoral immunity in mice

Biological Process	Effect of IgM deficiency	Reference
B cell subset development	Increased numbers CD5+ B-1 cells in PerC and spleen	Boes et al. 1998
	Increased numbers CD5+ CD21^{lo} CD23^{-} CD43- anergic B cells in PerC and spleen with enhanced turnover	Nguyen et al. 2015
	Reduced pre-B cell development and bone marrow B cell output	Nguyen et al. 2015
	Abnormal spleen development with increased marginal zone B cells Increased BCR signaling	Boes et al. 1998 Nguyen et al. 2015 Tsiantoulas D. et al. 2017
BCR-repertoire	Altered V_H usage in peripheral B cells	Nguyen et al. 2015
	Increased auto-antibody production: anti-dsDNA; anti-histone; ANA.	Boes et al. 2000; Ehrenstein et al. 2000 Nguyen et al. 2015
	Enhanced development of glomerulonephritis and other signs of antibody-mediated autoimmune disease	Boes et al. 2000 Ehrenstein et al. 2000
T-independent humoral immunity	No effect on total IgG, but enhanced IgG2a and reduced IgG2b responses to NP-Ficoll (1, 10 and 100 μg) immunization. Enhanced IgG 1, 2a, 2b and 3 responses to NP-Ficoll (5μg) to all IgG subclasses	Boes et al. 1998 Ehrenstein et al. 2000
T-dependent humoral immunity	Reduced IgG responses to low (1μg) but not higher (10 and 100 μg) NP-KLH immunization. Reduced IgG1 primary and secondary responses to NP-KLH (50μg). Delayed responses to NP-CG and phOx-CG immunization. Reduced affinity maturation. Normal secondary responses	Boes et al. 1998 Ehrenstein et al. 2000
	Reduced IgG1 and IgG2a responses to influenza infection Reduced IgG2a and IgG2b responses to influenza infection	Baumgarth et al. 2000; Nguyen et al. 2017 Kopf M et al. 2002

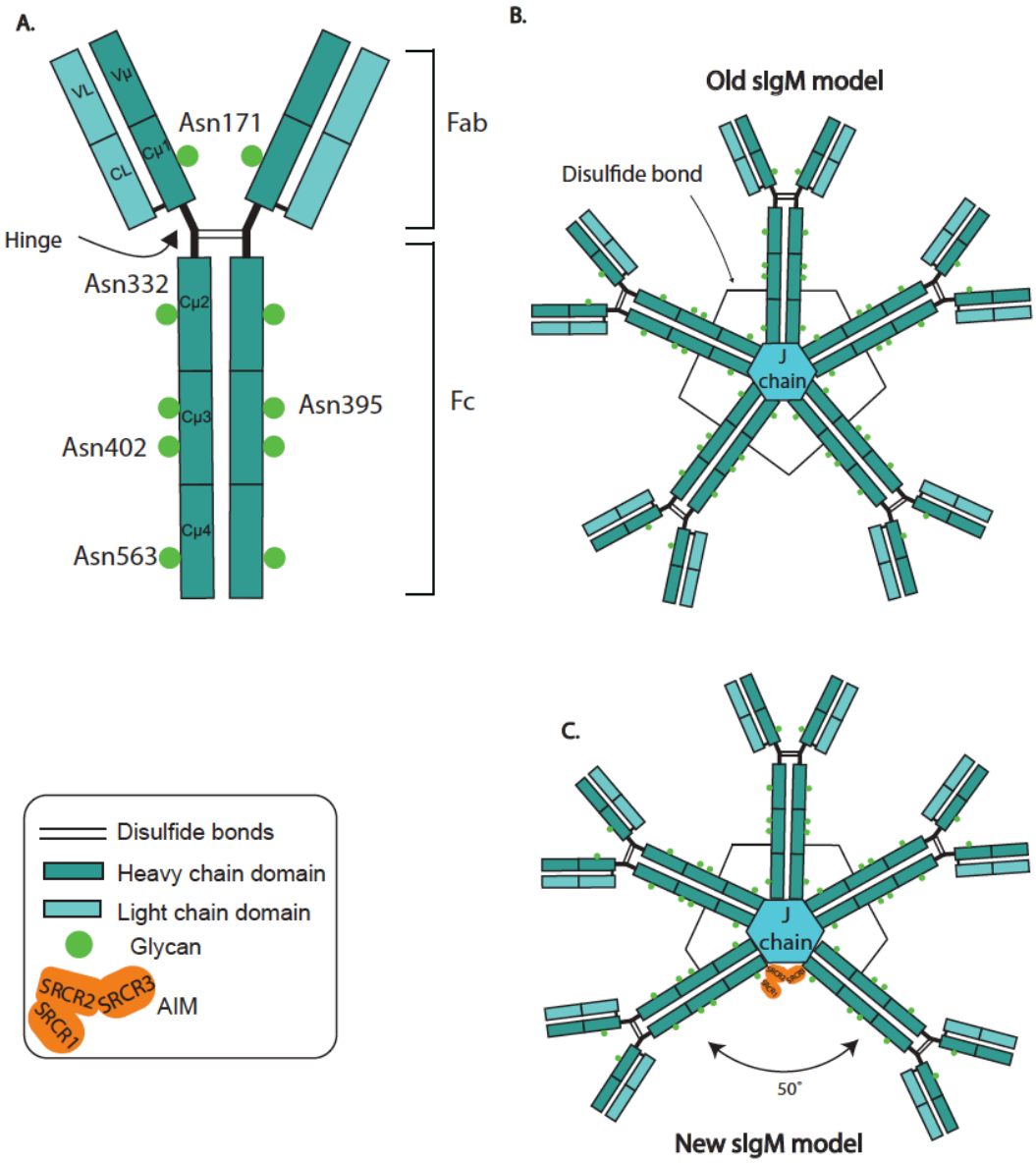
A.
VL
Vμ
CL
Cμ1
Asn171
Fab
Hinge
Asn332
Cμ2
Cμ3
Asn395
Asn402
Fc
Cμ4
Asn563
B.
Old sIgM model
Disulfide bond
J chain
C.
J chain
50°
New sIgM model
Disulfide bonds
Heavy chain domain
Light chain domain
Glycan
SRCR2
SRCR3
SRCR1
AIM

Fig. 1: Old versus new sIgM model. (A) Schematic structure of IgM monomer that possesses 2 heavy and 2 light chains. The monomer consists of a Fab region which consists of antigen binding sites and an Fc region which plays a major role in immune responses. There are 5 glycosylation sites that are attached to asparagine (Asn) on the IgM heavy chain molecule but no glycosylation sites on the light chain. (B) Classically, secreted IgM has always been thought to be a symmetric pentamer that contains a J chain. Each monomer of sIgM is linked via disulfide bonds. (C) New sIgM model that shows that sIgM is asymmetrical with a 50-degree groove that allows for 1 AIM (apoptosis inhibitor of macrophage) molecule to fit.

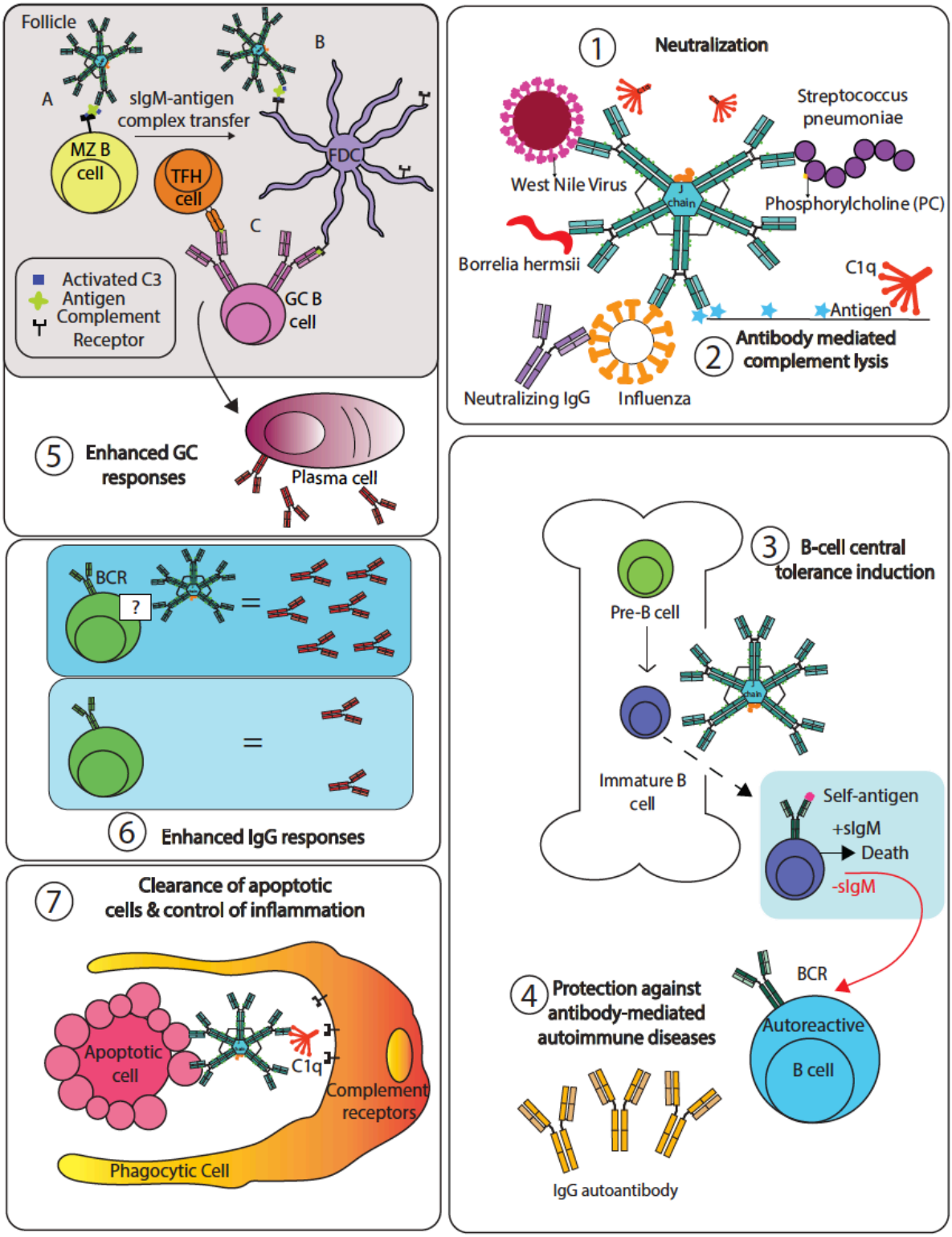
Follicle
A
B
sIgM-antigen complex transfer
MZ B cell
TFH cell
FDC
C
GC B cell
Activated C3
Antigen
Complement Receptor
5 Enhanced GC responses
Plasma cell
BCR
?
=
=
6 Enhanced IgG responses
7 Clearance of apoptotic cells & control of inflammation
Apoptotic cell
C1q
Complement receptors
Phagocytic Cell
1 Neutralization
Streptococcus pneumoniae
West Nile Virus
J chain
Phosphorylcholine (PC)
Borrelia hermsii
C1q
Antigen
2 Antibody mediated complement lysis
Neutralizing IgG
Influenza
3 B-cell central tolerance induction
Pre-B cell
Immature B cell
Self-antigen
+sIgM
Death
-sIgM
4 Protection against antibody-mediated autoimmune diseases
BCR
Autoreactive B cell
IgG autoantibody

Fig. 2: Secreted IgM functions. (1) Secreted IgM can neutralize pathogens which can subsequently block infection; either by blocking uptake into cells or causing virus particle aggregations. Natural IgM is polyreactive and can recognize homologous molecules such as phosphorylcholine (PC) present in the cell walls of *Streptococcus pneumoniae.* (2) sIgM can recruit complement components such as C5 convertase that initiates formation of the Membrane Attack Complex (MAC) that can result in lysis of the pathogen. (3) Although the mechanism is still unclear, sIgM plays an important role in central tolerance. Once the immature B cell is presented with self-antigen, if it binds too strongly- the B cell will undergo clonal deletion. (4) However, if sIgM is lacking there is a change in V-gene usage (not shown) which can then lead to increased autoantibodies. (5) A. In the follicle of the spleen, non-cognate MZ B cells capture sIgM-antigen complexes which consists of C3. B. The MZ B cell will then transfer the sIgM-antigen-C3 complex onto follicular dendritic cells (FDCs) through the complement receptor. C. The FDC will then internalize and present antigen to a germinal cell B cell which requires a T_{FH} cell to differentiate into a plasma cell which will then subsequently produce antibodies. (6) Although the mechanism is not yet understood, sIgM appears to support IgG responses. (7) IgM can help direct apoptotic cells to phagocytic cells via C1q. This is via the C1q binding to complement receptors present on the phagocytic cell this process can also be mediated by mannose binding lectin (MBL, not shown).

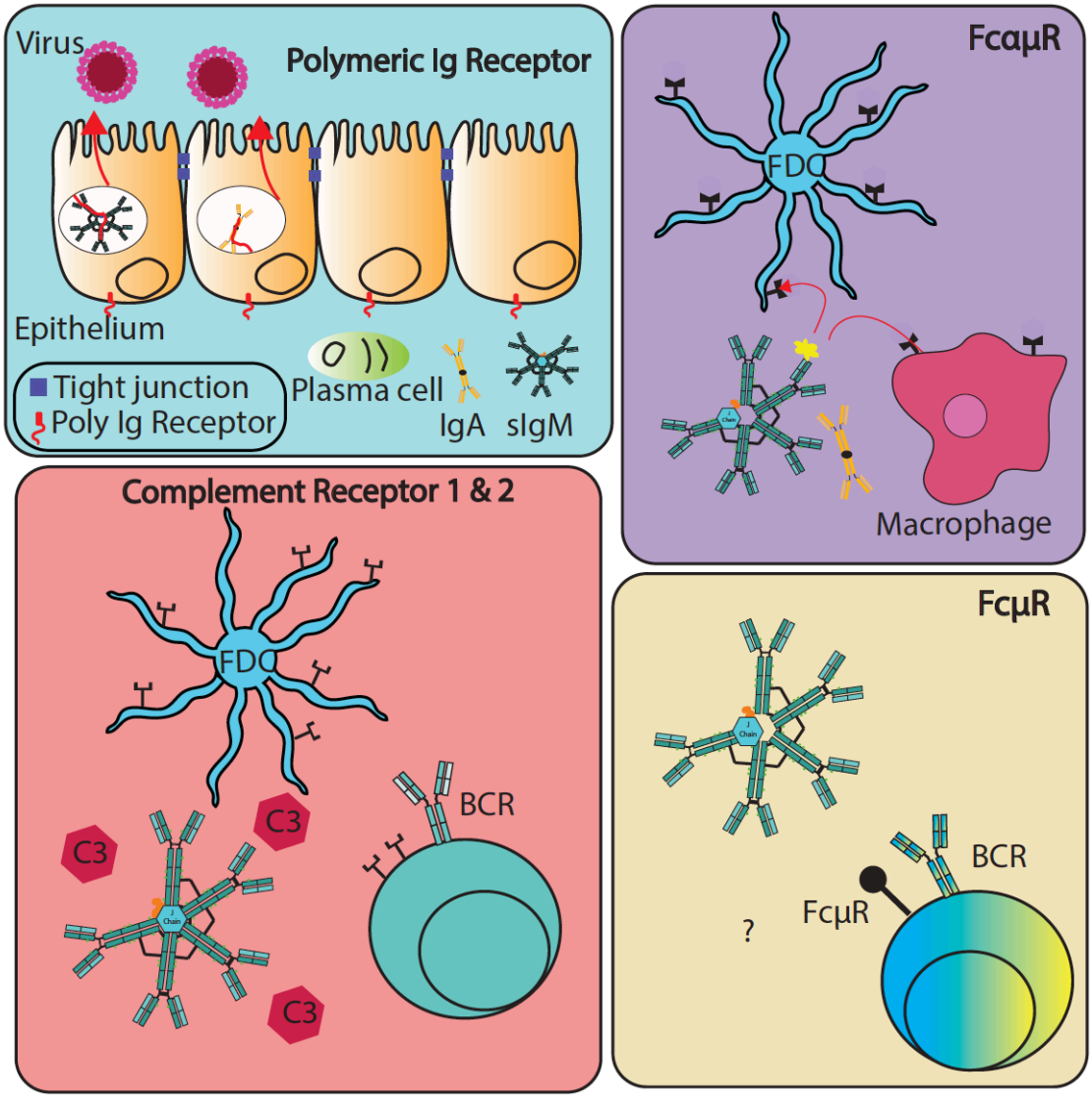
Virus
Polymeric Ig Receptor
Epithelium
Tight junction
Poly Ig Receptor
Plasma cell
IgA
sIgM
FcαμR
FDC
Macrophage
Complement Receptor 1 & 2
FDC
C3
C3
C3
BCR
FcμR
BCR
FcμR
?

Fig. 3: Receptors that bind Secreted IgM.

Polymeric Ig Receptor: pIgR can bind IgM as well as IgA via the J-chain resulting in transcytosis in epithelial cells. This receptor is mainly located on the epithelial cells of mucosal surfaces. Fc$\alpha\mu$R: The Fc$\alpha\mu$R can bind IgA and IgM and is expressed on macrophages as well as follicular dendritic cells. Its function is to mediate endocytosis of IgM-antigen complexes. This receptor binds to sIgM with high affinity and a moderate affinity to IgA. Complement Receptors: Complement receptor 1 is the C3b/C4b receptor and is present on a variety of immune cells such as B cells and follicular dendritic cells provides a mechanism for sIgM-antigen-C3 complexes onto FDCs. FcμR: The FcμR is highly expressed on B cells and binds to sIgM selectively. The role of sIgM- FcμR interactions are ongoing and show great promise for future studies.

Chapter 2
The Development of the SW_{HEL} System

Abstract

The immune system recognizes and disposes of invading pathogens such as viruses, bacteria, and fungi, all considered foreign antigens. B cells are essential components of the adaptive immune system, as they produce and secrete immunoglobulins (antibodies) that can bind and inactivate antigens in several ways: neutralization of pathogens to inhibit their adherence to host cells, opsonization for enhanced phagocytosis, and activation of complement to lyse pathogens and further enhance pathogen uptake. The evolutionary highly conserved immunoglobulin isotype M (IgM) is the first antibody to be secreted during an immune response. Secreted (s)IgM has 10 antigen-binding sites, which allows for high avidity and strong interactions with its cognate antigen. Although sIgM is produced transiently after an infection, its absence strongly reduces CD4 T cell-dependent IgG production after influenza infection or vaccination, increasing susceptibility to death following influenza virus challenge.

Thus, sIgM is regulating B cell responses resulting in enhanced production of IgG, but the mechanisms by which sIgM controls IgG responses are unknown. Yet, understanding this process is important as the generation of robust IgG responses is the protective mechanism behind most vaccinations given to-date. sIgM binds to the B cell surface via the Fc receptor for IgM, called FcμR. Recently our lab showed that the lack of FcμR on B cells caused similar reductions in IgG responses than those induced by the lack of sIgM, suggesting that sIgM- FcμR interactions are critical for maximal induction of protective IgG responses. Interestingly, we also provided evidence that B cells continuously internalize sIgM. In this chapter, the development and validation of a

linked antigen recognition model system that utilizes previously generated BCR and TCR-transgenic mice is described. Furthermore, generation of reagents is described with which to probe the mechanisms by which sIgM and the FcmR enhance T-dependent IgG responses.

Introduction

The humoral immune response is characterized by the production of antibodies via B lymphocytes and plasma cells to protect the host from infection (Baumgarth et al., 2000; Nguyen, Kläsener, et al., 2017). Antibodies are glycosylated immunoglobulins that are present either on the surface of a B cell or in a secreted form where they target and bind their antigen. The first immunoglobulin produced during a humoral immune response is (s)IgM. sIgM has a pentameric structure, which allows for high avidity and strong interactions with its antigen due to its 10 binding sites. In mice, at least 80% of circulating sIgM is derived by fetal-derived B-1 cells (Baumgarth et al., 2000; Choi et al., 2012; Savage et al., 2017; Smith et al., 2023). Natural IgM can recognize self-antigen, viral antigens, bacterial toxins, as well as other pathogens (Baumgarth et al., 2005; Ochsenbein et al., 1999). and has been shown to be required for early immune protection. A second immunoglobulin important for humoral responses is IgG. IgG is comprised of four subclasses in mice: IgG_1, $IgG_{2a/c}$, IgG_{2b}, and IgG_3 and can protect the host in numerous ways: 1) Binding to the invading microorganism, therefore blocking their ability to bind to host cell receptors; 2) binding to the microorganism so that phagocytic cells can engulf it; or 3) by activating complement via C1q (Merle et al., 2015). Depending on the cell surface receptor it binds to, and the antigen dose

administered, IgG can either have an enhancing or inhibitory effect on IgG responses. Both sIgM and IgG play essential roles in humoral immunity.

Mice lacking sIgM, ($\mu s^{-/-}$) are more susceptible to infection with influenza virus. They showed significantly decreased survival rates and increased viral loads compared to control mice after the infection (Baumgarth et al., 2000; Choi & Baumgarth, 2008; Savage et al., 2017; Waffarn et al., 2015). Previous studies have shown reductions in IgG responses when $\mu s^{-/-}$ mice were infected with influenza virus (Nguyen et al., 2015; Nguyen, Kläsener, et al., 2017). This was further confirmed when $\mu s^{-/-}$ (IgH_a) mice and control IgH_a mice were infected with influenza virus A/Puerto Rico/8/34 (A/PR8) and antiviral serum antibody titers were compared for one year. Results showed that $\mu s^{-/-}$ mice had significant reductions in antiviral IgG responses starting around day 8 after infection (Nguyen, Graf, et al., 2017). These results highlight the requirement for sIgM to mount a maximal antiviral IgG response.

The effects of IgG responses seen in $\mu s^{-/-}$ mice could suggest that there is a direct interaction between sIgM and B cells. On B cells, there are 4 receptors reported to bind to sIgM in a selective manner: The Fcα/μR (binds IgA and IgM), Complement receptors CR1 and CR2 (bind IgM-complement complexes) and the FcμR (Nguyen, Graf, et al., 2017). Previous experiments showed that after infection of $Fcamr^{-/-}$ and wildtype mice with influenza virus, there was no significant difference of virus specific serum IgG compared to controls (Nguyen, Graf, et al., 2017). Additionally, when complement was inhibited with Cobra Venom Factor (CVF), there was no effect on influenza specific IgG responses. However, when global $Fc\mu R^{-/-}$ mice were infected, there was reduced antiviral serum IgG titers, like what was observed in $\mu s^{-/-}$ mice.

Together, this suggests that sIgM-FcμR interactions plays a pivotal role in antiviral IgG responses. However, how sIgM regulates IgG responses is unknown.

Results

FcμR staining pattern differ between anti-FcμR mAb clones MM3 and 4B5

The Fc receptor specific for IgM (FcμR) has only recently been redefined by Kubagawa et. al (Kubagawa et al., 2009). In 1998, the receptor was originally identified as TOSO, encoded by Fas apoptosis inhibitory molecule (FAIM3) (Honjo et al., 2012). Because a mouse IgM monoclonal antibody (mAb) to Fas was able to inhibit apoptosis, which is now thought as having bound to the FcμR via its Fc-portion, not the antigen-binding site.

The mouse FcμR is a transmembrane receptor of ~ 60kDa and differs slightly in its composition compared to the human FcμR, as it contains more amino acids in both the extracellular region as well as the cytoplasmic domains (Kubagawa et al., 2009). FcμR expression has been reported on various cell types such as macrophages, B cells, dendritic cells, monocytes, and granulocytes. Our lab reported that expression was highest on follicular B cells, splenic B-1 cells and to a lesser extent marginal zone B cells (Nguyen, Graf, et al., 2017). To characterize total $Fc\mu R^{-/-}$ mice generated in our lab (Nguyen, Graf, et al., 2017), I studied FcμR expression using flow cytometric staining

on cell types that have been reported previously using two published mAb clones: MM3 and 4B5 (see Table 1) (Kubagawa et al., 2009; Nguyen, Kläsener, et al., 2017; Ouchida et al., 2012). However, previous studies with these clones have shown conflicting results. To characterize the surface staining of the two mAb clones, I used single cell suspensions from various tissues of global FcμR$^{-/-}$ (knock-out confirmed by genotyping) and wildtype C57BL/6 mice and measured staining by flow cytometry. Specifically, staining among B cells, T cells and non-T /non-B cells in spleen, bone marrow, peritoneal cavity (PERC) and pleural cavity (PLERC) was compared (Fig. 1A, B). Differences in staining of FcμR between MM3 (from BD) and 4B5 (from MBL) were apparent, especially in B cells (Fig.1B). Staining with the anti-FcμR mAb MM3 showed higher frequency of FcμR compared to staining with the mAb 4B5. As expected, there was a reduction in FcμR staining in the knockout mouse tissues tested, compared to the controls. In contrast, FcμR$^{-/-}$ knock-out cell staining with MM3 was comparable to staining seen with cells from C57BL/6 mice (Fig. 1C, upper right). Next anti-FcμR mAb (4B5) was biotinylated and the experiment was repeated, comparing B cells in the spleen to MM3 which was purchased from BD (conjugated to phycoerythrin (PE)). As expected, the biotinylated FcμR showed staining of most B cells in C57BL/6 mice (86%), while the FcμR$^{-/-}$ B cells showed little staining (6%). In contrast, the MM3 mAb stained C57BL/6 B cells at low frequencies (12%), not much different to FcμR$^{-/-}$ B cells (4%) (Fig. 1D). Together, these results showed clear differences in staining patterns among the MM3 and 4B5 clones and suggested that the MM3 mA does not bind the FcμR. Reported findings were sent to BD, who have since taken the MM3 mAb off the market.

FcμR total knockout mouse lacks mRNA expression of exons flanking target exon

Due to the staining pattern seen with the above tested mAb, the FcμR -/- mouse (Nguyen, Graf, et al., 2017) previously generated with help of the UC Davis Mouse Biology Program was explored. It is conceivable that this mouse may contain a truncated FcμR, given that the gene targeting strategy employed removed only the transmembrane-encoding exon 4. To test for this, I analyzed mRNA expression for the FcμR in wild type and gene-targeted mice, using primer probe sets that amplify each exon boundary (Table 2). Using whole spleen, whole bone marrow, PERC, PLERC and Peripheral blood mononuclear cells (PBMCs) harvested from wildtype (C57BL/6) or $Fc\mu R^{-/-}$ mice (Fig. 2A-2E) was compared. As expected, there was mRNA expression of all exons in all tissues tested in wildtype C57BL/6 mice. As expected also, mRNA expression was strongly reduced in $Fc\mu R^{-/-}$ mice. There appeared to be minimal expression of mRNA of exons 1-3 in all tissues tested (Fig 2A-2E). When compared to purified B cells (from spleen and bone marrow) of a C57BL/6 and $Fc\mu R^{-/-}$ mouse, there was a 10-fold decrease in expression of exons 1-3, a ~3000-fold decrease in exons 3-4, 14,000-fold decrease in exons 5-6, and a 5-11-fold decrease in exons 5-6, 6-7, and 7-8 (Supplemental Fig 1).

mRNA expression solely on B cells from $Fc\mu R^{+/+}$ and $Fc\mu R^{-/-}$ mice was investigated and compared to confirm mRNA expression levels in our mouse model. To do this, negatively enriched B cells from spleen and bone marrow were used. There

was very little exon expression of mRNA for FcμR in FcμR$^{-/-}$ B cells. Exons 3-4 and 4-5 had the least expression of FcμR (Fig 2F). This was expected as the targeted exon when generating the global knockout mouse was exon 4, which was confirmed by our data (Fig 2G). Thus, I found no significant mRNA expression in the FcμR -/- mice, suggesting that these mice do not carry a truncated FcμR.

Data in CLL patients have shown there exists a membrane and soluble form of the FcμR due to alternative splicing (skipping of exon 5) (Li et al., 2011). To determine whether the FcμR -/- mice lacking the transmembrane domain may have circulating soluble FcμR, an ELISA was performed in which plates were coated with 10ug/ml of α-FcμR followed by addition of sera from FcμR$^{+/+}$ and FcμR$^{-/-}$ mice. Results showed that both the wildtype (FcμR$^{+/+}$) control and the knockout (FcμR$^{-/-}$) mice lacked any detectable FcμR (data not shown). Although I did not have access to a positive control for this assay, the data suggested that there were no significant levels soluble FcμR in wildtype C57BL/6 nor FcμR-/- mice, consistent with findings that soluble FcμR has only been reported in human patients with CLL (Chronic Lymphocytic Leukemia) but not in healthy controls (Li et. al 2011).

B cell specific FcμR knockout mice show normal distribution of cell subsets

Previous data in the lab were generated in which FcμR floxed mice were bred to a global Cre-expressing (*Cmv*-Cre) mice to generate mice that completely lacked the FcμR (FcmR-/-), eventually resulting in the deletion of the *FcmR in* the germline.

Alternatively, the FcmR floxed mice were crossed with *Cd19-Cre$^{+/-}$ mice* to generate *Fcmr$^{flx/flx}$cd19-Cre$^{+/-}$* mice that contained a B cell-specific deletion of the FcμR, as well as CD19-Cre$^{-/-}$ negative littermates, which were used as controls (Nguyen, Graf, et al., 2017; Nguyen, Kläsener, et al., 2017).

Previously, the lab showed that the CD19 haploinsufficient CD19 Cre$^{+/-}$ FcμR$^{flx/flx}$ mice have a defect in B-1 cell generation, which was caused not by the lack of the FcμR, but the reduction in CD19 expression (Nguyen, 2017). Therefore, I created a mouse model in which CD19 was unaffected so that the effects of the FcμR could be studied, including on B-1 cells, (an important source of sIgM). To do this the FcμR$^{flx/flx}$ mice was crossed onto a Mb1-Cre$^{+/-}$ mice. These mice carry an allele in which exons 2 and 3 of the *mb1* gene (encoding CD79a) have been replaced with the gene for the Cre recombinase. Mb-1 Cre $^{-/-}$ mice were used as controls.

FcμR$^{flx/flx}$ CD19 Cre^{+}, FcμR$^{flx/flx}$ Mb1 Cre+ and FcμR$^{flx/flx}$ Mb1 Cre- mice were compared to characterize the different cell compartments of spleen, bone marrow, and peritoneal cavity with specific interest in the B1 cell population, which was identified among the CD93- cells.

To do this, tissue from the spleen, bone marrow and peritoneal cavity was harvested and analyzed via flow cytometry. Using the gating strategy (Fig 3A), B-1 cells (CD93-), T1-T3 transitional B cells, and follicular B cells were seen in all mice. There were no significant differences in the B cell population frequencies in the spleen (Fig 3B). However, IgM MFI in the marginal zone was significantly lower in Mb-1 Cre+ mice compared to CD19 Cre+ mice. No significant changes were observed in the follicular B cell subset (Fig 3C). Total B cell populations were comparable among all genotypes

tested (Fig 3D). B-1 cell frequencies showed significant difference between CD19 Cre+ compared to control (Cre-) and no significant difference among Mb-1 Cre+ and control B cells indicating that the Mb-1 line has comparable B-1 cell generation to control mice (Fig 3E).

Using the gating strategy (Fig 3F), immature, late (pre B) and mature B cell subsets in the bone marrow were measured using flow cytometry. Mature B cell subsets in the bone marrow showed significant differences among all genotypes with Mb1-Cre+ significantly the lowest compared to CD19Cre+ and control (mb-1 Cre-) (Fig 3G). MFI of IgM on these cells showed distinct differences on the immature and mature B cell populations with Mb-1 Cre+ and Cre- controls being comparable in the mature bone marrow population (Fig 3H).

Peritoneal cavity was investigated to measure B1 cells (Fig 3I). no significant differences in CD5+ or CD5- cells were found (Fig 3J). There were no overt MFI expression differences between Mb1 Cre+ and Mb1 Cre- control mice but I did see a significant difference between CD19Cre+ and Mb1 Cre+ B-1 cells (Fig 3K). Additionally, no there was no significant reductions or increases in the frequencies of B-1 cells in the peritoneal cavity among all genotypes (Fig 3L).

Lastly, serum IgM and total IgG levels were evaluated in each genotype. IgM serum levels were significantly lower in Mb-1 Cre+ and Mb-1 Cre- mice compared to CD19Cre+. In contrast, Mb-1 Cre+ and Mb-1 Cre- were comparable (Fig 3M). Total Ig levels were comparable among all three genotypes (Fig 3N). Overall, the data showed that backcrossing floxed FcmR-/- mice onto MB-1Cre mice resulted in the generation of mice lacking the FcμR only in B cells, without the changes in B cell subsets seen in the

CD19Cre- FcmR mice.

Generation of SwHEL x FcμR (+/+) and (-/-) mice to model T-dependent B cell responses

To study the effects of sIgM and the function of the FcμR, we generated a transgenic mouse model system by crossing the FcμR onto SW_{HEL} BCR transgenic mice. Mice were genotyped for HEL heavy and light chain using conventional PCR. FcμR genotyping was conducted through the Mouse Biology Program (MBP) using standard PCR. SW_{HEL} mice are homozygous for the HEL-specific Ig-heavy chain and heterozygous for the HEL-encoding Ig kappa light chain (Fig 4A), as light chain homozygosity leads to embryonic lethality, reducing the frequency of HEL-specific B cells in the SwHEL mice to about 50% of B cells. This was confirmed by flow cytometry after incubating B cells from SW_{HEL} BCR transgenic and control C57BL/6 mice with HEL protein (Sigma), followed by use of fluorescently labeled anti-HEL mAb (HYHEL9) (Fig 4B).

Generation of a linked antigen: HEL-OVA for transgenic B and T cell recognition

We next aimed to develop an *in vitro* system to study the effects of B cell-expressed FcμR on antigen specific T-dependent B cell responses in vitro. Since HEL does not include a T cell epitope in C57BL/6 mice, HEL-ovalbumin (OVA) conjugate was generated, which contains an I-A^b-restricted TCR OVA epitope (peptide 323-339). To do this, HEL protein (Sigma) was first conjugated to Succinimidyl-6-[(β-

maleimidopropionamido)hexaneoate]) (SMPH) and dialyzed this overnight. The next day, custom made OVA peptide (Genscript) was conjugated. Important for this OVA peptide generation was the addition of CGG at the C terminus of the peptide sequence. The rationale for this is the thiol group on cysteine will become activated by the maleimide. In addition, the glycine provided added flexibility to the conjugate. OVA peptide conjugation was then dialyzed for 2 days (Fig 5A) and conjugate size was checked using an SDS PAGE gel (Fig 5B). This data demonstrated successful conjugation of HEL to OVA, which was used for in vitro studies outlined in Chapter 3.

HEL-OVA conjugate successfully activates SW_{HEL} B and OT-II T cells

To test the HEL-OVA conjugate, transgenic mice as a source of B (SW_{HEL} mice) and CD4 T (OT-II) cells that have receptors specific for distinct antigens (HEL and OVA, respectively) were used. Using protein chemistry, a dual antigen HEL-OVA was constructed, that can be recognized by both the T and B cells. To test and ensure HEL-OVA conjugate can bind and activate SwHEL B cells, B cells were taken from either $Fc\mu R^{+/+}$ or $Fc\mu R^{-/-}$ spleens. Spleens were then processed and enriched for B cells. Results showed that HEL-OVA conjugate bound, and activated SwHEL B cells compared to controls. Adding LPS as a positive control yielded the most proliferation in B cells, which is expected as LPS is a mitogen. With varying concentrations and adding CD40L and IL-4 to mimic CD4 T cell help, minimal activation with only the addition of HEL protein was observed (Fig. 6A), which was also expected as HEL does not have a T cell epitope. However, when adding HEL along with IL-4 and CD40L, T cell proliferation was observed. (Fig. 6A). When adding the HEL-OVA conjugate together

with CD40L and IL-4, substantial CD4 T cell proliferation was observed (Fig.6B). B and T cells co-cultured with cytokines showed clear cell clustering in the presence of HEL-OVA and IL-4 and CD40L compared to the non-OVA conjugated HEL protein co-cultured otherwise under the same conditions. In addition, as the concentration of HEL-OVA conjugate was reduced, so did the clusters (Fig 6C). To test the T cell responsiveness of the HEL-OVA conjugate, OT-II T cells were enriched via autoMACS. For antigen presentation, irradiated splenocytes were used to present HEL-OVA conjugate to T cells. Addition of anti-CD3 and anti-CD28 was used as a positive control for T cell activation. IL-2 was added to the cultures to enhance T cell survival. T cell proliferation was optimal in culture wells that had HEL-OVA, IL-2 and irradiated antigen-presenting splenocytes (Fig 6D). Together the data showed that the HEL-OVA conjugate generated in our lab works successfully and activated HEL-specific B cells as well as transgenic OT-II T cells.

Materials and methods

Mice

Fcmr $^{flx/flx}$ were generated using embryonic stem cells (ES) with a floxed exon 4 of the Fcmr gene by the UC Davis Mouse Biology program ((MBP) gene identification, MGI: 1916419 https://www.komp.org/geneinfo.php?geneid=57632)) as previously described (Nguyen, Kläsener, et al., 2017). All procedure and experiments were approved by the Institutional Animal Care & Use Committee (IACUC) of the University of California, Davis.

To generate B cell specific FcμR knockout mice, Fcmr $^{flx/flx}$ mice were crossed onto cd19-Cre$^{+/-}$ mice (Nguyen, Graf, et al., 2017). To create B cell-specific FcμR deficient mice with a functional B-1 cell compartment, Fcmr$^{flx/flx}$ mice were used and backcrossed to mice in which exon 2 and 3 of the mb-1 gene (encoding CD79a) was replaced with an optimized Cre recombinase gene on one allele (https://www.jax.org/strain/020505). Additionally, published data using these mice have reported that Cre recombination occurs primarily in B cells with a low level of recombination in T cells in primary and secondary lymphoid tissues (Hobeika et al., 2006). Faim3 genotyping was done using simplex PCR with primers 5'-TGGGAAGATGAATGGACCTCTGAGC-3' for forward primer, 5'-GCTAGTGAGGTATCCAGGTAAGCCC-3' for reverse and ttR 5'-AGGCTTACTGTCTTCTGGACATGGG-3'. All mice were kept in specific-pathogen free housing conditions with food and water at libitum, a 12h day-night cycle and daily monitoring. Mice were euthanized by carbon dioxide overexposure. All experiments with mice were done after protocol approval by the UC Davis Institutional Animal Care and Use Committee.

Flow Cytometry

Single- cell suspensions from bone marrow, lymph nodes and spleens were prepared by using frosted end microscope slides and pressing the tissues with pressure. Red Blood cells were lysed with ACK buffer (150 mM NH4Cl, 10 mM KHCO3, 10 mM EDTA) for 1 minute on ice. Cell counts were determined using trypan blue and a hemocytometer or using the cellometer (Nexcelom Biosciences). All staining was performed using staining media (Buffered saline solution: 0.168 M NaCl, 0.168 M KCl, 0.112 M CaCl2, 0.168 M MsSO4, 0.168 M KH2PO4, 0.112 M K2HPO4, 0.336 M HEPES, 0.336 M NaOH, containing 3.5% heat-inactivated, filtered newborn calf serum, 1 mM EDTA, 0.02% sodium azide) for 20 minutes on ice. FcγR receptors were blocked by incubation of cells with anti-CD16/32 mAb for 20 minutes. Cells were then stained for the following surface antibodies: FcμR (MM3), FcμR (4B5).

Spleen cells were stained with CD19 (1D3), CD21 (BD), IgM (331), CD93(BD), CD8 (53-6.7.3.1), F4/80 (BM-8), GR-1 (RB6-8C5), CD4 (GK1.5), and CD23 (B3B4). Bone marrow cells were stained with CD24 (BD), BP-1, CD93(BD), IgD (11-26), CD43 (AF6-122), CD45R (eBioscience), GR-1 (RB6-8C5), CD4 (GK1.5), CD8 (53-6.7.3.1), F4/80 (BM-8), CD19 (1D3), IgM (331). Peritoneal cavity (PERC) staining was done using the same antibodies as bone marrow with addition of CD5 (53-7.8). FACS data were analyzed using FlowJo software (BD).

qRT-PCR for FcmR exon expression analysis

Total RNA was extracted immediately after tissue harvest using the Quiagen RNeasy Mini Kit (Lot: 154034579) and stored at -80 in RNA storage buffer (Ambion).

cDNA was made using random hexamers (Promega) with SuperScript II reverse transcriptase (Invitrogen). FcμR mRNA was measured using commercial primer-probe sets purchased from Invitrogen (Table 2). Relative expression was normalized to Ubiquitin C. Quantitative PCR was performed using a Real-Time PCR system (Quantstudio 6) with following cycles: 50°C for 2 min, 95°C for 10 min, and 40 cycles of 95°C for 15s and 60°C for 1 min. Relative expression was normalized to ubiquitin. Data are expressed using 2-ΔΔCT algorithm.

Magnetic B cell Enrichment

Spleen and bone marrow single cell suspensions were treated with Fc block and B cells were negatively enriched by autoMACS (Miltenyi Biotech) using depletion cocktails that consisted of a mixture of biotinylated antibodies ((anti-CD90.2 (30-H12), anti- Gr-1(RB6-8C5) anti F4/80 (BM8), and anti-Nk1.1(PK136)). Anti-biotin microbeads (Miltenyi Biotech) were used to label the antibody-stained cells. Lymph node CD4 T cells from OT-II mice were negatively enriched with anti- Gr-1(RB6-8C5) anti F4/80 (BM8), anti-Nk1.1(PK136), anti-CD19 (D3), anti TCRγλ (GL-3), anti- CD11b (M1/70), anti CD8a (53-6.7.3.1). Nylon-filtered bone marrow and splenocytes were separated using autoMACS (Miltenyi Biotech).

In vitro B cell and T cell proliferation labeling

Splenocytes were labeled using 0.5 μm CFSE diluted in sterile PBS at cell concentration of $1x10^7$ cells/ml for 10 minutes at 37°C, washed twice with quenching media (10% NCS) and resuspended in staining medium. Proliferation was measured using FlowJo software.

In vitro B and T cell cultures

B cells were cultured after autoMACS enrichment and then cultured at $2.25x10^5$ cells per well in medium containing 60 ng/ml IL-4, 100ug/ml CD40L, 20ug/ml LPS (Sigma) with HEL protein or HEL-OVA conjugate. T cells were cultured after autoMACS enrichment and then cultured at $1 x10^5$ cells per well in medium containing $4 x 10^5$ irradiated splenocytes, OVA protein, HEL-OVA conjugate, α-CD3 (10mg/ml), α-CD28, with HEL-OVA in 96-well flat-bottom plates for 72 hours at 37°C in 5% CO2. Purities for B and T cells were above 90%. Analysis of B and T cells was done via flow cytometry.

ELISA

Soluble FcμR was measured by first coating 10μg/ml of hen egg lysozyme (Sigma) and incubated overnight at room temperature. Plates were then washed, and plates were blocked for 1 hour with ELISA blocking buffer (0.1% milk powder, 0.05% Tween 20). 2-fold serially diluted serum samples in PBS were incubated for 2 hours.

Plates were incubated with biotinylated anti-FcμR for 1 hour. Revealing was done with incubation of streptavidin (SA)-horseradish peroxidase and subsequently with substrate (10 mg/ml 3,3V,5,5V-tetramethylbenzidine (TMB) in 0.05 mM citric acid, 3% hydrogen peroxide). Reactions were stopped with 1 N sulfuric acid and absorbance was read at 450 nm and reference wavelengths of 595 nm (Molecular Devices, Spectramax)

Generation of HEL-specific IgM

Generation of anti-mouse IgM are secreted by hybridomas from splenocytes taken from a 3-month-old BALB/c female mouse that was immunized with 50μg of HEL protein mixed in Complete Freund's Adjuvant. 5 days later, splenocytes (50×10^6) were fused with myeloma line X63 (25×10^6) in PEG for 3 minutes at 37 degrees and plated in 10 96-well flat bottom plates in HAT medium. Specificity of HEL IgM was done with HEL-coated plates (1 ug/ml) with anti-mouse IgM or anti-kappa secondary reagents. Positive cultures were cloned and expanded.

Discussion

To investigate whether sIgM-antigen-FcμR interactions plays a role for optimal activation and IgG responses, an *in vitro* system to model the dynamics of a T-dependent B cell response was developed. Because there is no transgenic system where the B and T cell recognize the same antigen, hen-egg lysosome (HEL)- and ovalbumin (OVA)-specific B and T cells, was used respectively, and generated a linked HEL-OVA antigen. The SW_{HEL} model was generated by inserting fully recombined VDJ heavy and VJ light chain genes into the Ig locus of C57BL/6 mice (Brink et al., 2015; Phan et al., 2003). FcμR was backcrossed onto the HEL mice background to generate mice that either possess the FcμR (Fc$\mu R^{+/+}$) or lack it (Fc$\mu R^{-/-}$). This was confirmed for HEL using conventional PCR and FcμR genotyping (conventional PCR) was conducted through the Mouse Biology Program (MBP). To generate an antigen that could be recognized by B cells and presented to CD4 T cells (linked-recognition), protein chemistry was used to conjugate HEL to a peptide from ovalbumin, that is recognized by transgenic CD4 OT-II T cells, which consist of CD4+ TCR Tg cells recognizing $OVA_{323-339}$ when presented by MHCII (specifically I-A^b) (Barnden, Allison, Heath, & Carbone, 1998). Successful stimulation of SwHEL B cells as well as OT-II T cells with the HEL-OVA conjugate was confirmed. A novel Mb-1 Cre+ line was generated, in which the FcμR is lacking on B cells and characterized it, demonstrating that these mice had normal B cell development and peripheral B cell subset distribution, including normal frequencies of B-1 cells. These reagents have been tested for use of experiments described in Chapter 3.

Table 1 mAb to FcmR used in experiments

	BD FcμR	MBL FcμR
Clone name	MM3	4B5
Conjugated	PE	Unconjugated
Concentration	0.2 mg/ml	1mg/ml
Lot # used	566030	D303-3
Isotype	mouse IgG_1 κ	rat IgG_1 κ,
Region binding to FcμR	Extracellular portion (exons 1-3)	Extracellular portion (exons 1-3)
Dilution used*	1:20	1:10

* Optimal dilution established after antibody titration

Table 2: Exon probes

	Exon boundary	Catalog number*	Amplicon length
Mm01302382_m1	1-2	4351372	73
Mm01302383_m1	2-3	4351372	79
Mm01302384_m1	3-4	4351372	91
Mm01302385_m1	4-5	4351372	67
Mm01302386_g1	5-6	4351372	92
Mm01302387_g1	6-7	4351372	130
Mm01302388_m1	7-8	4331182	106

* Catalog number identification

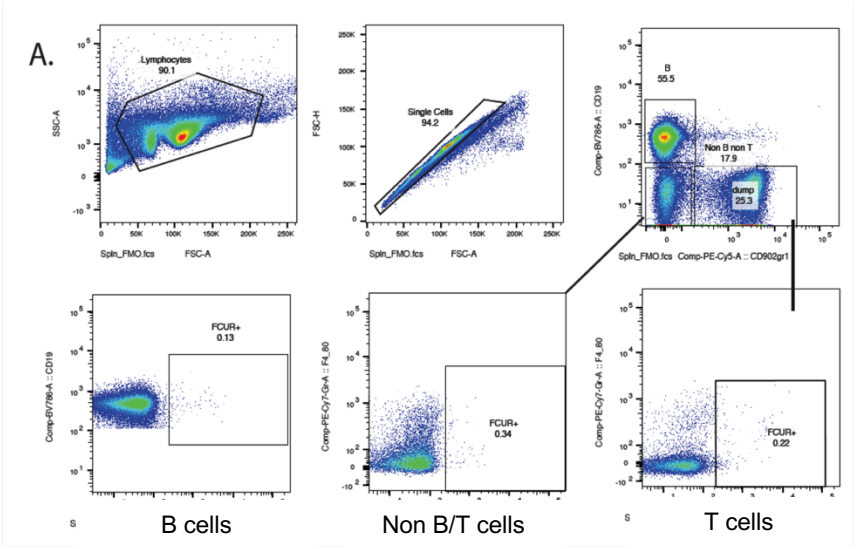
A.
Lymphocytes
90.1
SSC-A
Spln_FMO.fcs FSC-A
Single Cells
94.2
FSC-H
Spln_FMO.fcs FSC-A
B
55.5
Non B non T
17.9
dump
25.3
Comp-BV786-A :: CD19
Spln_FMO.fcs Comp-PE-Cy5-A :: CD902gr1
FCUR+
0.13
Comp-BV786-A :: CD19
FCUR+
0.34
Comp-PE-Cy7-Gr-A :: F4_80
FCUR+
0.22
Comp-PE-Cy7-Gr-A :: F4_80
B cells
Non B/T cells
T cells

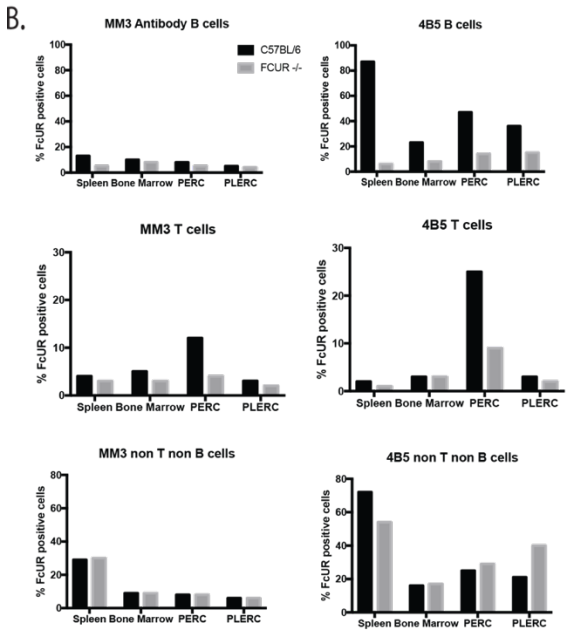
B.
MM3 Antibody B cells
C57BL/6
FCUR -/-
% FcUR positive cells
Spleen Bone Marrow PERC PLERC
4B5 B cells
MM3 T cells
4B5 T cells
MM3 non T non B cells
4B5 non T non B cells

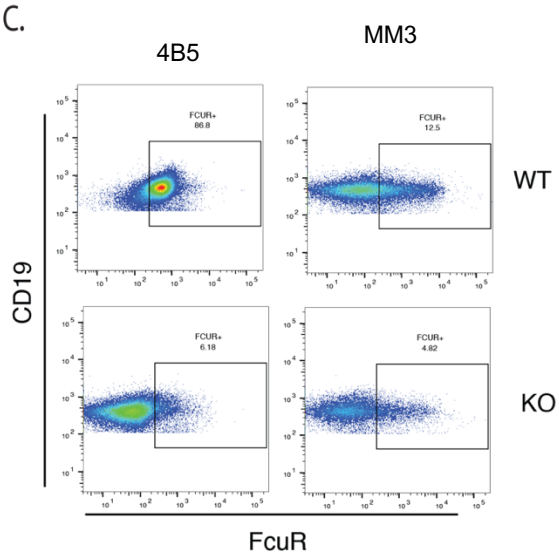
C.
4B5
MM3
FCUR+
86.8
FCUR+
12.5
WT
CD19
FCUR+
6.18
FCUR+
4.82
KO
FcuR

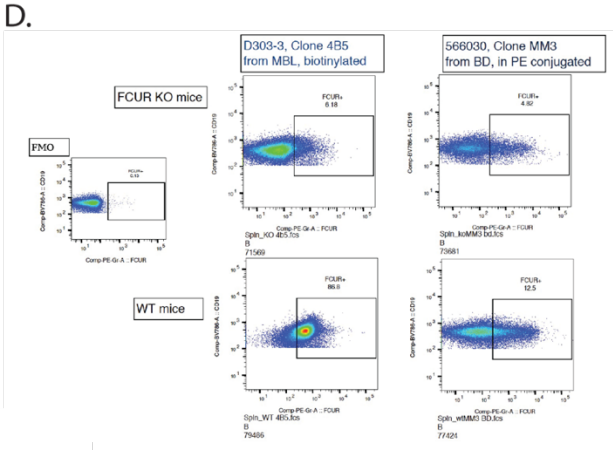
D.
D303-3, Clone 4B5
from MBL, biotinylated
566030, Clone MM3
from BD, in PE conjugated
FCUR KO mice
FMO
WT mice

Fig 1: Mab clones 4B5 and MM3 show differences in staining. (A) flow cytometry pseudocolor plots of spleen cells from C57BL\6 mouse. FMO of all subsets: B cells, T cells and non-B and T cells. (B) Shown are mean frequencies of cells stained with MM3 and 4B5 mAb, respectively, in spleen, bone marrow, PERC and PLERC. Quantification of (A) B cells (top) T cells (middle) and non-T and B cells (bottom). (C) FcμR staining in SW_{HEL} (+/+) and SW_{HEL} (-/-) mice with mAb clones 4B5 and MM3. (D) Staining with biotinylated (in-house) 4B5 and SA-PE of spleen cells from SW_{HEL} (+/+) and SW_{HEL} (-/-) mice (left) compared to staining with MM3-PE (right). Plots are from cells gated on CD19. Data are from one of 2 independent experiments done to verify staining, mice (*n*=2).

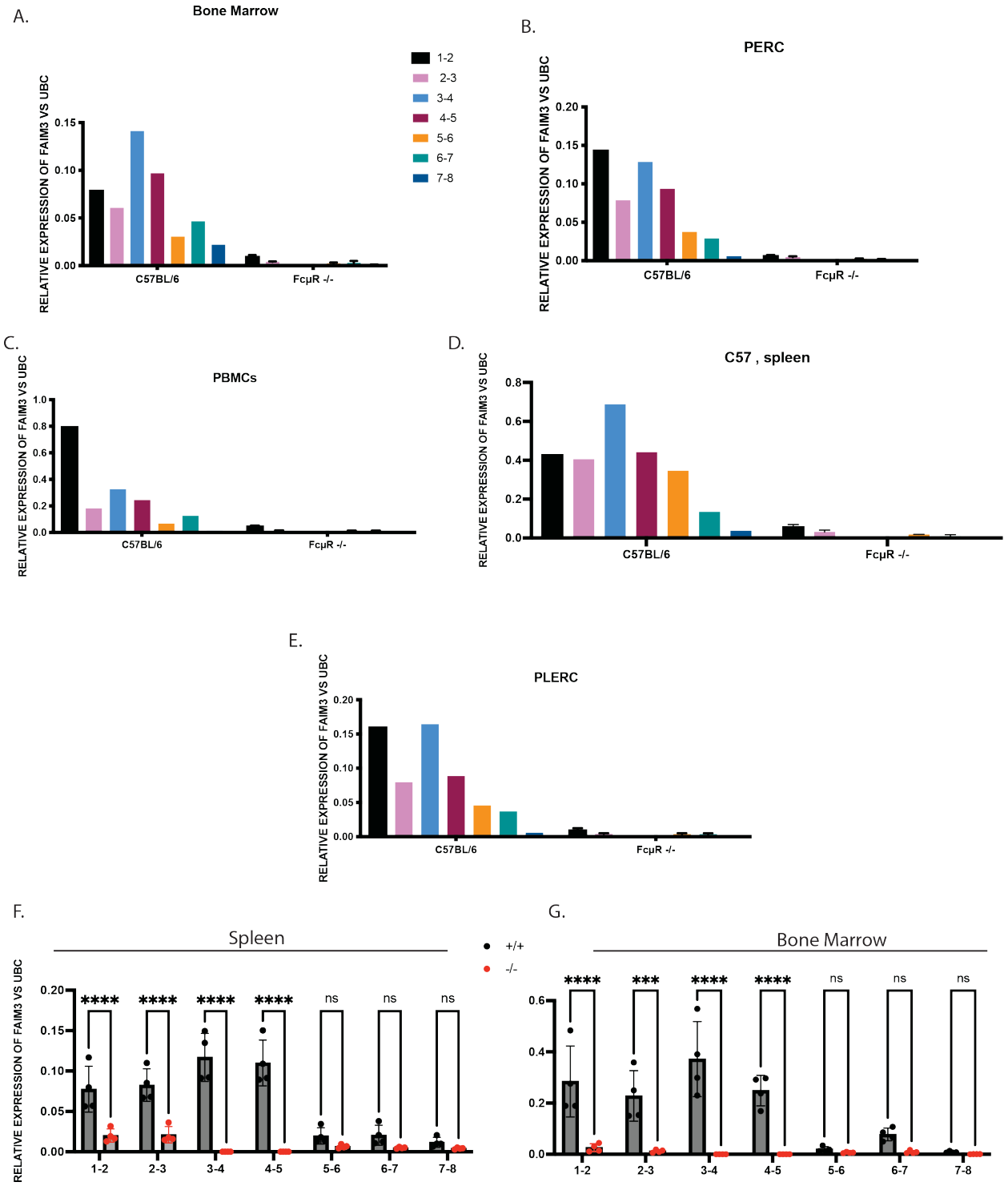

Fig 2: Fcmr expression of exons is absent in FcμR-/- mice

(A-E) Bar charts of relative expression levels for all exon boundaries of the gene encoding the FcμR assessed in (A) bone marrow (B) PERC (C) PBMCs (D) Spleen and (E) PLERC tissues from C57BL/6 and FcμR-/- mice. (F) Purified B cells harvested

from spleen or (G) bone marrow in SW_{HEL} (+/+) and SW_{HEL} (-/-) mice. Bar graphs represent the mean ± SD from (*n*=4) mice and was calculated using Student's *t* test. This experiment was repeated twice. *p < 0.05; **p < 0.01; ***p < 0.001; ****p < 0.0001; ns= not significant.

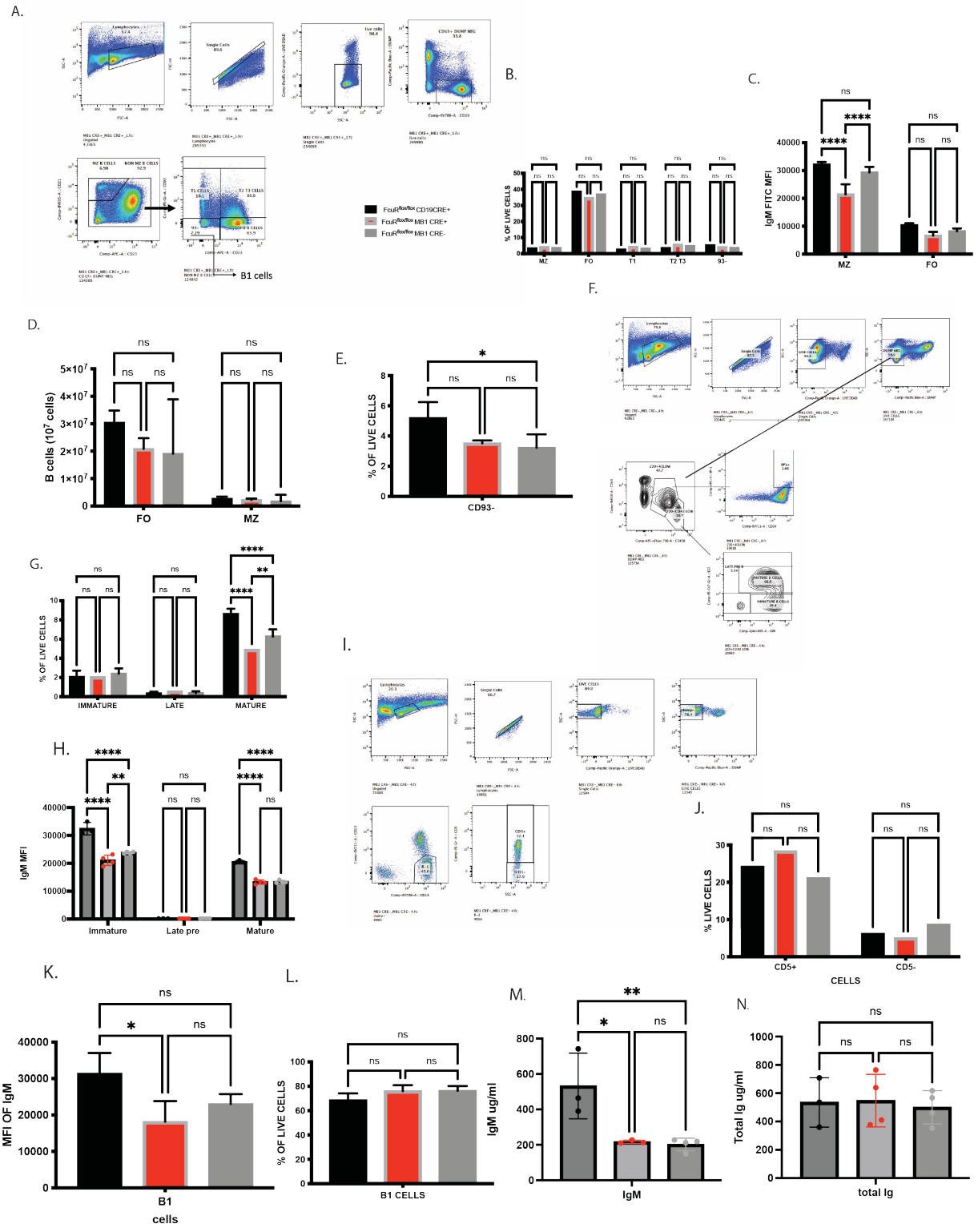
A.
B.
C.
D.
E.
F.
G.
H.
I.
J.
K.
L.
M.
N.
B1 cells
FcuR^flox/flox CD19CRE+
FcuR^flox/flox MB1 CRE+
FcuR^flox/flox MB1 CRE-
% OF LIVE CELLS
MZ
FO
T1
T2 T3
93-
IgM FITC MFI
B cells (10^7 cells)
CD93-
IMMATURE
LATE
MATURE
IgM MFI
Immature
Late pre
Mature
CD5+
CD5-
CELLS
MFI OF IgM
B1
cells
B1 CELLS
IgM ug/ml
IgM
Total Ig ug/ml
total Ig

Fig. 3: MB1 Cre+ FcmRfl/fl mice have normal B cell subsets. (A) pseudocolor plots indicating gating strategy to identify B cell subsets in spleen. (B) Summary of flow cytometric analysis of B cell subset, shown are means ± SD. (C) MFI of IgM on marginal zone (MZ) and follicular B cells (FO) ± SD. (D) Numbers ± SD of FO and MZ cells and (E) Frequency ± SD of CD93- cells among non-FO, non-MZ and non-Transitional B cells, indicative of B-1 cells *(n*=4 mice per group). (F) Pseudocolor plots indicating gating strategy of B cells in the bone marrow. (G) Summary of mean ± SD B cell frequencies. (H) MFI ± SD of IgM in compartments (Immature, Late pre-B and Mature). *(n*=4 mice per group). (I) Pseudocolor plots showing gating strategy to identify B cells in the peritoneal cavity (PERC). (J) Mean frequency ± SD of CD5+ B cells. (K) MFI of IgM ± SD. (L) Mean frequency of B1 cells ± SD *(n*=4 mice per group). (M) Serum ELISA of total IgM ± SD and (N) IgG in mice *(n*=4 mice per group). Statistics was calculated using 2-way ANOVA. *p < 0.05; **p < 0.01; ***p < 0.001; ****p < 0.0001; ns= not significant.

A.

HEL Light Chain

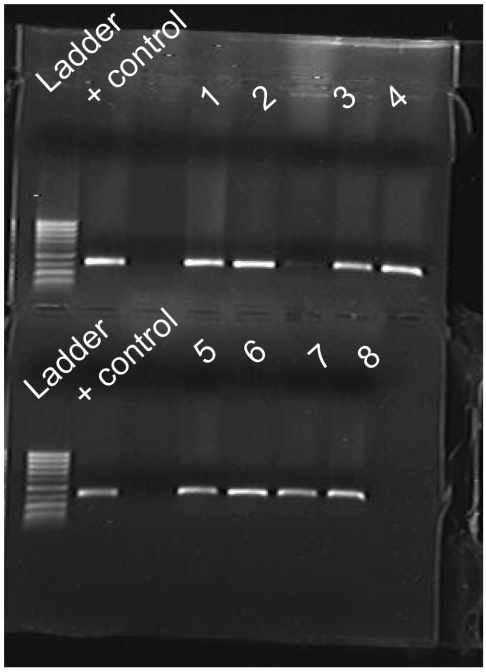

HEL Heavy Chain

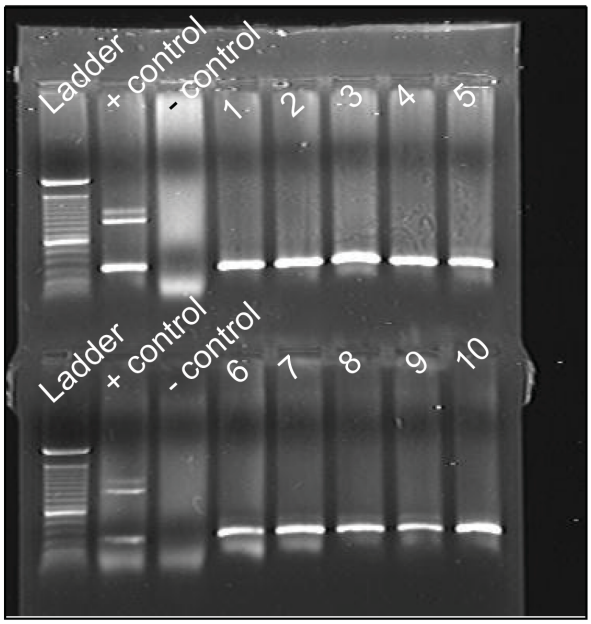

B.

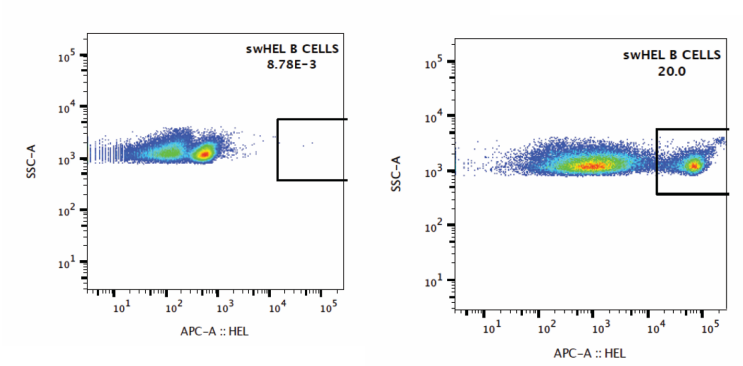

C57BL/6 mouse

SWHEL mouse

Fig. 4: Generation of SW_{HEL} mice

(A, left) Gel image of progeny positive for HEL Ig-light chain at 402 base pairs. Each number represents results from one mouse. Positive control is DNA from previously genotyped mouse breeder. No band is negative for transgene (targeted allele). (A, right) Gel image of mice progeny for HEL Ig-heavy chain at 302 base pairs (bp). Wildtype allele is at 865 bp to track HEL heavy chain heterozygous mice. Positive control was taken from a F2 heterozygous mouse and negative control is no template. (B) Pseudocolor flow plot showing the frequency of HEL+ total cells in a SW_{HEL} mouse and a C57BL/6 mouse as a control.

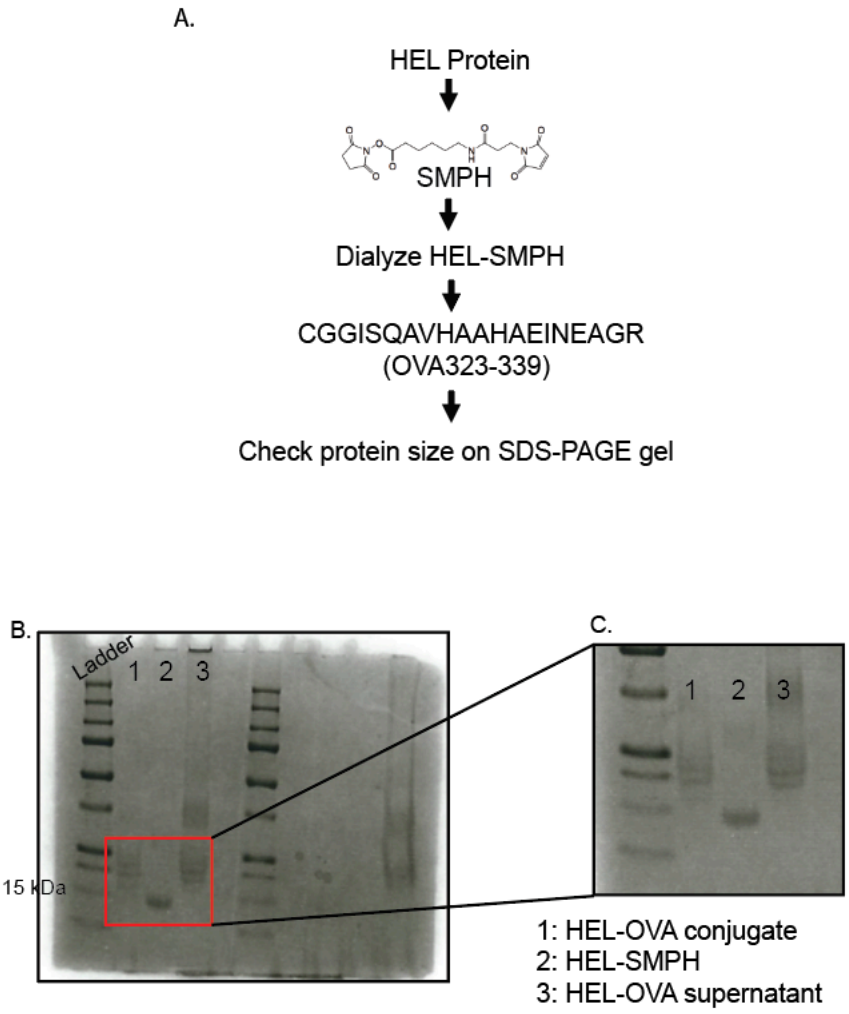

Figure 5: Workflow of HEL-OVA conjugate. (A) HEL protein (sigma) was conjugated to (Succinimidyl-6-[(β-maleimidopropionamido)hexaneoate]) (SMPH) and dialyzed. Maleimide-activated OVA (Genscript) was conjugated to sulfhydrylated-HEL (Sigma) this generating HEL-OVA conjugates. (B) SDS-PAGE gel showing HEL conjugated to SMPH in the middle lane (lane 1 and 3) molecular weight shift indicates successful conjugation (~14kDa to ~20kDa). HEL-SMPH was ran as a negative control (lane 2). (C) close up image of the same gel (boxed in red).

A.

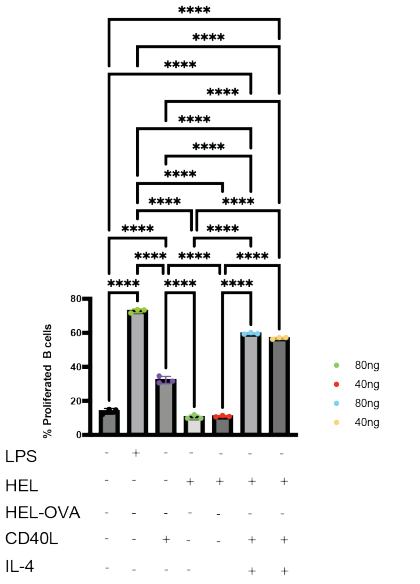
HEL
% Proliferated B cells
80ng
40ng
80ng
40ng
LPS
HEL
HEL-OVA
CD40L
IL-4

B.

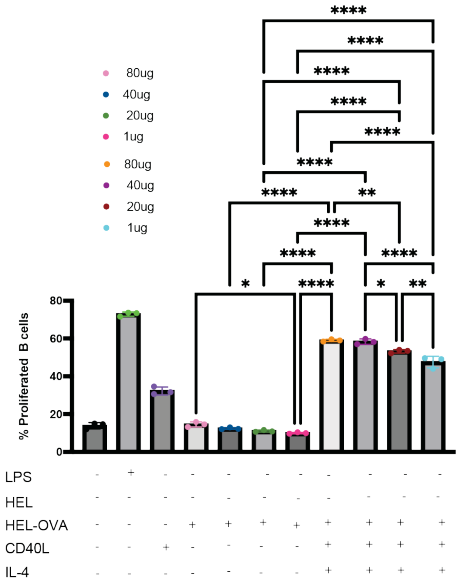
HEL-OVA
80ug
40ug
20ug
1ug
80ug
40ug
20ug
1ug
% Proliferated B cells
LPS
HEL
HEL-OVA
CD40L
IL-4

C.

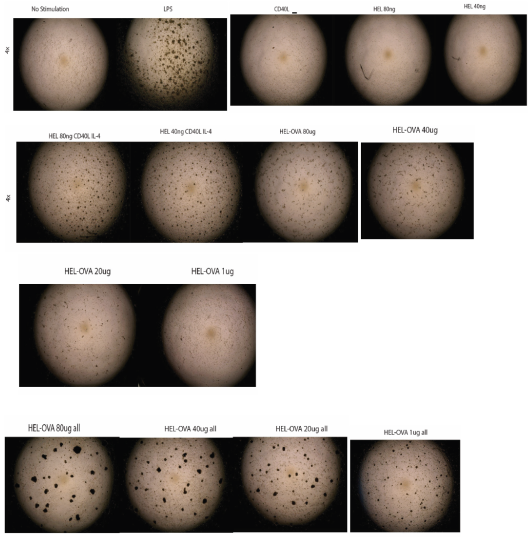
No Stimulation
LPS
CD40L
HEL 80ng
HEL 40ng
HEL 80ng CD40L IL-4
HEL 40ng CD40L IL-4
HEL-OVA 80ug
HEL-OVA 40ug
HEL-OVA 20ug
HEL-OVA 1ug
HEL-OVA 80ug all
HEL-OVA 40ug all
HEL-OVA 20ug all
HEL-OVA 1ug all

D.

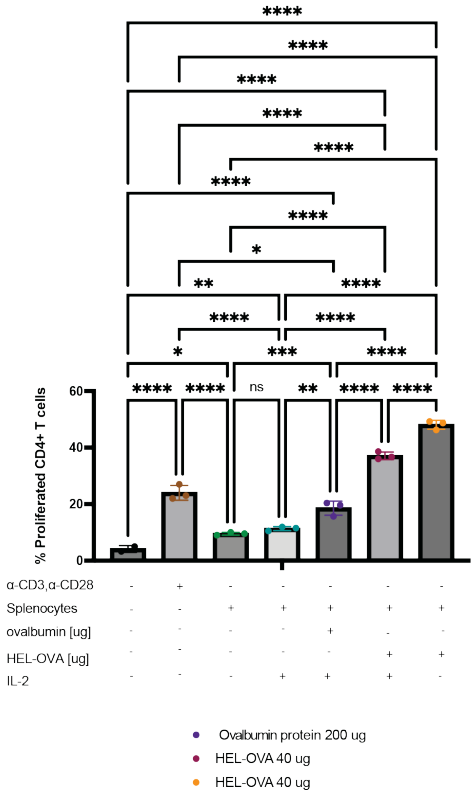
% Proliferated CD4+ T cells
ns
α-CD3,α-CD28
Splenocytes
ovalbumin [ug]
HEL-OVA [ug]
IL-2
Ovalbumin protein 200 ug
HEL-OVA 40 ug
HEL-OVA 40 ug

Figure 6: HEL-OVA conjugate stimulates antigen specific B and T cells

(A) Analysis of CFSE labeled B cells stimulated with varing concentrations of HEL protein (Sigma) or (B) HEL-OVA conjugate. Each condition was done in triplicates (*n*=3) and each symbol is mean ± SD from one culture well. (C) Visualization of B and T cells co-cultured with HEL-OVA at different concentrations. (D) Quantification of mean ± SD of OT-II T cells labeled with CFSE and co-cultured with SW_{HEL} B cells with varying concetrations of HEL-OVA in culturefor 72 hours. Statistics was calculated using 2-way ANOVA. *p < 0.05; **p < 0.01; ***p < 0.001; ****p < 0.0001; ns= not significant. Each symbol is representative of one culture well. Results in A-D are representative of 2 independent experiments.

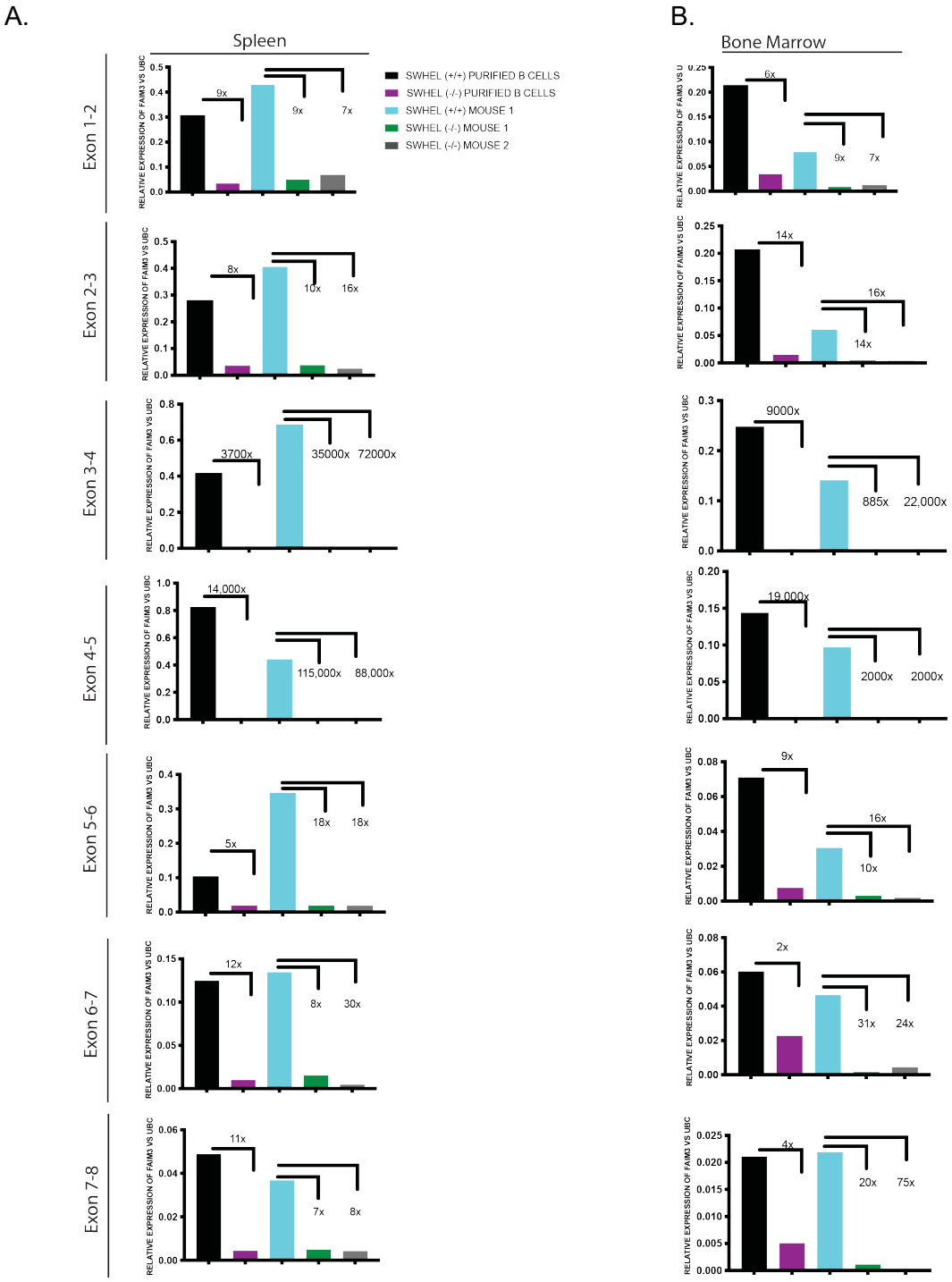

Supplemental Figure 1: Exon boundaries of faim3 in spleen and bone marrow show successful deletion of fcmR. (A-B) Bar charts of each exon boundary in (A) spleen and (B) bone marrow. Bar graphs represented with mean ± SD (*n*=2).

CHAPTER 3:

The FcμR Facilitates Antigen Uptake and Presentation via MHCII by Binding to Soluble and Membrane Bound IgM-Antigen Complexes

Abstract:

The evolutionary conserved immunoglobulin isotype M (IgM) is the first antibody expressed by developing B cells as part of the B cell receptor (BCR) complex and the first to be secreted during an immune response. Previous work has shown that both, secreted (s)IgM and its receptor FcμR, which is expressed predominantly on B cells, are required for maximal IgG responses to immunization and infection, but the mechanisms by which this receptor-ligand pair supports humoral responses is unknown. Confocal and STED imaging was used to demonstrate that SW_{HEL} transgenic B cells, either expressing or not the FcμR, acts as a chaperone for antigen IgM-BCR complexes, significantly increasing antigen internalization, processing, and presentation on MHCII. In a co-culture system with HEL-ovalbumin as antigen, presence of the FcμR on SwHEL B cells supported enhanced proliferation of ovalbumin-specific transgenic OTII CD4 T cells, compared to the SW_{HEL} x FcμR-/- B cells, which was further enhanced by the addition of HEL-specific sIgM. Thus, the FcμR supports T-dependent B cell responses by facilitating cognate T-B interaction.

Introduction

Efficient IgG responses are the basis for most vaccine strategies. The cells that produce antibodies are plasmablasts and plasma cells. The latter are terminally differentiated B cells (Nutt et al., 2015). B cells are a key component of the adaptive immune response. Their differentiation into high affinity antibody-producing plasma cells or memory B cells is a result of activation steps that involve interaction with CD4 T cells via antigen internalization, processing and presentation to CD4+ T cells via MHC class II molecules (Yuseff et al., 2013). This process is facilitated by the internalization of antigen captured by surface B cell receptor (BCR). Following presentation to CD4+ T cells, the B and T cell will become further activated and enter differentiation programs. B cells selected to enter the germinal center reaction are called germinal center B cells and T cells selected to enter the same reaction are called T follicular helper cells (T_{FH}) (Pissani & Streeck, 2014). This reaction leads to the development of both memory B cells and plasma cells.

Antibody producing plasma cells secrete immunoglobulins such as IgG. High affinity IgG antibodies can then neutralize pathogens before they can spread (Martínez-Riaño et al., 2018). Understanding the mechanism for maximal IgG response induction can be applied to vaccine development and design as well as understanding immunity to infections. Numerous experiments investigating the role of sIgM have shown that when secreted IgM is absent, IgG responses are reduced. Previous data from our lab and others showed that mice lacking sIgM and infected with influenza virus showed strong reductions in IgG production, increasing their susceptibility to death and inability

to clear infection compared to controls (Baumgarth et al., 2000; Boes, 2000; Kopf et al., 2002; Nguyen, Kläsener, et al., 2017). In addition, sIgM deficiency also resulted in pathogenic IgG autoantibody appearance (Ehrenstein & Notley, 2010; Nguyen, Graf, et al., 2017). Together, this suggested that sIgM is critical for effective IgG, However, the mechanisms by which sIgM regulates IgG responses, are not understood.

Although sIgM has been reported to bind various Fc receptors, there is only one receptor identified to date that binds to sIgM with high affinity: the FcμR. The FcμR is highly expressed on B cells in humans and mice (Kubagawa et al., 2009; Li et al., 2011; Nguyen, Kläsener, et al., 2017; Ouchida et al., 2012). HeLa cells transfected with a FcμR expression vector were able to bind and internalize IgM-conjugated beads (Shima et al., 2009), suggesting that the FcμR can bind and internalize sIgM-antigen complexes. Recently, our lab showed that mice lacking the FcμR ($FcμR^{-/-}$), have strongly reduced IgG responses after influenza infection, similar to sIgM-deficient mice (Nguyen, Graf, et al., 2017; Nguyen, Kläsener, et al., 2017). Therefore, I hypothesize that the FcμR mediates uptake and processing of sIgM-antigen complexes for antigen presentation to CD4 T cells, resulting in enhanced subsequent IgG responses.

Confocal and STED microscopy following *in vitro* exposure of transgenic "SW_{HEL}" B cells, specific for hen egg lysozyme (HEL), to HEL-BODIPY demonstrated a lack of IgM-BCR "polarization" on SW_{HEL} B cells that lacked the FcμR compared to FcμR-expressing SW_{HEL} B cells. The $FcμR^{-/-}$ cells also retained higher amounts of antigen on their surface compared to the SW_{HEL} x $FcμR^{+/+}$ cells. This reduced antigen-internalization led to diminished peptide-MHCII complex expression and diminished proliferation of antigen-specific CD4 T cells during co-culture. Addition of sIgM further

enhanced antigen presentation by SW_{HEL} x $Fc\mu R^{+/+}$ but not SW_{HEL} x $Fc\mu R^{-/-}$ B cells. This data showed that the FcμR acts as a non-redundant chaperone that optimizes IgM-BCR antigen internalization and processing and sIgM-antigen complex capture to support T-dependent B cell responses.

SW_{HEL} x $Fc\mu R^{-/-}$ B cells have significantly reduced IgG1 responses following immunization *in vivo.*

To better understand how the FcμR plays a role in IgG responses, an *in vivo* model that reflects the diminished IgG responses following influenza infection in the absence of the FcμR on B cells (Nguyen, Graf, et al., 2017; Nguyen, Kläsener, et al., 2017) was created. To do this, a previously published BCR knock-in mouse model (SW_{HEL}) wherein B cells express a knock-in of both, Ig heavy and light chain variable genes from the HYHEL10 hybridoma specific for HEL was crossed with FcμR-/- mice, described previously (Nguyen, Kläsener, et al., 2017), to create SW_{HEL} BCR knock-in mice that either expressed (SW_{HEL} x $Fc\mu R^{+/+}$) or did not express (SW_{HEL} x $Fc\mu R^{-/-}$) the FcμR.

In both strains of mice, about 20% of B cells were HEL-specific, measured by flow cytometry, revealing binding to HEL with a fluorescently-labeled anti-HEL antibody (Brink et al., 2008). Groups of these mice were immunized with 40μg HEL-OVA conjugate (made in-house) mixed with alum, and measured for HEL specific IgM and IgG1 at various time points over 42 days (Fig. 1A). Mice were bled prior to immunization as controls and were boosted subcutaneously with an additional 40ug of HEL-OVA in

alum at day 14 after initial immunization (Fig 1A). HEL specific IgM ELISA showed no significant differences between mice expressing or not the FcμR either prior to boost or after (Fig 1B). In contrast, HEL specific serum IgG1 concentrations in SW_{HEL} x FcμR $^{-/-}$ were significantly reduced by day 21 after immunization and boost, compared to SW_{HEL} x FcμR $^{+/+}$ mice (Fig 1C).

To understand whether the decreased IgG1 levels seen in SW_{HEL} x FcμR $^{-/-}$ mice was due to B cell intrinsic factors, and to establish models with more physiological levels of antigen-specific B cells, mixed bone marrow chimeras (MBCs) were generated. To do this, 2% transgenic SW_{HEL} total bone marrow cells either from SW_{HEL} x FcμR $^{-/-}$ or SW_{HEL} x FcμR $^{+/+}$ mice (both expressing the CD45.2 allo-antigen) and mixed each with 98% bone marrow cells from congenic C57BL/6 mice expressing the CD45.1 marker were used. Mixed bone marrow cells were injected intravenously into lethally irritated CD45.1 mice. After 6 weeks of reconstitution, mice were tail bled and immunized subcutaneously with 40ug HEL-OVA conjugate in alum as previously described in chapter 2 (Fig. 1D). At day 14 after immunization, there was a significant reduction in anti-HEL IgM in the SW_{HEL} x FcμR $^{-/-}$ chimeric mice compared to the SW_{HEL} x FcμR $^{+/+}$ chimeras, while anti-HEL IgM levels at all other timepoints were comparable (Fig. 1E). Conversely, IgG1 levels were significantly reduced in mice lacking FcμR from day 14 and beyond (Fig. 1F). Because all HEL-specific B cells lacked the FcμR in the SW_{HEL} x FcμR $^{-/-}$ chimeras, while 98% of all other cells expressed the receptor, the data show that the receptor supports IgG responses in a B cell intrinsic manner.

The FcμR is expressed on the surface and intracellularly by mature B cells.

To evaluate the FcμR, flow cytometry was used to confirm its expression. For that two lots of mAb MM5 (MBL), 002 and 003, were biotinylated, dialyzed and then used to stain splenocytes from SW_{HEL} x FcμR $^{+/+}$ and SW_{HEL} x FcμR $^{-/-}$ mice. Antibodies were titrated for use in future experiments (Fig. 2A). To understand where the FcμR is localized on the cell in relation to the IgM-BCR, confocal microcopy was used to determine if IgM-BCR and the FcμR are internalized together or separately following B cell antigen encounter. To do this, B cells from SW_{HEL} x FcμR $^{+/+}$ and SW_{HEL} x FcμR $^{-/-}$ spleens were magnetically enriched. B cells were incubated for 30 minutes on ice with HEL-BODIPY antigen and then unbound antigen was washed away and B cells were incubated in a 37-degree water bath for designated time points. B cells were stained with IgM-BCR and FcμR (red, green respectively). Confocal microscopy showed that there was a certain staining background using the anti-FcμR mAb in mice lacking the FcμR, however, the staining intensity was greatly lower compared to SW_{HEL} x FcμR $^{+/+}$ B cells (Fig. 2B). Cell surface/internalized staining shows colocalization of the FcμR with IgM-BCR at time 0 and 15 min (Fig. 2C, D) and to a lesser extent at 60 min (Fig. 2E). Measuring MFI of FcμR in SwHEL x FcμR $^{+/+}$ showed that as early as 15 min the FcμR was internalization, similar to what was seen with IgM-BCR, suggesting that the FcμR is internalized as a complex with IgM-BCR: antigen (Fig. 2F). Surface staining showed that the FcμR was strongly re-expressed at 60 minutes, as was seen also with IgM-BCR

(Fig. 2G). Co-localization of FcμR and IgM-BCR occurred also at 15, and 60 minutes on the surface of the B cell (Fig. 2I). Thus, the data show co-localization of the FcμR with antigen complexed IgM-BCR.

Lack of FcμR in SW_{HEL} -/- B cells cause a delay in IgM-BCR surface re-expression following antigen-triggered internalization

Previous data suggested that FcμR interacts with IgM-BCR to help keep B cells activated during an immune response (Kubagawa et al., 2009; Ouchida et al., 2012).

To understand the role the FcμR plays during an immune response and how it affects BCR-IgM internalization and antigen processing, confocal microscopy was utilized; specifically, to visualize the location of antigen and the IgM-BCR. For that, SW_{HEL} B cells were negatively enriched using magnetic cell separation (Figs. 3A, B). Cells were incubated with antigen (HEL-BODIPY) for 30 minutes on ice, which was subsequently washed away. Cells were then incubated in the 37° water bath for 0, 5, 15, 30, 60, and 120 minutes. To stop antigen processing, cells were washed with ice cold PBS and fixed with PFA, followed by saponin to look at intracellular kinetics (from here on referred to as surface staining, and surface/internalized respectively). Stained IgM-BCR in SW_{HEL} x FcμR $^{-/-}$ showed stronger expression of the IgM-BCR compared to SW_{HEL} x FcμR $^{+/+}$ BCR (Fig. 3C), consistent with what was observed previously with cells from C57BL/6 FcμR-/- mice (Nguyen, Graf, et al., 2017; Nguyen, Kläsener, et al., 2017). Median fluorescent intensity (MFI) of the IgM-BCR on the surface of SW_{HEL} x FcμR-/- B cells did not significantly change from time 0 to 15 min. In contrast, SW_{HEL} x FcμR+/+ B cells showed dynamic changes of the IgM-BCR over this time frame,

suggesting a need for the FcμR for internalization of IgM-BCR: antigen complexes (Fig. 3C). Although both, SW_{HEL} x $Fc\mu R^{+/+}$ and SW_{HEL} x $Fc\mu R^{-/-}$ B cells internalized some IgM-BCR, it is notable that at 15, 30 and 60 minutes, the MFI for the IgM-BCR of SW_{HEL} x $Fc\mu R^{-/-}$ was significantly greater than that of the SW_{HEL} x $Fc\mu R^{+/+}$ B cells, suggesting that although SW_{HEL} x $Fc\mu R^{-/-}$ B cells can internalize IgM-BCR: antigen complexes, their ability to do this efficiently is compromised when the FcμR is absent (Fig. 3D, E). At 60 to 120 min surface IgM-BCR on SW_{HEL} x $Fc\mu R^{-/-}$ B cells remained unchanged (Fig. 3C, D). Due to the changes seen on the surface of B cells with and without the FcμR, the data indicate that the FcμR is involved with internalization and mobilization of the IgM-BCR following antigen encounter.

SW_{HEL} B cells lacking the FcμR show delayed IgM-BCR intracellular mobilization.

To determine the effects of the FcμR on IgM-BCR and antigen processing, permeabilized B cells were studied using the same experimental setup as described (Fig 3) to measure intracellular localization of the IgM-BCR with and without the FcμR. The MFI of IgM-BCR at 60 and 120 min in SW_{HEL} x $Fc\mu R^{-/-}$ B cells did not significantly change (Fig. 4A), as seen for the surface staining as well (Fig. 3).

Cell polarity is a mechanism in which a B cell can rapidly polarize their microtubule organizing center (MTOC) and other molecules such as MHCII+ lysosomes. It is thought to help acquire antigen and optimize their activation (Yuseff et al., 2013). Notably, visualization of cell polarization was apparent in SW_{HEL} x $Fc\mu R^{+/+}$ B cells but

was largely absent in SW_{HEL} x $Fc\mu R^{-/-}$ B cells at 60 min and at 120 min (Fig. 4B). Overall, the IgM-BCR MFI was significantly higher in SwHEL x $Fc\mu R^{-/-}$ B cells at time 0, as previously shown (Fig. 3). However, at all other time points measured, the signal was significantly reduced compared to that of the SW_{HEL} x $Fc\mu R^{+/+}$ B cells (Fig 4C). Collectively these results show that the absence of the FcμR leads to delayed mobilization of the IgM-BCR.

FcμR supports antigen internalization

To visualize location of antigen during an immune response, B cells were enriched from SW_{HEL} x $Fc\mu R^{+/+}$ and SW_{HEL} x $Fc\mu R^{-/-}$ mice using the experimental set up as outlined in Figure 3. Quantification of antigen MFI in SW_{HEL} x $Fc\mu R^{-/-}$ B cells showed no significant changes at 30 min compared to 120 min (Fig. 5A). It was also evident from confocal imaging that at 120 min most of the antigen was internalized by SW_{HEL} x $Fc\mu R^{+/+}$ B cells, whereas SW_{HEL} x $Fc\mu R^{-/-}$ B cells still showed prominent antigen staining (Fig. 5B).

Merged images show that there was clear polarization of antigen and IgM-BCR as early as 15 minutes in SW_{HEL} x $Fc\mu R^{+/+}$ but not in SW_{HEL} x $Fc\mu R^{-/-}$ B cells (Fig 5C). At 2 hours, there was significantly more antigen present in SW_{HEL} x $Fc\mu R^{-/-}$ B cells (Fig 5D), suggesting that these B cells were unable to process antigen efficiently. Together, the data showed that the FcμR supports antigen internalization, and that its absence slows down efficient antigen processing.

STED imaging shows an accumulation of antigen on the surface of B cells lacking the FcμR

To observe antigen internalization and processing at higher resolution, particularly to differentiate between cell surface and internalized antigen, Stimulated Emission Depletion (STED) microscopy was used. In addition, staining of a surface marker expressed on all B cells (CD45R/B220) that does not immediately internalize after B cell activation was done to visualize the cell surface. The cells were further co-stained for IgM-BCR and HEL-BODIPY, which was used to visualize antigen. At time 0, there was successful binding of antigen to both, SW_{HEL} x $Fc\mu R^{+/+}$ and SW_{HEL} x $Fc\mu R^{-/-}$ B cells. (Fig. 6A). SW_{HEL} x $Fc\mu R^{-/-}$ B cells at all time points had increased amounts of antigen on the surface compared to SW_{HEL} x $Fc\mu R^{+/+}$ B cells, where antigen was minimal (Fig. 6B). In addition, a unique phenotype was seen amongst the SW_{HEL} x $Fc\mu R^{-/-}$ B cells at 15- and 30-min time points, which was termed “membrane kissing”, where two antigen-specific B cells were seen to form apparent membrane fusion (Fig. 6C). IgM-BCR was seen along the shared cell membranes, suggesting that there was an exchange of IgM- BCR between these cells. Collectively, the data suggest that the FcμR acts as a chaperone for IgM-BCR in antigen processing and presentation.

Lack of FcμR reduces antigen internalization when antigen is continuously provided.

To understand whether continuous exposure to antigen by SW_{HEL} B cells impacted the B cells' ability to internalize antigen and/or IgM-BCR, cultures of SW_{HEL} B cells were set up and HEL-BODIPY was provided as antigen throughout the study.

Consistent with what was observed at steady state (Nguyen, Kläsener, et al., 2017), SW_{HEL} x $Fc\mu R^{-/-}$ B cells expressed more surface IgM-BCR at time 0 compared to SW_{HEL} x $Fc\mu R^{+/+}$ B cells (Fig. 7A). As early as 15 minutes of continuous antigen exposure, there was obvious polarization in SW_{HEL} x $Fc\mu R^{+/+}$ B cells but not SW_{HEL} x $Fc\mu R^{-/-}$ B cells (Fig. 7B). At 45 minutes there was a visible difference in the polarization of IgM-BCR and antigen in SW_{HEL} x $Fc\mu R^{+/+}$ B cells compared to SW_{HEL} x $Fc\mu R^{-/-}$ B cells (Fig. 7C). IgM-BCR and antigen MFI at 60 and 120 min was significantly higher in SwHEL x $Fc\mu R^{-/-}$ B cells compared to controls (Fig. 7D-F), suggesting that SW_{HEL} x $Fc\mu R^{-/-}$ B cells are unable to process antigen and likely cannot present antigen as efficiently as SW_{HEL} x $Fc\mu R^{+/+}$ B cells, both when antigen is limited, or when antigen is present throughout.

Lack of $Fc\mu R^{-/-}$ expression affects LAMP-1 expression

To discern whether the lack of antigen presentation in SW_{HEL} x $Fc\mu R^{-/-}$ B cells is due to a defect of endosomal trafficking of antigen-IgM complexes to the lysosome, late endosome (LE)/lysosomal marker lysosomal-associated membrane protein 1 (LAMP-1) was used. In this work, confocal microscopy to follow antigen through the LAMP-1+ B

cells was utilized. There were no significant changes in LAMP-1+ expression in SW_{HEL} x $Fc\mu R^{+/+}$ and SW_{HEL} x $Fc\mu R^{-/-}$ B cells at times 0, 15, and 120 minutes. However, at 30 and 60 min SW_{HEL} x $Fc\mu R^{-/-}$ B cells had significantly lower LAMP-1+ expression (Fig. 8A). At time 0 LAMP-1 expression in SW_{HEL} x $Fc\mu R^{+/+}$ and SW_{HEL} x $Fc\mu R^{-/-}$ B cells was comparable (Fig. 8B). Stronger co-localization of BCR and LAMP-1 occurred in the $Fc\mu R^{+/+}$ B cells compared to SW_{HEL} x $Fc\mu R^{-/-}$ as well as antigen colocalization at 30 min (Fig. 8C). At 60 min there was still significantly decreased expression of LAMP-1 in SW_{HEL} x $Fc\mu R^{-/-}$ B cells (Fig. 8D). The kinetics of LAMP-1 expression among SW_{HEL} x $Fc\mu R^{+/+}$ B cells showed no significant changes other than at times 60 and 120 min compared to time 0 (Fig. 8E). Conversely, SW_{HEL} x $Fc\mu R^{-/-}$ B cells had significant LAMP-1 fluctuations from 15 -30 min and 60 -120 minutes (Fig, 8F). Collectively, this data suggests that there is LE/lysosomal misdirection when FcμR expression is absent and that IgM-BCR antigen complexes cannot get to the lysosome effectively in the absence of the FcμR.

Lack of $Fc\mu R^{-/-}$ suggests a different endosomal pathway is used to internalize antigen

The results seen when the $Fc\mu R^{-/-}$ is absent were surprising, as we are unaware of any literature that describes the FcμR in an antigen processing and presentation context. To gain further insight into differences in endosomal compartments that could be utilized with FcμR during B cell processing, splenocytes were taken from SW_{HEL} x $Fc\mu R^{+/+}$ and SW_{HEL} x $Fc\mu R^{-/-}$ mice, and incubated with HEL-BODIPY on ice for 30

minutes. Once antigen was washed away, splenocytes were incubated at 37C and then stained with intracellular markers and co-stained for IgM-BCR (IgM, alexa488), DAPI and HEL-BODIPY. We looked at early endosome antigen 1 (EEA1) and a slow recycling G protein, Rab11.

EEA1 is a well characterized protein that is present in early endosomes and is implicated in docking of endocytic vesicles before fusing with early endosomes (Wilson et al., 2000). At 60 minutes, there was clear expression of EEA1 in SW_{HEL} x $Fc\mu R^{+/+}$ splenocytes but little to no expression in SW_{HEL} x $Fc\mu R^{-/-}$ splenocytes (Fig. 9A). This data suggest that EEA1 is abrogated when the FcμR is absent. However, further experiments are needed to quantify and visualize EEA1 at different time points.

In classical antigen processing and presentation, there is constant intracellular recycling of vesicles with cargo (such as IgM-BCR: antigen complexes) and vesicles being transported to the cell surface (such as MHC-II) (Drake et al., 1997). Rab11 has been shown to be involved with cellular trafficking pathways such as recycling endosomes, post-Golgi vesicles, late recycling and other cell processes (Welz et al., 2014). To visualize if antigen as well IgM-BCR can be recycled with and without the FcμR, confocal microscopy was utilized. At time 0 there appeared to be no significant differences in Rab11 expression between SW_{HEL} x $Fc\mu R^{+/+}$ and SW_{HEL} x $Fc\mu R^{-/-}$ B cells (Fig. 9B). However, at 60 minutes Rab11 expression was seen in SW_{HEL} x $Fc\mu R^{+/+}$ but not SW_{HEL} x $Fc\mu R^{-/-}$ B cells, indicative that there is slowed or halted recycling in the absence of the FcμR (Fig, 9C). Further experiments are needed to quantify and visualize Rab11 at different time points.

IgD-BCR is strongly expressed on B cells and can bind antigen. Additionally, IgM

and IgD can “replace” each other (Noviski et al., 2018). To test whether IgD-BCR on SW_{HEL} B cells can also bind antigen and be internalized with or without the FcμR, confocal microscopy was used. Clear expression of IgD (green) was seen at time 0 in SW_{HEL} x $Fc\mu R^{+/+}$ B cells, but very little expression in SW_{HEL} x $Fc\mu R^{-/-}$ cells (Fig. 9D). At 60 min, IgD expression was comparable (Fig. 9D). Importantly, there was no co-localization of antigen with the IgD-BCR at times 0 and 60 minutes (Fig, 9D). Previously our lab showed that in B cell development the FcμR restrains IgM-BCR but not IgD-BCR surface expression (Nguyen, Kläsener, et al., 2017). Given these apparent conflicting results further studies on the IgD-BCR are required.

The data indicate that the FcμR affects effective endosomal processing of antigen following IgM-BCR internalization.

Lack of $Fc\mu R^{-/-}$ on B cells reduces formation of surface peptide-MHC-II complexes

To quantify B cell MHC-complexes, HEL-OVA conjugate coupled to an immunogenic IEα peptide that can be presented on I-A^b MHCII was used. Enriched B cells from SW_{HEL} mice were incubated with HEL alone or HEL- IEα-OVA conjugates. The IEα peptide:I-A^b MHC II complexes on B cells were then quantified by flow cytometry, using a monoclonal antibody (Y-Ae) that detects these complexes. Exposure of B cells to HEL- IEα-OVA but not HEL alone resulted in staining with Y-Ae (Fig. 10A).

Comparison of B cells from SW_{HEL} mice either expressing or not the FcμR demonstrated that as early as 15 minutes post antigen exposure, there was a significant reduction in IEα-MHCII complexes on the surface of B cells lacking the FcμR (Fig. 10B,

C). Thus, the FcμR is required for maximal presentation of antigen via MHC-II.

Soluble IgM supports antigen uptake and presentation by MHC-II

Previously, we showed that the lack of sIgM resulted in significantly reduced IgG responses (Nguyen, Graf, et al., 2017). To determine if sIgM affects peptide-MHC-II complex formation, I utilized HEL-specific sIgM from hybridoma NB 9.1 in splenocyte cultures, in which cells from SW_{HEL} x FcμR $^{+/+}$ and SW_{HEL} x FcμR$^{-/-}$ mice were isolated and incubated with HEL- IEα-Ova for 30 min on ice. Antigen was then washed away and cells were incubated for up to 60 minutes at 37C with or without HEL-IgM, at which time cells were stained for flow cytometry (Fig. 11A). Cells kept at 4C throughout the 1h time course were used as negative controls.

There was a significant difference in peptide MHCII expression, as assessed by measuring the frequencies of Y-Ae+ B cells from SW_{HEL} x FcμR$^{+/+}$ (~45%) and SW_{HEL} x FcμR $^{-/-}$ (~18%) mice (Fig. 11A). Addition of sIgM with HEL- IEα-Ova significantly increased Y-Ae frequencies in SW_{HEL} x FcμR$^{+/+}$ (~60%) but not SW_{HEL} x FcμR$^{-/-}$ (~35%) B cells (Fig. 11A). B cells that contained SW_{HEL} x FcμR$^{+/+}$ showed a significant difference as early as 30 minutes after transfer to 37C, compared to those that lacked it (Fig. 11B). However, at 30 min, the addition of HEL-specific sIgM did not further enhance Yae staining compared to cells that received IEα peptide: I-A^b alone (Fig. 11B). At 60 min, there was a significant increase in antigen presentation by B cells compared to time 0 and this was enhanced with sIgM at 60 minutes in SW_{HEL} x FcμR $^{+/+}$ B cells (Fig. 11B).

To confirm that this effect was specific to SW_{HEL} B cells and that antigen

presentation was not due to other antigen presenting cells present in the spleen, such as macrophages or dendritic cells, I gated on HEL negative cells and measured Y-Ae staining. At all timepoints, as well as the 4C control, Y-Ae was not expressed (Fig. 11C). Thus, the Y-Ae expression was based solely on B cells suggesting that B cells expressing the FcμR$^{+/+}$ can present antigen significantly better than B cells lacking it. An effect that was enhanced at 60 minutes with sIgM.

Analysis of SW_{HEL} x FcμR $^{+/+}$ and SW_{HEL} x FcμR $^{-/-}$ splenocytes incubated with HEL- IEα-Ova showed that there was a significantly higher expression of Y-Ae at 60 minutes compared to 0 min (Fig. 11D). However, when the two genotypes were compared side by side, Y-Ae staining was stronger in SW_{HEL} x FcμR $^{+/+}$ compared to FcμR-/- B cells (Fig. 11E). The data demonstrate that the FcμR participates in IgM-BCR:antigen as well as sIgM-antigen complex internalization and peptide presentation on MHCII.

Lack of FcμR $^{-/-}$ reduced cognate T-B interaction and T cell proliferation.

The results seen suggest that B cells lacking the FcμR are unable to present antigen efficiently. To understand whether the observed lack of MHCII peptide complex formation affects T-B interaction and T cell proliferation, SW_{HEL} x FcμR $^{+/+}$ and SW_{HEL} x FcμR $^{-/-}$ B cells were enriched and co-cultured with enriched ovalbumin-specific OT-II CD4 T cells in the presence of varying doses HEL-OVA conjugate (Fig. 12A). Results showed antigen-dose dependent increases in proliferation of OT-II T cells in the presence of FcμR expressing B cells but not those lacking the receptor. (Fig. 12B).

Consistent with the reduced T cell proliferation, the MFI of MHCII expression by SW_{HEL} x $Fc\mu R^{-/-}$ B cells were significantly reduced compared to the FcμR-expressing cells at all timepoints (Fig. 12C). MFI in SW_{HEL} x $Fc\mu R^{+/+}$ showed a significant decrease in MHCII when given 0.3 ug/ml of HEL-OVA conjugate and SW_{HEL} x $Fc\mu R^{-/-}$ B cells showed no difference at this concentration (Fig. 12D). The data demonstrate that the FcμR supports CD4 T cell-B cell interaction and T cell activation.

Secreted IgM enhances cognate T-B interaction when FcμR is present

To further assess whether sIgM aids in "mopping" up antigen to bring to the IgM-BCR as well as the FcμR, flow cytometry was used. Purified SW_{HEL} x $Fc\mu R^{+/+}$ and SW_{HEL} x $Fc\mu R^{-/-}$ B cells and CFSE labeled OT-II T cells were co-cultured in presence or absence of HEL-OVA conjugate and varying doses of soluble IgM for 3 days. OT-II T cell proliferation was measured as a readout of their activation by B cells. In cultures with HEL-OVA conjugate, SW_{HEL} x $Fc\mu R^{-/-}$ B cells and OT-II T cells, T cell proliferation was significantly reduced compared to cultures with SW_{HEL} x $Fc\mu R^{+/+}$ B cells (Fig. 13A). With the addition of sIgM at the highest concentration (10ug/ml), there was a drastic and significant increase of proliferation of T cells cultured with SW_{HEL} x $Fc\mu R^{+/+}$ B cells but not with SW_{HEL} x $Fc\mu R^{-/-}$ B cells (Fig. 13A). Conversely, addition of sIgM to SwHEL x $Fc\mu R^{-/-}$ B cells did not significantly increase T cell proliferation, indicating that enhancement of antigen presentation by sIgM requires the FcμR (Fig. 13B). Collectively, these results reveal a novel function for the FcμR in antigen internalization, processing and presentation following interaction with both, membrane-bound and sIgM.

Discussion

B cells are antigen presenting cells whose mode of antigen uptake is thought to be exclusively through binding of antigen by the IgM-BCR. Previous studies showed that lack of sIgM or lack of FcμR on B cells resulted in diminished IgG responses after influenza virus infection (Nguyen, Graf, et al., 2017) . For the first time, this study revealed a novel role of the FcμR in antigen processing and presentation, and addition of sIgM enhanced this process. Various stains, whether confocal, or flow cytometry were used to visualize and measure the role of the FcμR and sIgM (Fig. 14A). The differences seen between SW_{HEL} x FcμR $^{+/+}$ and SW_{HEL} x FcμR $^{-/-}$ B cells are summarized in (Fig 14B).

Unexpectedly, SW_{HEL} x FcμR $^{-/-}$ B cells showed cell to cell membrane touching (as termed “kissing”) at 15 minutes (data not shown) and 30 minutes via confocal and STED microscopy (Fig. 4), whereas in SW_{HEL} x FcμR $^{+/+}$ B cells, this phenotype was not detected at any time point. Previously reported, IgM-BCR can become donated to bystander B cells to present antigen to CD4+ T cells (Quah et al., 2008). This could be a mechanism enacted by SwHEL x FcμR $^{-/-}$ B to receive continuous activation to internalize IgM-BCR without FcμR. However further experiments are needed to test this.

Various endosomal markers (EEA1, RAB11, LAMP-1) showed that FcμR is implicated in antigen internalization and processing and its absence abrogates their roles. Thus, the FcμR is a chaperone for the IgM-BCR and the presence of this receptor aids in internalization of the IgM-BCR: antigen complexes and is enhanced with the addition of sIgM.

Materials and Methods:

Mice:

BCR transgenic mice expressing a knock-in of a BCR specific for HEL (SW_{HEL}) were obtained from Dr. Roger Sciammas (UC Davis, Davis, CA) with kind permission from Dr. Robert Brink, (Centenary Institute, Sydney, Australia) and bred onto $Fcmr^{flx/flx}$ mice to the desired genotype. All mice were kept in specific-pathogen-free housing, in HVAC-filtered filter-top cages and were monitored for the absence of 17 common mouse pathogens. Mice were euthanized by overexposure to carbon dioxide. The Animal Use and Care Committee of the University of California, Davis, approved all procedures and experiments involving animals.

Generation of Chimeras

Mixed bone marrow chimeras were generated by adoptively transferring 2% SW_{HEL} (CD 45.2) and 98% wildtype CD 45.1 bone marrow cells into lethally irradiated CD45.1 C57BL/6 wildtype mice intravenously. Chimeric mice rested for 6 weeks before use.

HEL-OVA immunization and boost

Mice were injected subcutaneously in the left hind leg with 40ug of HEL-OVA conjugate mixed with Imject alum (Thermofisher Scientific). Mice were boosted 14 days later in the same leg with the same amount of antigen.

Immunofluorescence and Confocal Microscopy

Splenic B cells were negatively enriched from SW_{HEL} x FcμR $^{+/+}$ and SW_{HEL} x FcμR $^{-/-}$ mice by autoMACS (anti-CD 90.2 (30-H12), anti-F4/80 (BM8),anti-Gr-1 (RB6-8C5), and anti-NK1.1 (PK136) biotin). B cells were incubated with HEL-BODIPY on ice for 30 minutes. Antigen was washed away 3 times and B cells were stained with IgM^b biotin followed by SA-Alexa fluor 488 each for 20 minutes. For membrane markers, Rab11a, LAMP-1, EEA1 were incubated with purified B cells for 30 minutes followed by Alexa fluor 647 anti-rabbit Ig. FcμR was biotinylated and was followed by SA-Alexa 488 for 20 minutes. Cells were transferred into 30ul PBS to slides and mounted with Prolong Diamond Antifade Mountant. Images were acquired on a Leica 100X microscope. For STED Imaging IgM-BCR (331), B220 (in house) and HEL-BODIPY (in house) was imaged on Leica 100X and depletion was done with a 592 nm laser for alexa488, and 775 nm laser for both Alexa 647 and HEL-BODIPY TRX.

Quantification for confocal images were analyzed using Bitplane Imaris software. The spot function was used to fit the cell nuclei, spots were manually corrected to make sure all cells were included. Spots were enlarged 1.5 to cover the cells. Cell positions and mean intensities for all channels were read and touching cells excluded using MATLAB code written for this purpose.

HEL-BODIPY

BODIPY TR-X NHS Ester (succinimidyl Ester) (ThermoFisher Scientific) was prepared and conjugated to HEL protein (sigma) using the calculation provided by manufacturer. Conjugate was purified using a Nap-5 column (Cytiva) and stored in 4 degrees for use.

Magnetic B cell Enrichment

Spleen (for SW_{HEL} B cells) and lymph node (for OT-II T cells) cell suspensions were treated with Fc block. B and CD4 T cells were negatively enriched by autoMACS (Miltenyi Biotech) using depletion cocktails that consisted of a mixture of biotinylated antibodies. For B cells: ((anti-CD90.2 (30-H12), anti- Gr-1(RB6-8C5) anti F4/80 (BM8), and anti-Nk1.1(PK136)). For CD4 T cells: anti- Gr-1(RB6-8C5) anti F4/80 (BM8), anti-Nk1.1(PK136), anti-CD19 (D3), anti TCR$\gamma\lambda$ (GL-3), anti- CD11b (M1/70), anti CD8a (53-6.7.3.1). Anti-biotin microbeads (Miltenyi Biotech) were used to label the antibody-stained cells. Nylon-filtered bone marrow and splenocytes were separated using autoMACS (Miltenyi Biotech).

HEL^{2X}-IEα Protein

Protein was gifted by Sciammas lab (Cook et al., 2021) and was made in
Purified B cells were incubated with protein for 30 minutes on ice and then washed away. Y-Ae/Ea 52–68 mAb (eBioY-Ae) was obtained commercially (eBioscience) and used to stain surface I-A^b-Ieα complexes.

Flow Cytometry

Spleen cells were stained with CD19 (1D3), IgM (331), and Y-Ae (Invitrogen) followed by streptavidin-APC (Invitrogen), CD4 (GK1.5), HYHEL9 mAb (first incubated for 20 min with 1ug/ml of HEL protein ((Sigma), followed by HYHEL9) and dead cells were excluded using live/dead (Invitrogen). Single- cell suspensions from lymph nodes and spleens were prepared by using frosted end microscope slides and pressing the tissues with pressure. Red Blood cells were lysed with ACK buffer (150 mM NH4Cl, 10 mM KHCO3, 10 mM EDTA) for 1 minute on ice. Cell counts were determined using trypan blue and a hemocytometer or using the cellometer (Nexcelom Biosciences). All staining was performed using staining media (Buffered saline solution: 0.168 M NaCl, 0.168 M KCl, 0.112 M CaCl2, 0.168 M MsSO4, 0.168 M KH2PO4, 0.112 M K2HPO4, 0.336 M HEPES, 0.336 M NaOH, containing 3.5% heat-inactivated, filtered newborn calf serum, 1 mM EDTA, 0.02% sodium azide) for 20 minutes on ice. FcγR receptors were blocked by incubation of cells with anti-CD16/32 mAb for 20 minutes. FACS data were analyzed using FlowJo software (BD).

In vitro CFSE labeling and co-culture of B and T cells

B cells were cultured after autoMACS enrichment and then cultured at $2.25x10^5$ cells per well in medium. Splenocytes and/or OT-II T cells were labeled using 0.5 μm CFSE diluted in sterile PBS at cell concentration of $1x10^7$ cells/ml for 10 minutes at 37°C, washed twice with quenching media (10% NCS) and resuspended in staining medium. T cells were cultured after autoMACS enrichment and then cultured at 1 $x10^5$ cells per well in medium. Cultures contained HEL-OVA conjugate, Positive control:

α-CD3 (10mg/ml), α-CD28, in 96-well flat-bottom plates for 72 hours at 37°C in 5% CO2. Purities for B and T cells were above 90%. Analysis of B and T cells was done via flow cytometry and proliferation was measured using FlowJo software.

Generation of HEL-specific IgM

Generation of anti-mouse IgM are secreted by hybridomas from splenocytes taken from a 3-month-old BALB/c female mouse that was immunized with 50μg of HEL protein mixed in Complete Freund's Adjuvant. 5 days later, splenocytes (50 x 10^6) were fused with myeloma line X63 (25 x 10^6) in PEG for 3 minutes at 37 degrees and plated in 10 96-well flat bottom plates in HAT medium. Specificity of HEL IgM was done with HEL-coated plates (1 ug/ml) with anti-mouse IgM or anti-kappa secondary reagents. Positive cultures were cloned and expanded.

ELISA:

IgM and IgG1 were measured by first coating 10ug/ml HEL (Sigma) and incubated overnight at room temperature. Plates were then washed and blocked for 1 hour with ELISA blocking buffer (0.1% milk powder, 0.05% Tween 20). 2-fold serially diluted serum samples in PBS were incubated for 2 hours. Plates were incubated with biotinylated anti-IgM or IgG1 for 1 hour. Revealing was done with incubation of streptavidin (SA)-horseradish peroxidase and subsequently with substrate (10 mg/ml 3,3V,5,5V-tetramethylbenzidine (TMB) in 0.05 mM citric acid, 3% hydrogen peroxide). Reactions were stopped with 1 N sulfuric acid and absorbance was read at 450 nm and

reference wavelengths of 595 nm (Molecular Devices, Spectramax). A standard curve was made to calculate concentration of anti-IgM or IgG1 antibody.

Generation of recombinant anti-HEL IgG

HEL-specific IgM and IgG1 was generated by transfecting Chinese Hamster Ovary (CHO) cells with HEL IgM or IgG1 heavy and light chain plasmids (kind gift of Dr. R. Brink, Centenary Institute, Sydney Australia) at a ratio of 4:1 Kappa Light chain DNA to heavy chain DNA. Supernatants were harvested and stored in -80.

Statistical analysis

Statistical analysis was done using one-way ANOVA or 2-way ANOVA function with Prism software (GraphPad). *$p < 0.05$; **$p < 0.01$; ***$p < 0.001$; ****$p < 0.0001$; ns= not significant. All data are shown as mean $\pm$ standard deviation unless otherwise noted.

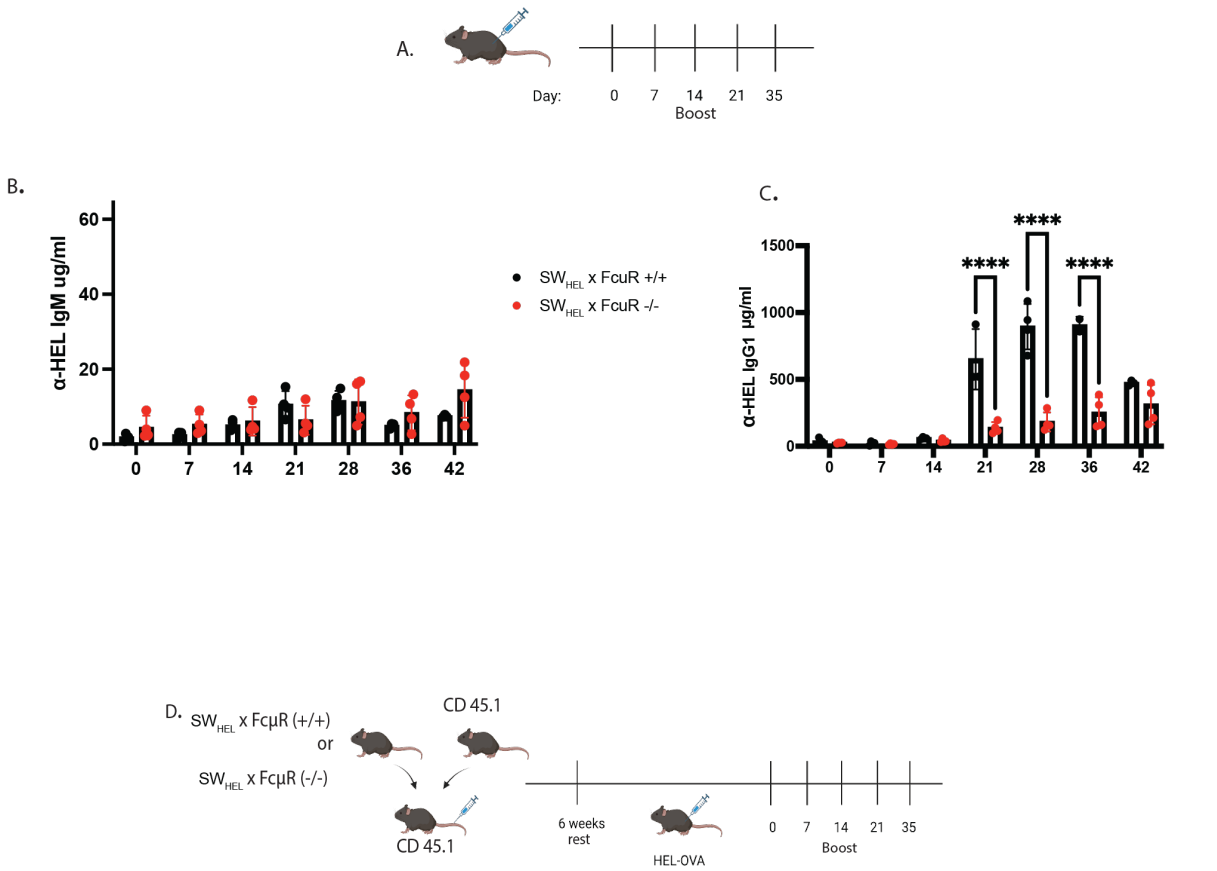
A.
Day: 0 7 14 21 35
Boost
B.
α-HEL IgM ug/ml
SW$_{HEL}$ x FcuR +/+
SW$_{HEL}$ x FcuR -/-
C.
α-HEL IgG1 µg/ml
****
D.
SW$_{HEL}$ x FcµR (+/+)
or
SW$_{HEL}$ x FcµR (-/-)
CD 45.1
CD 45.1
6 weeks rest
HEL-OVA
0 7 14 21 35
Boost
E.
α-HEL IgM ug/ml
SW$_{HEL}$ x FcuR +/+
SW$_{HEL}$ x FcuR -/-
F.
α-HEL IgG1 ug/ml

Figure 1: IgM and IgG1 responses with HEL-OVA conjugate *In vivo*.

(A) Schematic of experimental layout. SW_{HEL} x FcμR+/+ and SW_{HEL} x FcμR-/- mice were injected with 40ug/ml of HEL-OVA conjugate via subcutaneous injection. Mice were bled via tail and HEL specific antibody response for (B) IgM and (C) IgG1 were measured by ELISA. (D-F) IgM and IgG1 responses with HEL-OVA conjugate in mixed bone marrow chimera mice. (D) Schematic of experimental layout; To generate chimera in which only small numbers of B cells are specific for the immunogen, mixed bone marrow (BM) chimeras were generated. BM cells were injected via tail vein into groups of lethally irradiated CD45.1 mice. After 6 weeks reconstitution, SW_{HEL} x FcμR+/+ and SW_{HEL} x FcμR-/- chimeras were injected with 40ug/ml of HEL-OVA conjugate via subcutaneous injection. Mice were bled via tail vein and (E) HEL specific IgM and (F) IgG1 concentrations were measured by ELISA. Bar graphs represent the mean ± SD serum concentrations from (*n*=4) mice (fig 1B,1C) and (*n*=7) (Fig 1E,1F). Each dot represents results from one mouse. Statistics were calculated using one-way ANOVA. *p < 0.05; **p < 0.01; ***p < 0.001; ****p < 0.0001; ns= not significant.

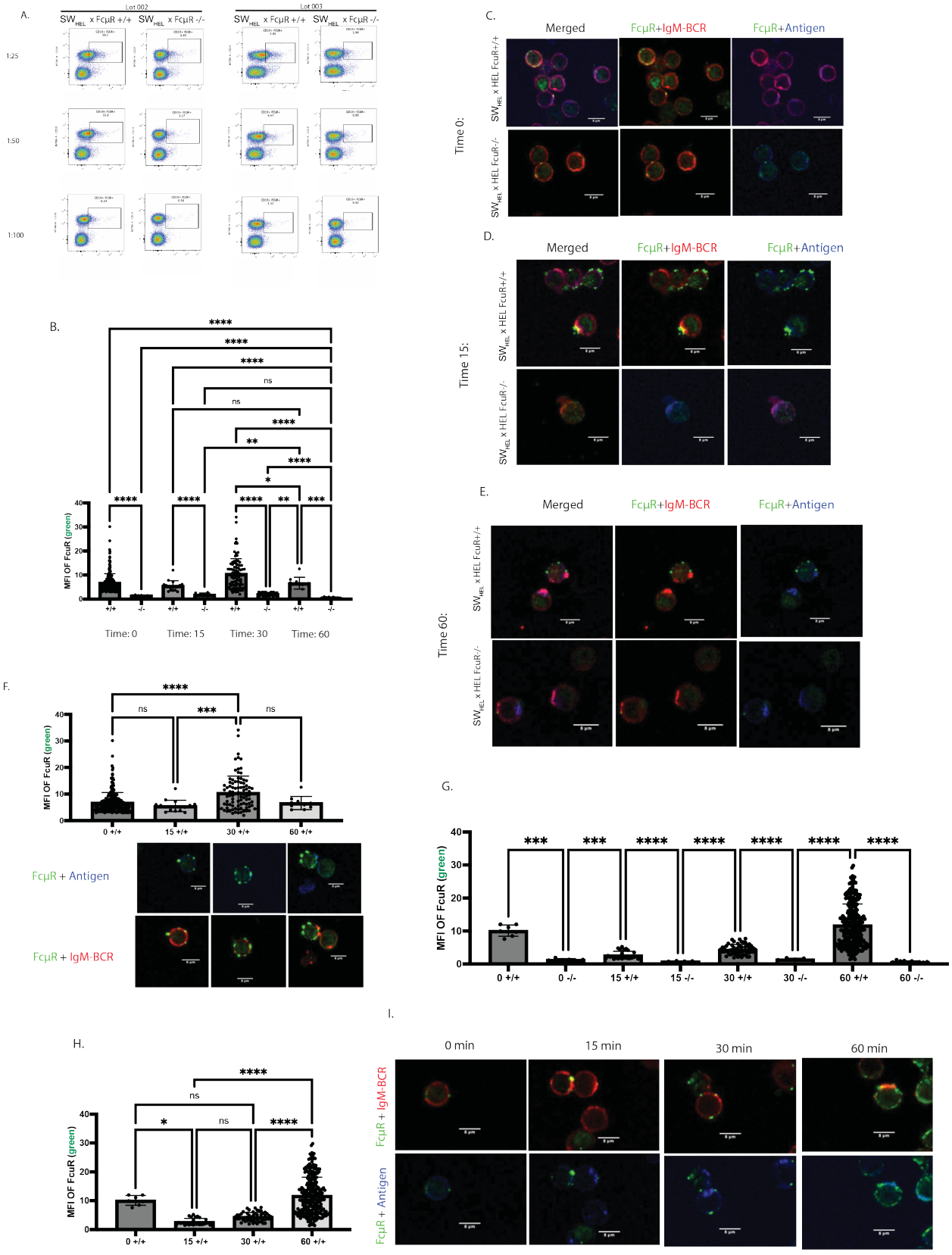
A.
Lot 002
Lot 003
SWHEL x FcμR +/+
SWHEL x FcμR -/-
1:25
1:50
1:100
B.
MFI OF FcuR (green)
Time: 0
Time: 15
Time: 30
Time: 60
C.
Merged
FcμR+IgM-BCR
FcμR+Antigen
Time 0:
SWHEL x HEL FcuR+/+
SWHEL x HEL FcuR-/-
D.
Time 15:
E.
Time 60:
F.
FcμR + Antigen
FcμR + IgM-BCR
G.
0 +/+
0 -/-
15 +/+
15 -/-
30 +/+
30 -/-
60 +/+
60 -/-
H.
I.
0 min
15 min
30 min
60 min

Figure 2: FcμR expression colocalizes with IgM-BCR on surface and intracellularly. (A) Pseudocolor plots show staining of spleen cells from indicated mouse strains with anti-FcμR mAb MM5 with two different lots that were conjugated to biotin and titrated. (B) MFI ± SD of permeabilized B cells from SW_{HEL} x FcμR+/+ and SW_{HEL} x FcμR-/- B cells at indicated time points (*n=177 cells* for SW_{HEL} x FcμR+/+ and *n=16 cells for* HEL x FcμR-/- B cells). (C-E,). Confocal image of single plane images of intracellularly/surface of merged, FcμR IgM-BCR, and FcμR-antigen wherein IgM- BCR (red) ,FcμR (green) and antigen (Blue) at (C) 0 minutes (D) 15 minutes (E) and 60 minutes. (F) MFI ± SD with single place confocal images below at time 15, 30 and 60 minutes. (G-H) MFI ± SD of PFA B cells from SW_{HEL} x FcμR+/+ and SW_{HEL} x FcμR-/- B cells at indicated time points (*n= 76 cells* for SW_{HEL} x FcμR+/+ and *n=18 cells for* SW_{HEL} x FcμR-/- B cells) at indicated time points. (I) SW_{HEL} x FcμR+/+ with representative single plane images at indicated time points. All bar graphs were calculated using one-way ANOVA *p < 0.05; **p < 0.01; ***p < 0.001; ****p < 0.0001; ns= not significant. This experiment was done once. Each dot represents a cell.

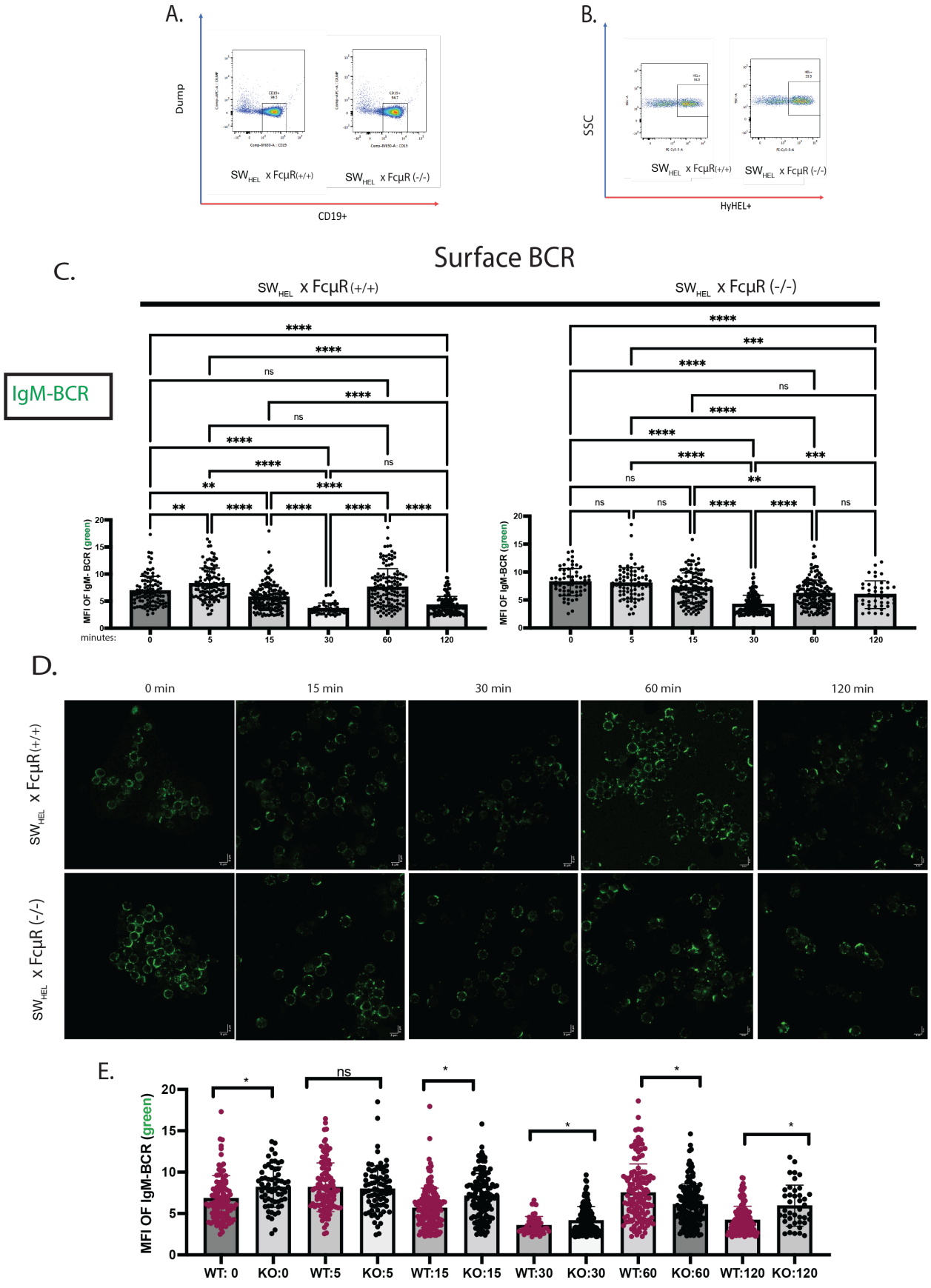
A.
Dump
CD19+
SW HEL x FcμR(+/+)
SW HEL x FcμR (-/-)
B.
SSC
HyHEL+
SW HEL x FcμR(+/+)
SW HEL x FcμR (-/-)
C.
Surface BCR
SW HEL x FcμR (+/+)
SW HEL x FcμR (-/-)
IgM-BCR
MFI OF IgM- BCR (green)
MFI OF IgM-BCR (green)
minutes:
0
5
15
30
60
120
D.
0 min
15 min
30 min
60 min
120 min
SW HEL x FcμR(+/+)
SW HEL x FcμR (-/-)
E.
MFI OF IgM-BCR (green)
WT: 0
KO:0
WT:5
KO:5
WT:15
KO:15
WT:30
KO:30
WT:60
KO:60
WT:120
KO:120

Figure 3: Reduced IgM-BCR expression in B cells lacking the FcμR

(A) pseudocolor plots of purity check between SW_{HEL} x FcμR+/+ and SW_{HEL} x FcμR-/- B cells and (B) frequency of antigen specific B cells. (C-E) Confocal microscopy images of pulse-chase experiment showing kinetics of surface IgM-BCR (green). B cells from SW_{HEL} x FcμR +/+ mice and SW_{HEL} x FcμR-/- were enriched using autoMACS and incubated with HEL-BODIPY for 30 min. Antigen was washed away three times and cells then incubated in warm culture media until at indicated time points, they were fixed and stained with IgM-BCR and DAPI. (C) Quantification of mean fluorescent intensity (MFI) of BCR-IgM fixed with paraformaldehyde (surface IgM-BCR) in indicated genotypes and (D) Representative confocal images on indicated timepoints and mice. (E) Quantification of IgM-BCR MFI between genotypes. Each dot represents an individual cell (*n=90 cells* for SW_{HEL} x FcμR +/+ and 98 cells for SW_{HEL} x FcμR-/-) . All bar graphs are MFI of IgM-BCR $\pm$ SD and was calculated using one-way ANOVA *p < 0.05; **p < 0.01; ***p < 0.001; ****p < 0.0001; ns= not significant.

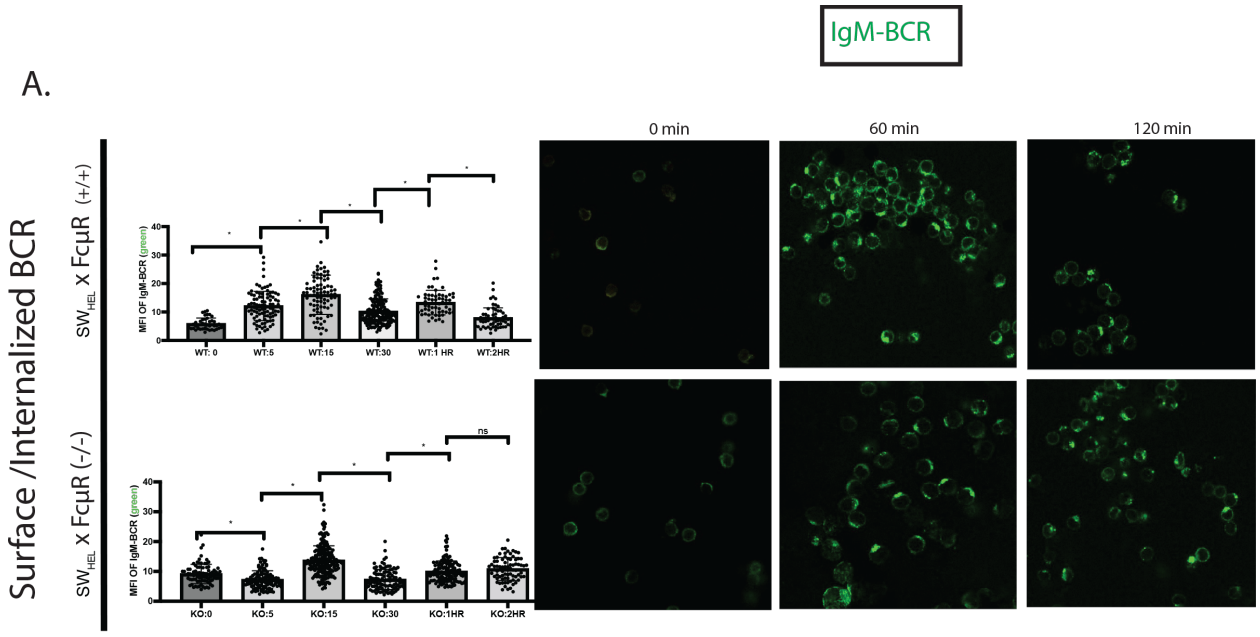
IgM-BCR
A.
Surface /Internalized BCR
SWHEL x FcμR (+/+)
SWHEL x FcμR (-/-)
MFI OF IgM-BCR (green)
WT: 0
WT:5
WT:15
WT:30
WT:1 HR
WT:2HR
KO:0
KO:5
KO:15
KO:30
KO:1HR
KO:2HR
ns
0 min
60 min
120 min

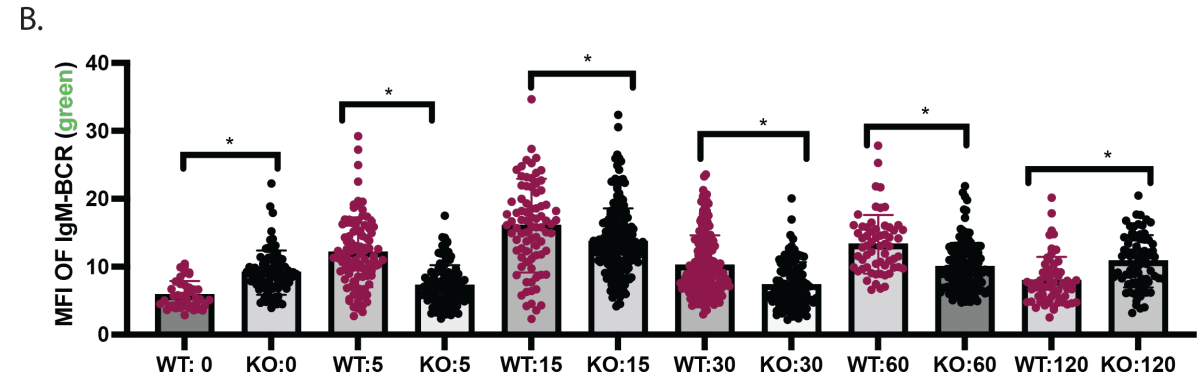
B.
MFI OF IgM-BCR (green)
WT: 0
KO:0
WT:5
KO:5
WT:15
KO:15
WT:30
KO:30
WT:60
KO:60
WT:120
KO:120

Figure 4: Absence of FcμR creates a delay in IgM-BCR mobilization. Experimental setup is the same as figure 3. (A,left) Half the samples were fixed with paraformaldehyde and permeabilized with saponin to visualize surface and internalized IgM-BCR at 0, 5, 60 and 120 min for SW_{HEL} x FcμR +/+ and SW_{HEL} x FcμR -/- B cells. (A,right) Representative confocal images on indicated timepoints and mice. (B) MFI of IgM-BCR ± SD at tested time points between genotypes. Single confocal planes are shown. Each dot represents an individual cell n= *90 cells* for SW_{HEL} x FcμR +/+ and 98 for SW_{HEL} x FcμR-/-) . All bar graphs are MFI of IgM-BCR ± SD and was calculated using one-way ANOVA *p < 0.05; **p < 0.01; ***p < 0.001; ****p < 0.0001; ns= not significant.

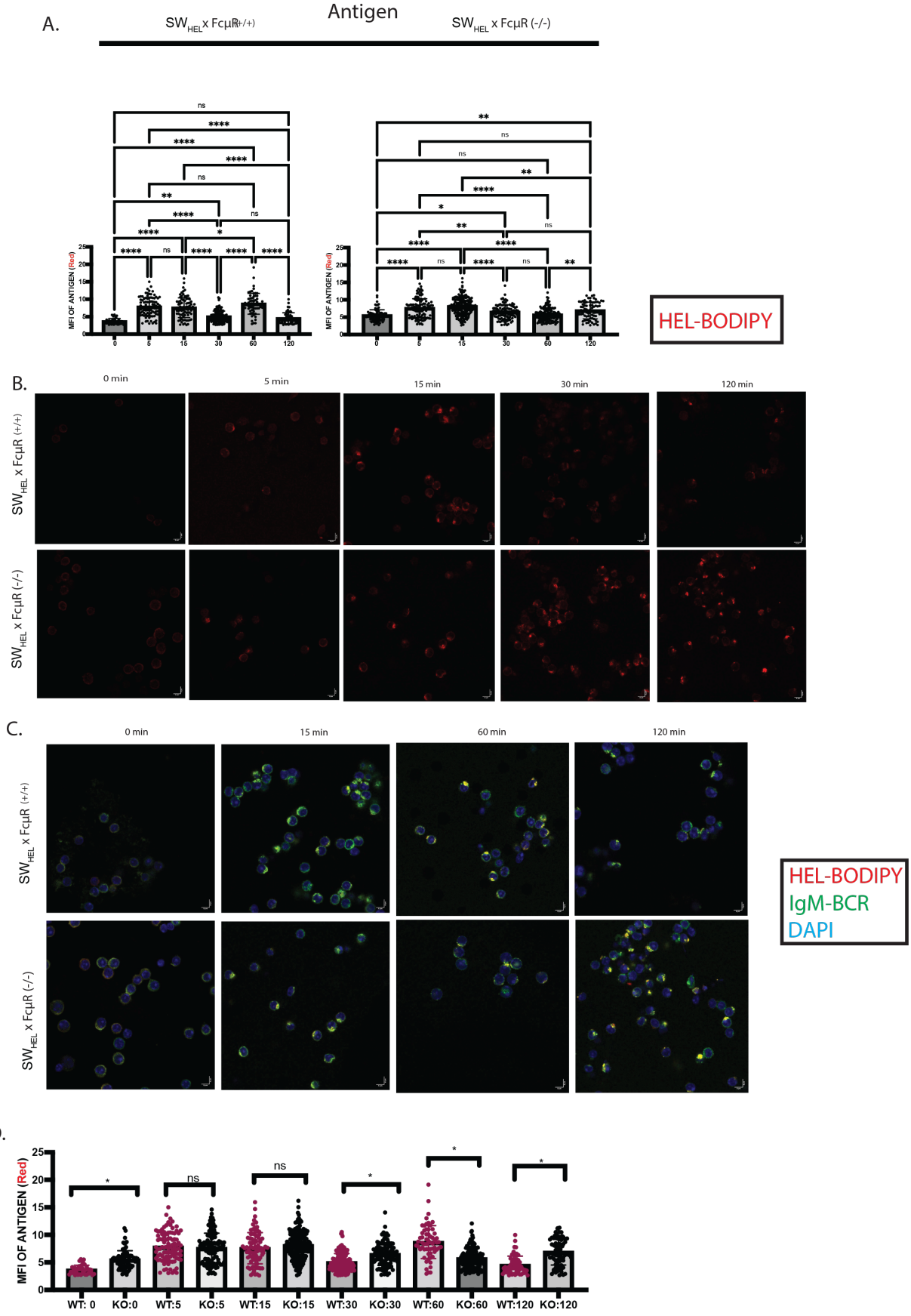
A.
Antigen
SW$_{HEL}$ x FcμR$^{+/+}$
SW$_{HEL}$ x FcμR (-/-)
MFI OF ANTIGEN (Red)
HEL-BODIPY
B.
0 min
5 min
15 min
30 min
120 min
SW$_{HEL}$ x FcμR (+/+)
SW$_{HEL}$ x FcμR (-/-)
C.
0 min
15 min
60 min
120 min
SW$_{HEL}$ x FcμR (+/+)
SW$_{HEL}$ x FcμR (-/-)
HEL-BODIPY
IgM-BCR
DAPI
D.
MFI OF ANTIGEN (Red)
WT: 0
KO:0
WT:5
KO:5
WT:15
KO:15
WT:30
KO:30
WT:60
KO:60
WT:120
KO:120

Figure 5: Antigen kinetics are stalled when FcμR is absent. Experimental setup is the same as Figure 3. (A) Half of the samples were fixed with paraformaldehyde and permeabilized with saponin. Antigen kinetics of HEL-BODIPY (red) with SW_{HEL} x FcμR+/+ B cells and SW_{HEL} x FcμR-/- B cells at 0,15, 30,120 min. (B) Representative single plane confocal images from indicated timepoints and mice. (C) Merged panel of all markers of SW_{HEL} x FcμR +/+ and SW_{HEL} x FcμR-/- B cells at 0, 60 and 120 min. (D) MFI ± SD of IgM-BCR of indicated genotypes at different timepoints. Single confocal planes are shown. Each dot represents an individual cell (*~90 cells* for SW_{HEL} x FcμR +/+ and 98 per for SW_{HEL} x FcμR-/-) . All bar graphs are MFI of IgM-Antigen ± SD and was calculated using one-way ANOVA *p < 0.05; **p < 0.01; ***p < 0.001; ****p < 0.0001; ns= not significant.

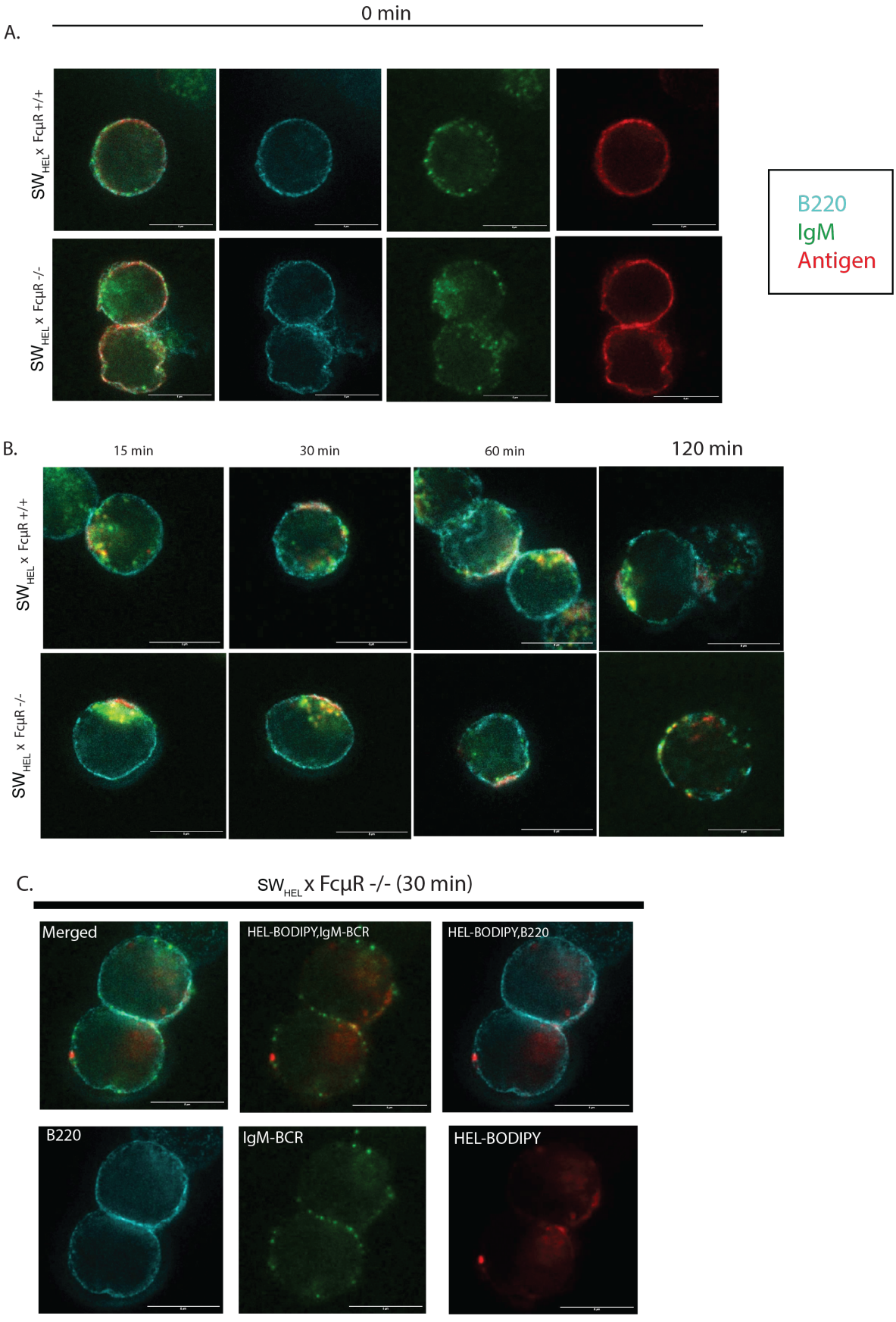
A.
0 min
SW HEL x FcμR +/+
SW HEL x FcμR -/-
B220
IgM
Antigen
B.
15 min
30 min
60 min
120 min
SW HEL x FcμR +/+
SW HEL x FcμR -/-
C.
SW HEL x FcμR -/- (30 min)
Merged
HEL-BODIPY,IgM-BCR
HEL-BODIPY,B220
B220
IgM-BCR
HEL-BODIPY

Figure 6: STED imaging of SWHEL x FcμR-/- cells demonstrate accumulation of antigen on the surface of B cells compared to controls. (A) Stimulated Emission Depletion microscopy (STED) images of SwHEL B cells when antigen is limited. Experimental setup is the same in Figs. 3-5. (A) STED images of SW_{HEL} x FcμR +/+ and SW_{HEL} x FcμR-/- B cells at time 0 with HEL-BODIPY(red), co-stained with HEL-BCR (green) and B220 (cyan). (B) Representative single plane images of B cells at designated time points from each genotype. (C) Representative STED image of HEL x FcμR-/- B cells at 30 min sharing membrane. Single confocal planes are shown. Each timepoint (*n*=20 images per time point, per genotype).

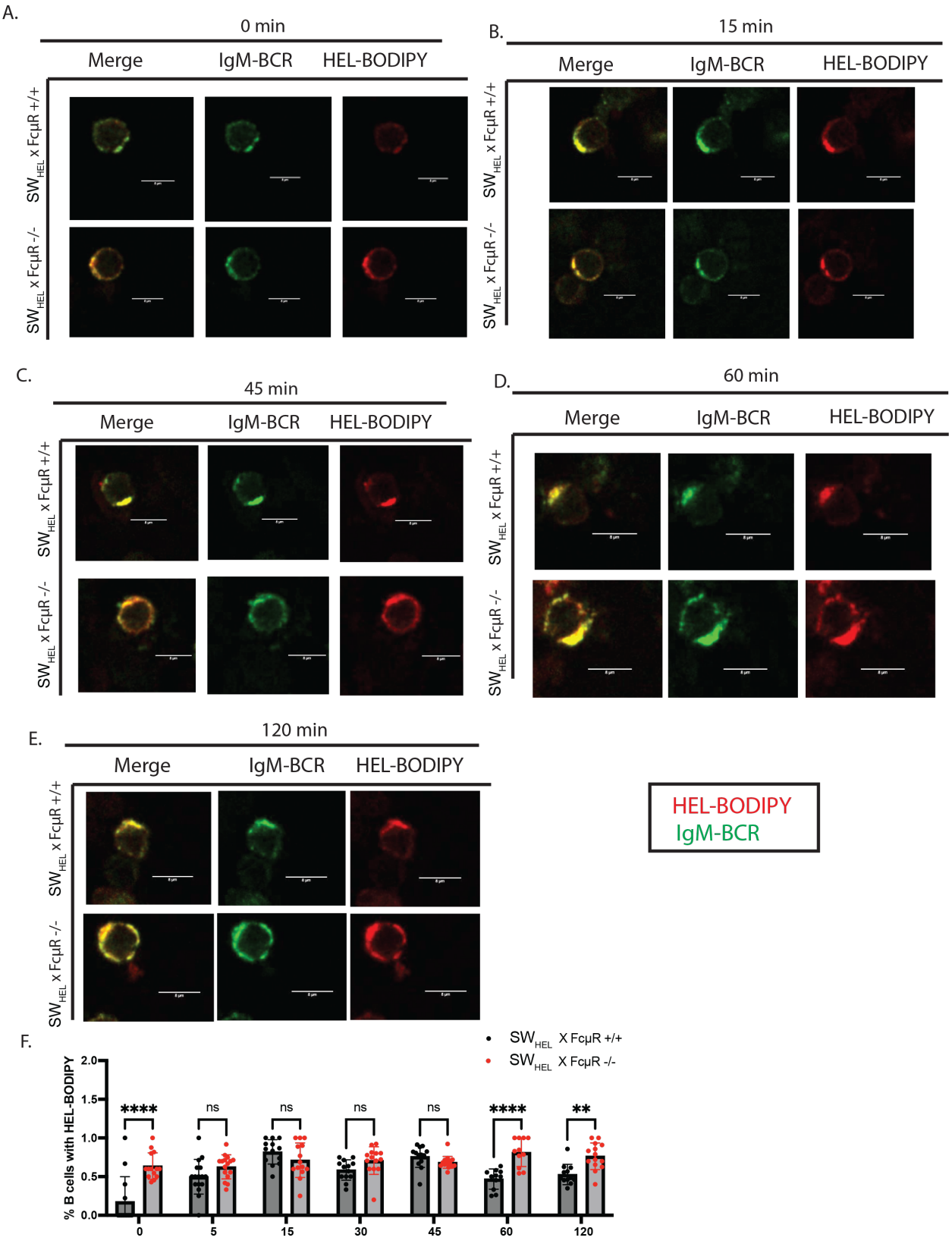
A.
0 min
Merge
IgM-BCR
HEL-BODIPY
SW$_{HEL}$ x FcμR +/+
SW$_{HEL}$ x FcμR -/-
B.
15 min
C.
45 min
D.
60 min
E.
120 min
HEL-BODIPY
IgM-BCR
F.
SW$_{HEL}$ X FcμR +/+
SW$_{HEL}$ X FcμR -/-
% B cells with HEL-BODIPY
2.0
1.5
1.0
0.5
0.0
****
ns
ns
ns
ns
****
**
0
5
15
30
45
60
120

Figure 7:Confocal images of SWHEL B cells when antigen is continuously provided to B cells. (A-E) Experimental setup is the same as Figs. 3-5 with exception to washing away antigen. Confocal images of SW_{HEL} B cells activated with HEL-BODIPY (antigen) for (A) 0 minutes, (B) 15 minutes (C) 45 minutes (D), 60 minutes (E) and 120 minutes and co-stained with HEL-BCR (green). (F) Bar graphs represent the mean ± SD (*~12 cells per time point* for SW_{HEL} x FcμR +/+ and 14 per timepoint for SW_{HEL} x FcμR-/- mice). % B cells was calculated by dividing the total number of cells with B cells and was calculated using 2-way ANOVA. *p < 0.05; **p < 0.01; ***p < 0.001; ****p < 0.0001; ns= not significant. Single confocal planes are shown.

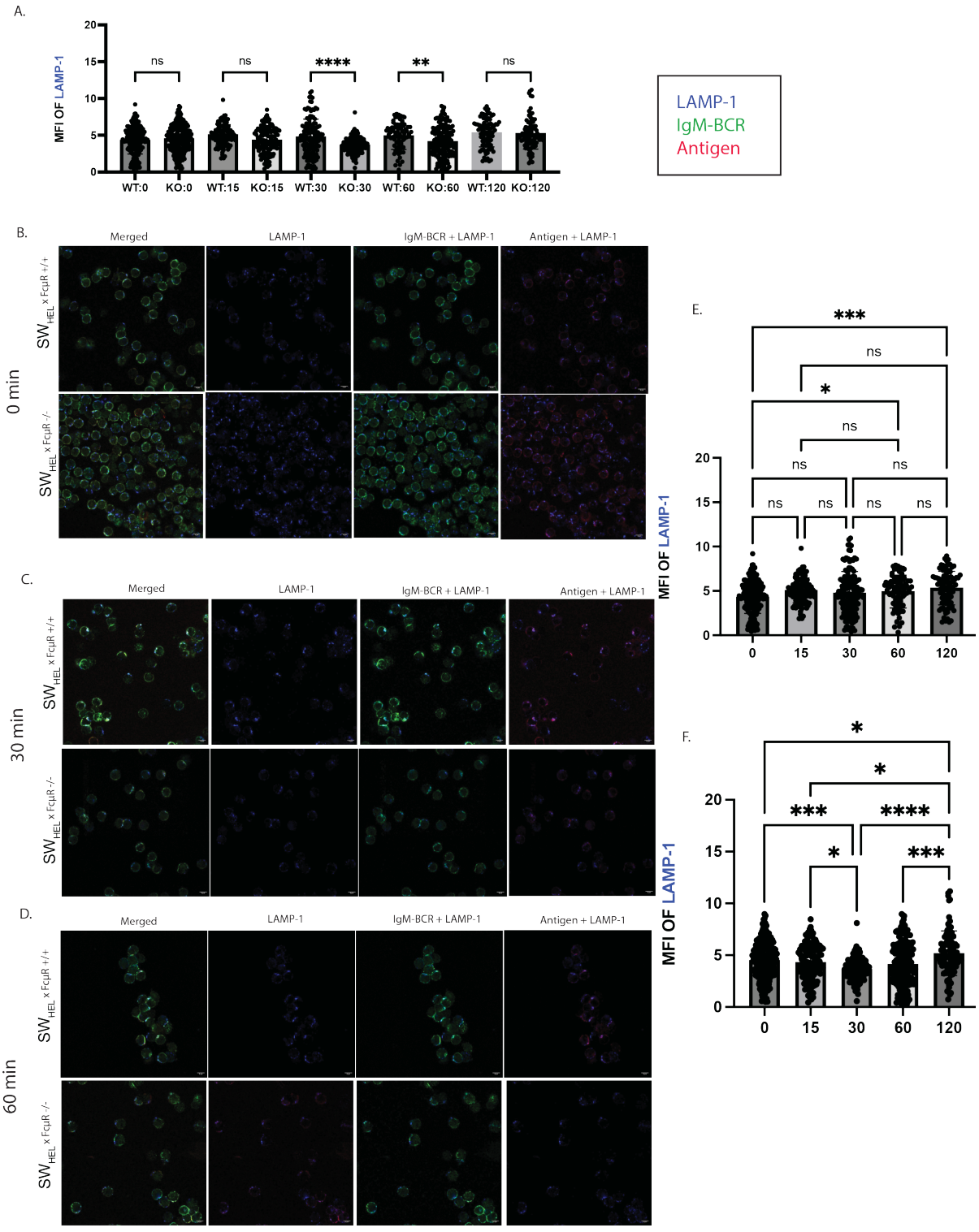
A.
MFI OF LAMP-1
ns
ns
****
**
ns
WT:0
KO:0
WT:15
KO:15
WT:30
KO:30
WT:60
KO:60
WT:120
KO:120
LAMP-1
IgM-BCR
Antigen
B.
Merged
LAMP-1
IgM-BCR + LAMP-1
Antigen + LAMP-1
0 min
SWHEL x FcμR +/+
SWHEL x FcμR -/-
C.
30 min
D.
60 min
E.
***
ns
*
ns
ns
ns
ns
ns
ns
ns
MFI OF LAMP-1
0
15
30
60
120
F.
*
*
***
****
*
***
MFI OF LAMP-1

Figure 8: LAMP-1 expression is altered when FcμR is absent. (A) Bar graph showing MFI ± SD of LAMP-1 from either SW_{HEL} x FcμR+/+ and SW_{HEL} x FcμR-/- B cells over different time points. (B) Confocal single plane images of LAMP-1 (blue) co-stained with IgM-BCR (green) and antigen (red) at (C) 30 minutes (D) 60 minutes. (E, top) MFI ± SD of LAMP-1 in SW_{HEL} x FcμR+/+ or (E, bottom) in SW_{HEL} x FcμR-/- B cells. All images are single confocal planes. Bar graphs represent the mean ± SD (*n=123 cells* for SW_{HEL} x FcμR +/+ and 152 for SW_{HEL} x FcμR-/- mice). was calculated using 2-way ANOVA. *p < 0.05; **p < 0.01; ***p < 0.001; ****p < 0.0001; ns= not significant.

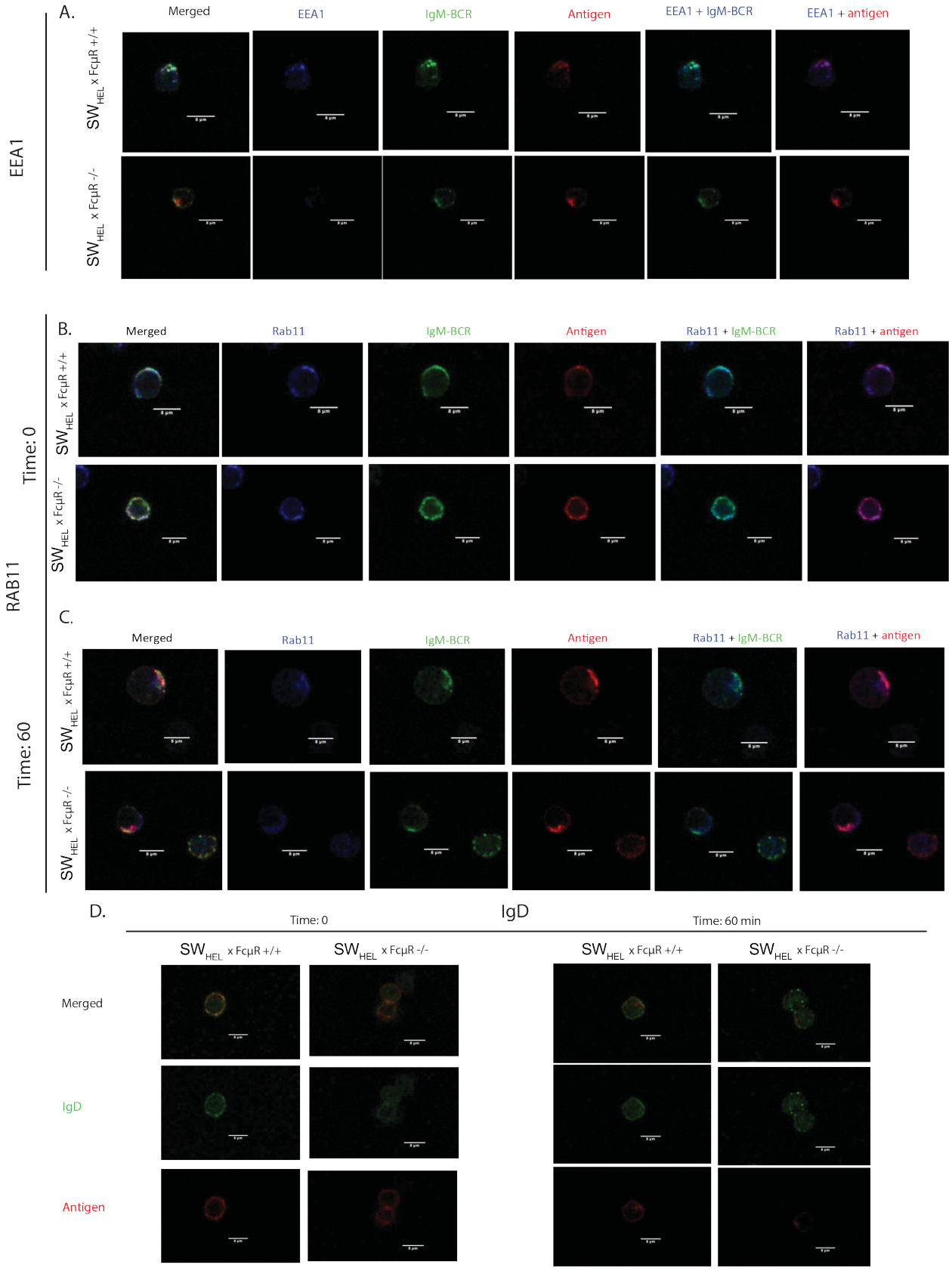
A.
Merged
EEA1
IgM-BCR
Antigen
EEA1 + IgM-BCR
EEA1 + antigen
EEA1
SWHEL x FcμR +/+
SWHEL x FcμR -/-
B.
Merged
Rab11
IgM-BCR
Antigen
Rab11 + IgM-BCR
Rab11 + antigen
RAB11
Time: 0
SWHEL x FcμR +/+
SWHEL x FcμR -/-
C.
Merged
Rab11
IgM-BCR
Antigen
Rab11 + IgM-BCR
Rab11 + antigen
Time: 60
SWHEL x FcμR +/+
SWHEL x FcμR -/-
D.
IgD
Time: 0
Time: 60 min
SWHEL x FcμR +/+
SWHEL x FcμR -/-
SWHEL x FcμR +/+
SWHEL x FcμR -/-
Merged
IgD
Antigen

Figure 9: Endosomal and IgD expression in B cells. (A) Confocal single plane images showing kinetics of EEA1 (blue) co-stained with antigen (red) with IgM-BCR (green) at 60 min. (B-C) Confocal single plane images Rab11 (blue) splenocytes at different time points co-stained with antigen (red) and IgM-BCR (green) on SW_{HEL} x FcμR+/+ and SW_{HEL} x FcμR-/+ B cells at (B) 0 minutes and (C) 60 minutes. (D) Confocal single plane of IgD expression (green) co-stained with antigen (red) at (D,left) time 0 and (D,right) 60 min. Each group (*n=6 cells*) per time point. This experiment was done once.

A.

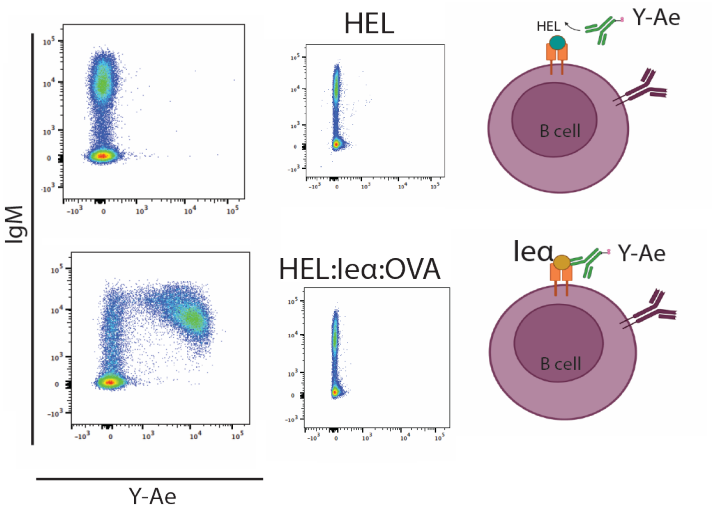
HEL
HEL
Y-Ae
B cell
IgM
HEL:Iea:OVA
Iea
Y-Ae
B cell
Y-Ae

B.

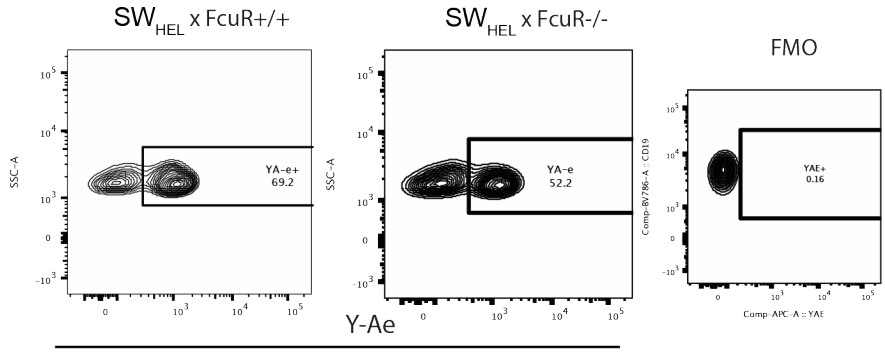
SW HEL x FcuR+/+
SW HEL x FcuR-/-
FMO
SSC-A
YA-e+
69.2
SSC-A
YA-e
52.2
Comp-BV786-A :: CD19
YAE+
0.16
Y-Ae

C.

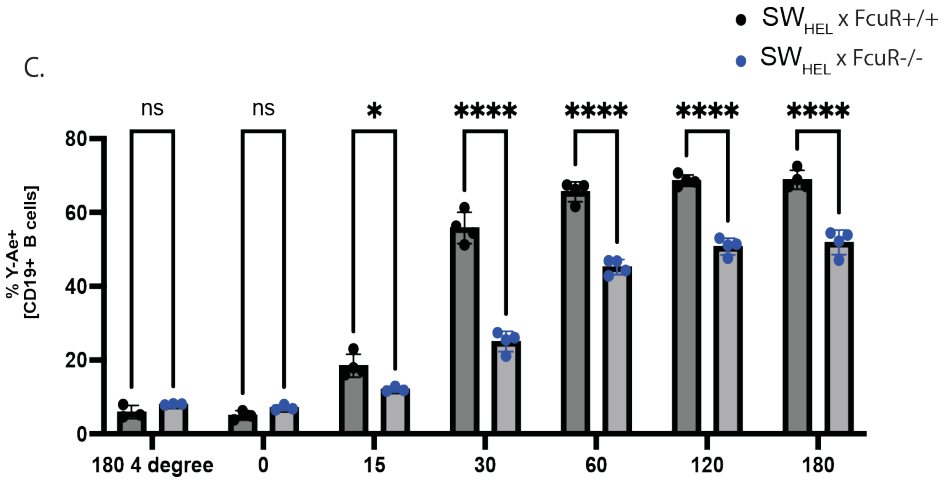
SW HEL x FcuR+/+
SW HEL x FcuR-/-
ns
ns
*
****
****
****
****
% Y-Ae+
[CD19+ B cells]
80
60
40
20
0
180 4 degree
0
15
30
60
120
180

Figure 10: Lack of FcμR-/- on B cells reduced the formation of peptide-MHC-II complexes on the cell surface. (A, top) Pseudocolor flow cytometry plots of B cells given HEL or (A, bottom) purified HEL-Ieα −OVA (Detection of IEα-peptide: I-A^b MHC II complexes on B cells were measured using mAb Y-Ae). (B) contour plots showing representative FACS staining at 180 min with (B, far right) florescence minus one (FMO). (C) Bar graphs with mean ± SD frequency of Y-Ae from of enriched B cells from SW_{HEL} x FcμR +/+ and SW_{HEL} x FcμR-/- B cells with 4 degree control at 180 minutes (*n*=6 mice) This experiment was repeated in 2 independent experiments and calculated using 2-way ANOVA. *p < 0.05; **p < 0.01; ***p < 0.001; ****p < 0.0001; ns= not significant.

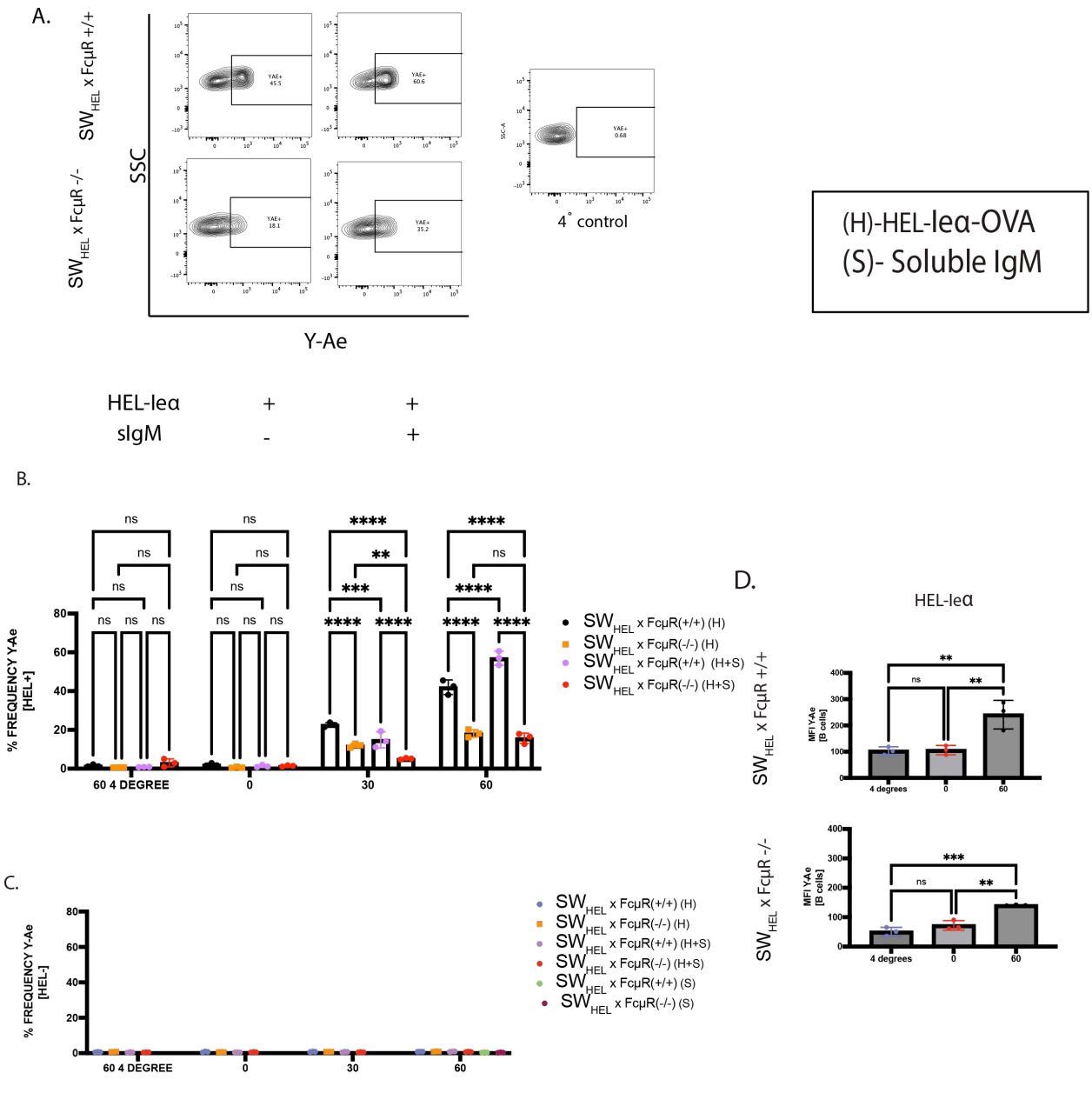
A.
SW$_{HEL}$ x FcμR +/+
SW$_{HEL}$ x FcμR -/-
SSC
Y-Ae
4° control
(H)-HEL-leα-OVA
(S)- Soluble IgM
HEL-leα + +
sIgM - +
B.
% FREQUENCY Y-Ae [HEL+]
60 4 DEGREE
0
30
60
SW$_{HEL}$ x FcμR(+/+) (H)
SW$_{HEL}$ x FcμR(-/-) (H)
SW$_{HEL}$ x FcμR(+/+) (H+S)
SW$_{HEL}$ x FcμR(-/-) (H+S)
C.
% FREQUENCY Y-Ae [HEL-]
SW$_{HEL}$ x FcμR(+/+) (S)
SW$_{HEL}$ x FcμR(-/-) (S)
D.
HEL-leα
SW$_{HEL}$ x FcμR +/+
SW$_{HEL}$ x FcμR -/-
MFI Y-Ae [B cells]
4 degrees
E.
MFI Y-Ae [B cells]
SW$_{HEL}$ x FcμR +/+
SW$_{HEL}$ x FcμR +/+

Figure 11: Soluble IgM Supports antigen uptake and presentation in MHCII

(A)Contour plots of splenocyte cells from SW_{HEL} x FcμR+/+ and SW_{HEL} x FcμR-/- mice incubated with HEL-Ieα-OVA alone or with HEL-Ieα-OVA incubated with purified HEL-specific IgM. (B) Summary of quantification of means ± SD of HEL specific splenocytes at 4 degrees, 0, 30, and 60 minutes compared to (C) non-HEL specific splenocytes under the same conditions. (D) MFI ± SD of Y-Ae in individual genotypes at 0 and 60 minutes with a 4-degree control (60 minutes). (E) MFI ± SD of Y-Ae amongst mice at time 0 and 60 minutes (E). Each condition was done in triplicates (*n*=3) and each symbol is mean ± SD from one well and was calculated using One-way ANOVA *p < 0.05; **p < 0.01; ***p < 0.001; ****p < 0.0001; ns= not significant. This is one of two independent experiments.

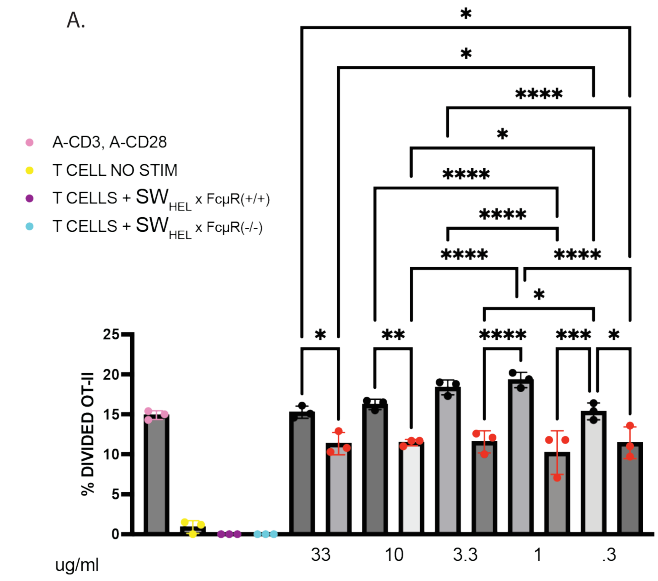
A.
A-CD3, A-CD28
T CELL NO STIM
T CELLS + SW HEL x FcμR(+/+)
T CELLS + SW HEL x FcμR(-/-)
% DIVIDED OT-II
ug/ml
33
10
3.3
1
.3

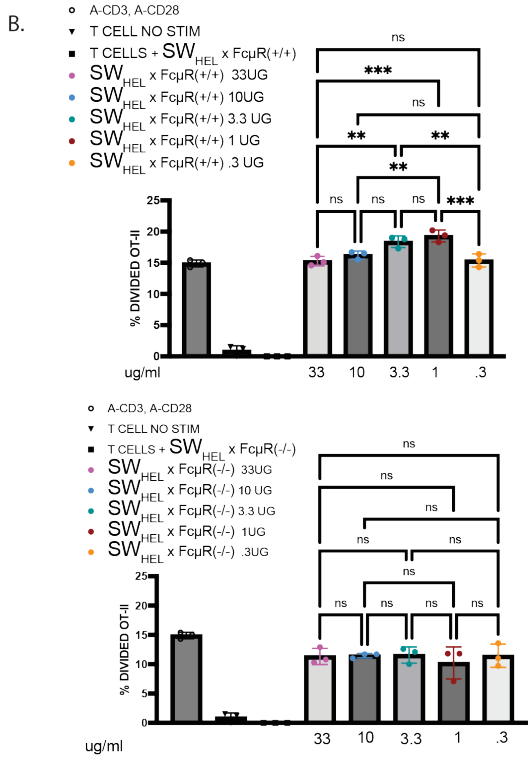
B.
A-CD3, A-CD28
T CELL NO STIM
T CELLS + SW HEL x FcμR(+/+)
SW HEL x FcμR(+/+) 33UG
SW HEL x FcμR(+/+) 10UG
SW HEL x FcμR(+/+) 3.3 UG
SW HEL x FcμR(+/+) 1 UG
SW HEL x FcμR(+/+) .3 UG
% DIVIDED OT-II
ug/ml
33
10
3.3
1
.3
A-CD3, A-CD28
T CELL NO STIM
T CELLS + SW HEL x FcμR(-/-)
SW HEL x FcμR(-/-) 33UG
SW HEL x FcμR(-/-) 10 UG
SW HEL x FcμR(-/-) 3.3 UG
SW HEL x FcμR(-/-) 1UG
SW HEL x FcμR(-/-) .3UG
% DIVIDED OT-II
ug/ml
33
10
3.3
1
.3

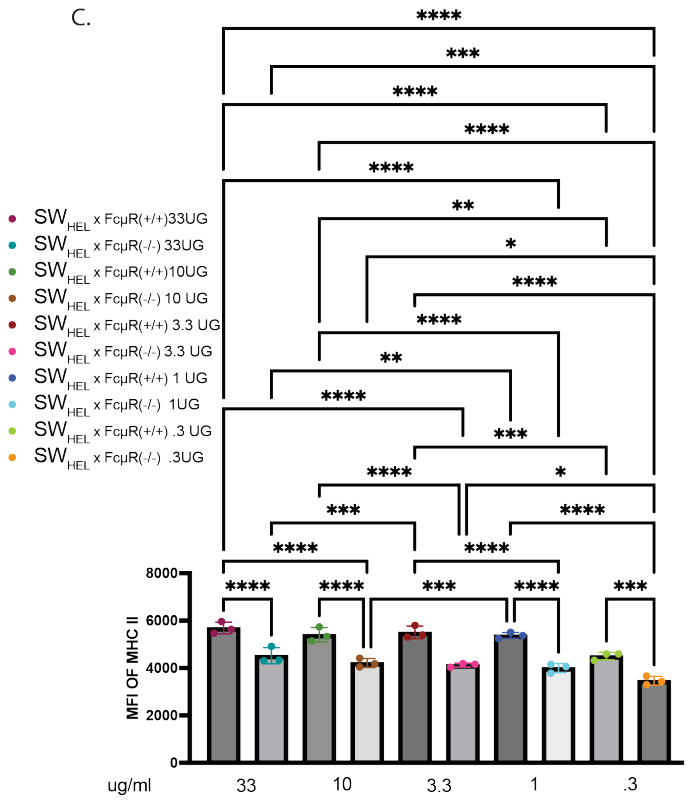
C.
SW HEL x FcμR(+/+)33UG
SW HEL x FcμR(-/-) 33UG
SW HEL x FcμR(+/+)10UG
SW HEL x FcμR(-/-) 10 UG
SW HEL x FcμR(+/+) 3.3 UG
SW HEL x FcμR(-/-) 3.3 UG
SW HEL x FcμR(+/+) 1 UG
SW HEL x FcμR(-/-) 1UG
SW HEL x FcμR(+/+) .3 UG
SW HEL x FcμR(-/-) .3UG
MFI OF MHC II
ug/ml
33
10
3.3
1
.3

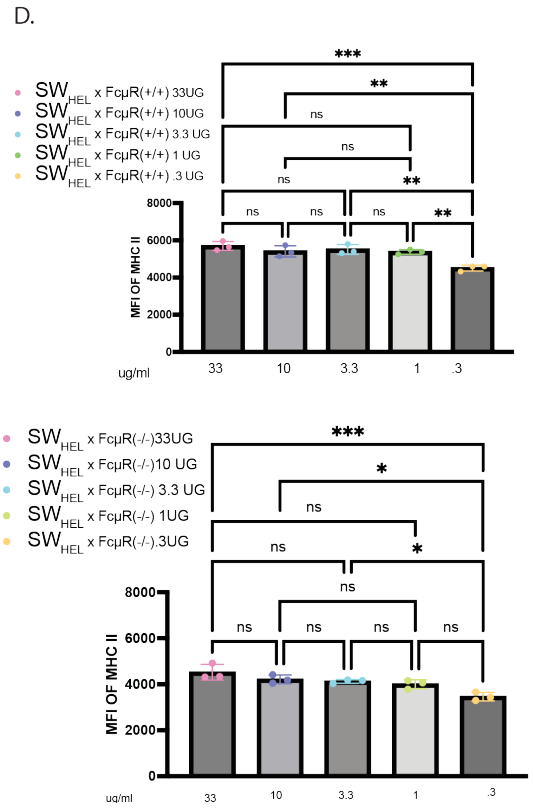
D.
SW HEL x FcμR(+/+) 33UG
SW HEL x FcμR(+/+) 10UG
SW HEL x FcμR(+/+) 3.3 UG
SW HEL x FcμR(+/+) 1 UG
SW HEL x FcμR(+/+) .3 UG
MFI OF MHC II
ug/ml
33
10
3.3
1
.3
SW HEL x FcμR(-/-)33UG
SW HEL x FcμR(-/-)10 UG
SW HEL x FcμR(-/-) 3.3 UG
SW HEL x FcμR(-/-) 1UG
SW HEL x FcμR(-/-).3UG
MFI OF MHC II
ug/ml
33
10
3.3
1
.3

Figure 12: Lack of FcμR on B cells reduces cognate T-B interaction and T cell proliferation.
Proliferation of transgenic CFSE labeled T cells incubated with enriched SW_{HEL} x FcμR+/+ and SW_{HEL} x FcμR-/- B cells cultured with varying concentrations of HEL-OVA for 3 days. (A) Analysis of CFSE labeled B cells stimulated with different concentrations of HEL-OVA. Each condition was done in triplicates (*n*=3) and each dot is mean ± SD from one culture well.(B) MFI ± SD of T cell proliferation with SW_{HEL} x FcμR+/+ B cells at 0 and 60 minutes with a 4-degree control (60 minutes). (c) MFI ± SD of T cell proliferation with SW_{HEL} x FcμR-/- B cells at 0 and 60 minutes with a 4-degree control (60 minutes). (D) MFI ± SD of B from each genotype and T cells co-cultured with HEL-OVA at different concentrations.). Data was calculated with One-way ANOVA *p < 0.05; **p < 0.01; ***p < 0.001; ****p < 0.0001; ns= not significant. This is one of two independent experiments.

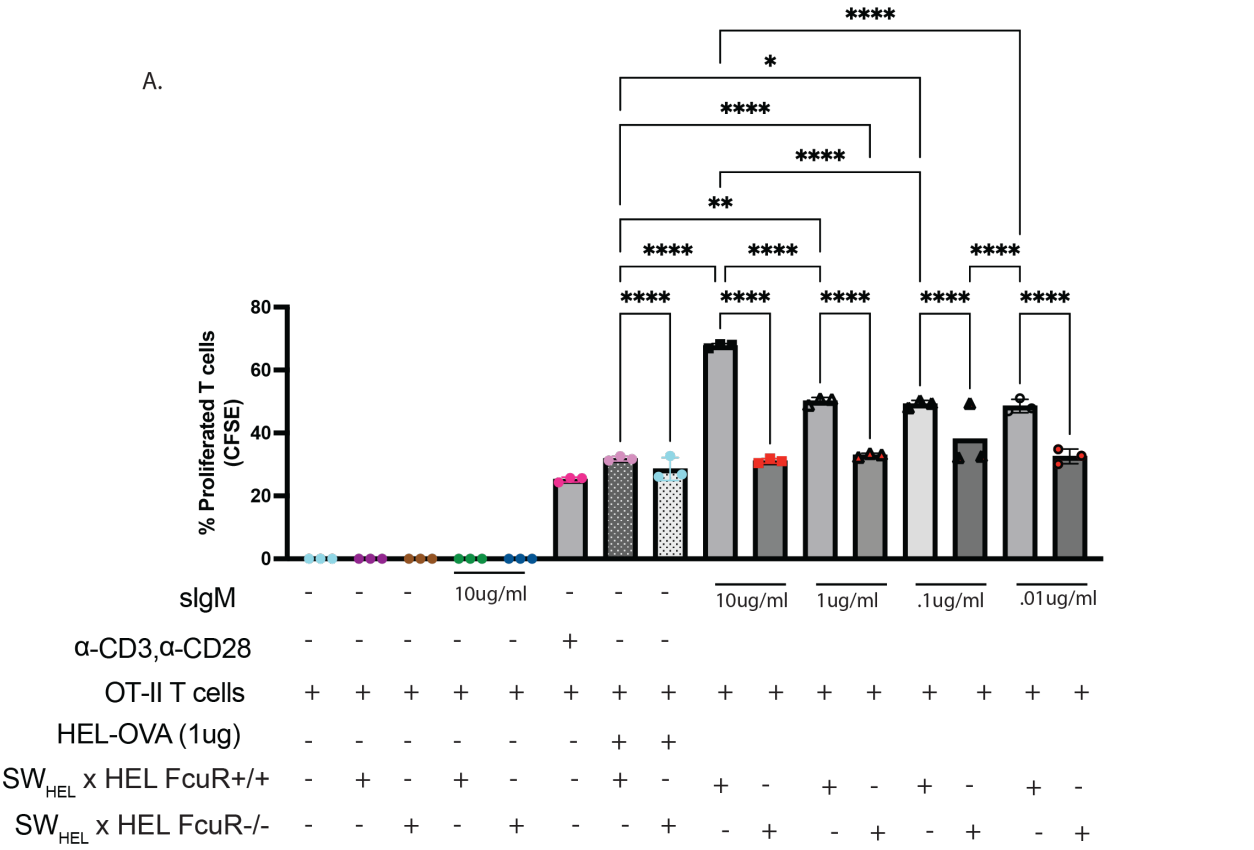
A.
% Proliferated T cells (CFSE)
sIgM
α-CD3,α-CD28
OT-II T cells
HEL-OVA (1ug)
SWHEL x HEL FcuR+/+
SWHEL x HEL FcuR-/-
10ug/ml
1ug/ml
.1ug/ml
.01ug/ml

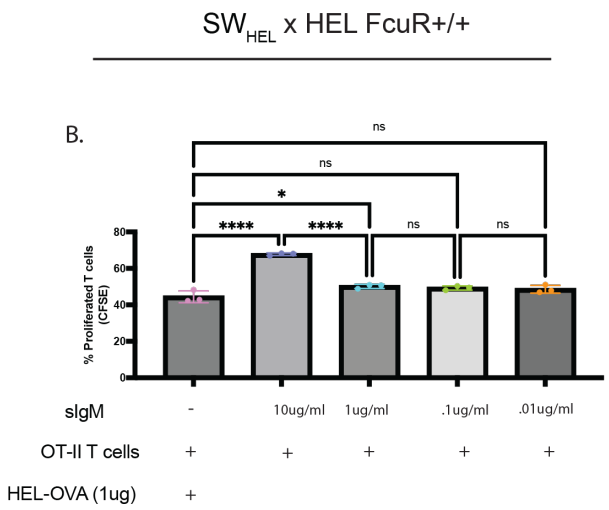
SWHEL x HEL FcuR+/+
B.
% Proliferated T cells (CFSE)
sIgM
OT-II T cells
HEL-OVA (1ug)
10ug/ml
1ug/ml
.1ug/ml
.01ug/ml

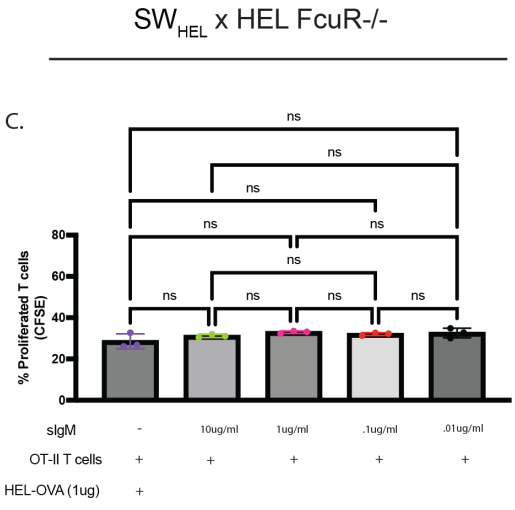
SWHEL x HEL FcuR-/-
C.
% Proliferated T cells (CFSE)
sIgM
OT-II T cells
HEL-OVA (1ug)
10ug/ml
1ug/ml
.1ug/ml
.01ug/ml

Figure 13: Soluble IgM Supports cognate B-T cell activation**.** (A) Analysis of CFSE labeled OT-II T cells stimulated with 1ug/ml HEL-OVA conjugate with varying concentrations of sIgM. Each condition was done in triplicates (*n*=3) and each symbol is mean ± SD from one culture well. (B) Quantification of mean ± SD of OT-II T cells labeled with CFSE and co-cultured with SW_{HEL} x FcμR+/+ B cells with HEL-OVA and secreted IgM in varrying concentrations in culture for 72 hours. (C) Quantification of mean ± SD of OT-II T cells labeled with CFSE and co-cultured with SW_{HEL} x FcμR-/- B cells with HEL-OVA and secreted IgM in varying concentrations in culture for 72 hours. Statistics was calculated using one-way ANOVA. *p < 0.05; **p < 0.01; ***p < 0.001; ****p < 0.0001; ns= not significant. Each symbol is representative of one culture well.

A.

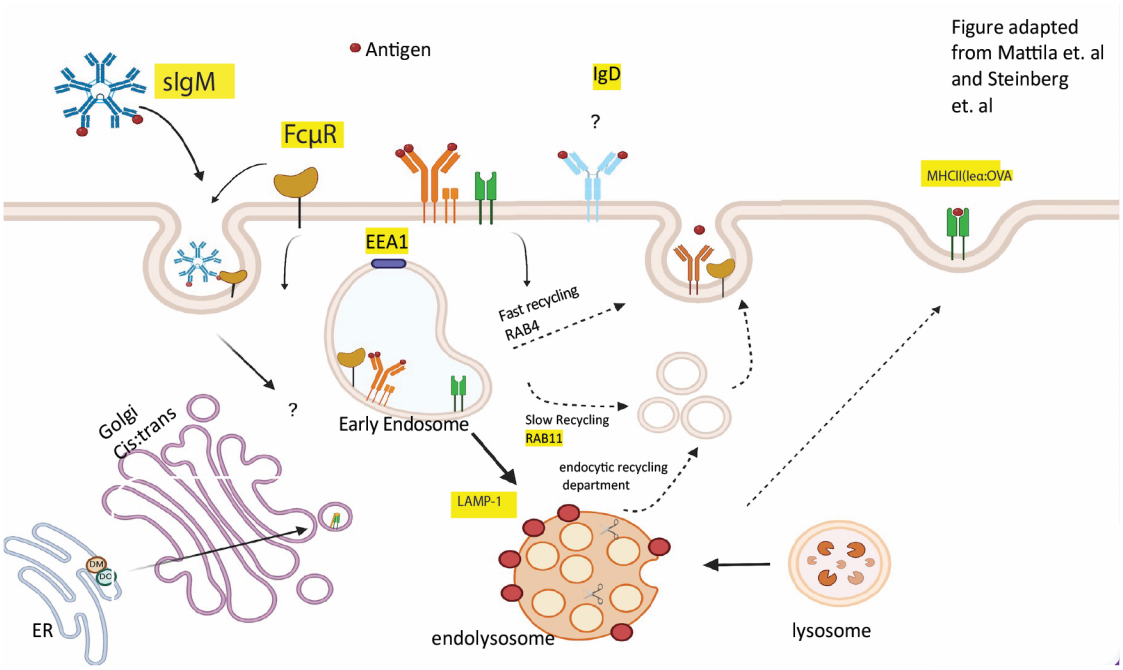
Figure adapted from Mattila et. al and Steinberg et. al
Antigen
sIgM
FcμR
IgD
?
MHCII(Iea:OVA
EEA1
Fast recycling RAB4
Slow Recycling RAB11
endocytic recycling department
Early Endosome
Golgi Cis:trans
?
LAMP-1
ER
endolysosome
lysosome

B.

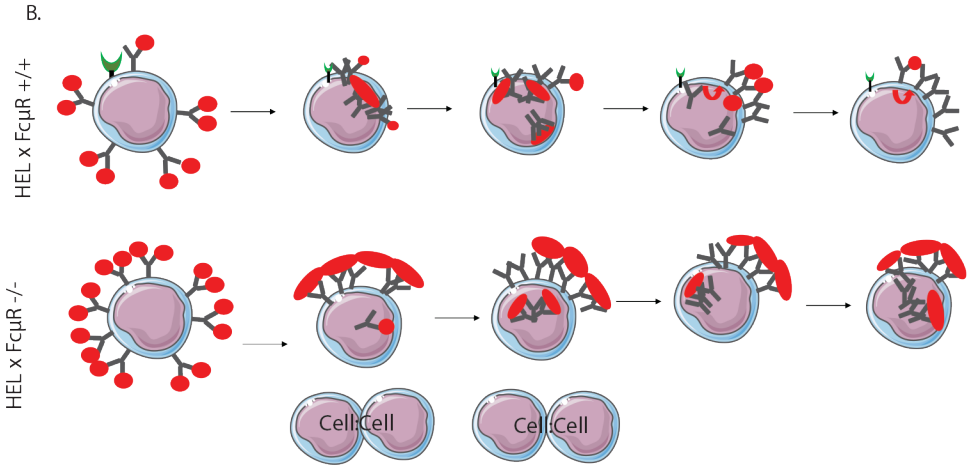
HEL x FcμR +/+
HEL x FcμR -/-
Cell:Cell
Cell:Cell

Figure 14:Conclusion Schematic of summary data with various markers used in our studies (A) Schematic of intracellular and surface markers used to characterize SW_{HEL} x FcμR +/+ and SW_{HEL} x FcμR-/- B cells in the context of antigen. (B) Summary schematic from STED and confocal analysis of antigen internalization in SW_{HEL} x FcμR +/+ and SW_{HEL} x FcμR-/- B cells at different time points.

References

Barnden, M. J., Allison, J., Heath, W. R., & Carbone, F. R. (1998). Defective TCR expression in transgenic mice constructed using cDNA-based alpha- and beta-chain genes under the control of heterologous regulatory elements. *Immunol Cell Biol, 76*(1), 34-40. doi:10.1046/j.1440-1711.1998.00709.x

Baumgarth, N., Herman, O. C., Jager, G. C., Brown, L. E., Herzenberg, L. A., & Chen, J. (2000). B-1 and B-2 cell-derived immunoglobulin M antibodies are nonredundant components of the protective response to influenza virus infection. *J Exp Med, 192*(2), 271-280.

Boes, M. (2000). Role of natural and immune IgM antibodies in immune responses. *Mol Immunol, 37*(18), 1141-1149.

Brink, R., Paus, D., Bourne, K., Hermes, J. R., Gardam, S., Phan, T. G., & Chan, T. D. (2015). The SW(HEL) system for high-resolution analysis of in vivo antigen-specific T- dependent B cell responses. *Methods Mol Biol, 1291*, 103-123. doi:10.1007/978-1- 4939-2498-1_9

Choi, S. C., Wang, H., Tian, L., Murakami, Y., Shin, D. M., Borrego, F., . . . Coligan, J. E. (2013). Mouse IgM Fc receptor, FCMR, promotes B cell development and modulates antigen-driven immune responses. *J Immunol, 190*(3), 987-996. doi:10.4049/jimmunol.1202227

Ehrenstein, M. R., & Notley, C. A. (2010). The importance of natural IgM: scavenger, protector and regulator. *Nat Rev Immunol, 10*(11), 778-786. doi:10.1038/nri2849

Kopf, M., Brombacher, F., & Bachmann, M. F. (2002). Role of IgM antibodies versus B cells in influenza virus-specific immunity. *Eur J Immunol, 32*(8), 2229-2236. doi:10.1002/1521-4141(200208)32:8<2229::AID-IMMU2229>3.0.CO;2-T

Kubagawa, H., Oka, S., Kubagawa, Y., Torii, I., Takayama, E., Kang, D. W., . . . Wang, J. Y. (2009). Identity of the elusive IgM Fc receptor (FcmuR) in humans. *J Exp Med, 206*(12), 2779-2793. doi:10.1084/jem.20091107

Nguyen, T. T., & Baumgarth, N. (2016). Natural IgM and the Development of B Cell-Mediated Autoimmune Diseases. *Crit Rev Immunol, 36*(2), 163-177. doi:10.1615/CritRevImmunol.2016018175

Nguyen, T. T., Klasener, K., Zurn, C., Castillo, P. A., Brust-Mascher, I., Imai, D. M., . . . Baumgarth, N. (2017). The IgM receptor FcmuR limits tonic BCR signaling by regulating expression of the IgM BCR. *Nat Immunol, 18*(3), 321-333. doi:10.1038/ni.3677

Nguyen, T. T. T., Graf, B. A., Randall, T. D., & Baumgarth, N. (2017). sIgM-FcmuR Interactions Regulate Early B Cell Activation and Plasma Cell Development after Influenza Virus Infection. *J Immunol, 199*(5), 1635-1646. doi:10.4049/jimmunol.1700560

Ouchida, R., Mori, H., Hase, K., Takatsu, H., Kurosaki, T., Tokuhisa, T., . . . Wang, J. Y. (2012). Critical role of the IgM Fc receptor in IgM homeostasis, B-cell survival, and humoral immune responses. *Proc Natl Acad Sci U S A, 109*(40), E2699-2706. doi:10.1073/pnas.1210706109

Phan, T. G., Amesbury, M., Gardam, S., Crosbie, J., Hasbold, J., Hodgkin, P. D., . . .

Brink,R. (2003). B cell receptor-independent stimuli trigger immunoglobulin (Ig) class switch recombination and production of IgG autoantibodies by anergic self-reactive B cells. *J Exp Med, 197*(7), 845-860. doi:10.1084/jem.20022144

Schroeder, H. W., Jr., & Cavacini, L. (2010). Structure and function of immunoglobulins. *J Allergy Clin Immunol, 125*(2 Suppl 2), S41-52. doi:10.1016/j.jaci.2009.09.046